NORSAR

NORSAR Scientific Report No. 2-2011

Semiannual Technical Summary

1 January - 30 June 2011

Frode Ringdal (ed.)

Kjeller, August 2011

REPORT DOCUMENTATION PAGE

Form Approved
OMB No. 0704-0188

PLEASE DO NOT RETURN YOUR FORM TO THE ABOVE ADDRESS.

1. REPORT DATE *(DD-MM-YYYY)*	2. REPORT TYPE	3. DATES COVERED *(From - To)*
15-08-2011	Semiannual Technical Summary	1 January - 30 June 2011

4. TITLE AND SUBTITLE

Semiannual Technical Summary, 1 January - 30 June 2011

5a. CONTRACT NUMBER

FA2521-06-C-8003

5b. GRANT NUMBER

5c. PROGRAM ELEMENT NUMBER

NDC Support / R&D

6. AUTHOR(S)

Frode Ringdal (Ed.)

5d. PROJECT NUMBER

T/6110

5e. TASK NUMBER

SOW Task 4.2 & 4.3

5f. WORK UNIT NUMBER

CDRL sequence nos. A001-A004

7. PERFORMING ORGANIZATION NAME(S) AND ADDRESS(ES)

Stiftelsen NORSAR
Post Box 53
NO-2027 Kjeller
Norway

8. PERFORMING ORGANIZATION REPORT NUMBER

Scientific Report No. 2-2011

9. SPONSORING/MONITORING AGENCY NAME(S) AND ADDRESS(ES)

AFTAC/TTS, 1030 South Highway A1A MS 1000, Patrick AFB, FL 32925-3002

10. SPONSOR/MONITOR'S ACRONYM(S)

AFTAC/TTS

11. SPONSOR/MONITOR'S REPORT NUMBER(S)

12. DISTRIBUTION/AVAILABILITY STATEMENT

Approved for public release; distribution unlimited

13. SUPPLEMENTARY NOTES

14. ABSTRACT

This report describes activities carried out at NORSAR under Contract No. FA2521-06-C-8003 (T/6110) for the period 1 January - 30 June 2011. In addition, it provides summary information on operation and maintenance (O&M) activities at the Norwegian National Data Center (NOR-NDC) during the same period. The O&M activities, including operation of transmission links within Norway and to Vienna, Austria, are being funded jointly by the CTBTO/PTS and the Norwegian Government, with the understanding that the funding of O&M activities for primary stations in the International Monitoring System (IMS) will gradually be transferred to the CTBTO/PTS. The O&M statistics presented in this report are included for the purpose of completeness, and in order to maintain consistency with earlier reporting practice. The cost of transmission of selected data from the Norwegian NDC to the United States NDC is covered by the United States Government. Research activities described in this report are mainly (cont.)

15. SUBJECT TERMS

NORSAR, Norwegian Seismic Array

16. SECURITY CLASSIFICATION OF:			17. LIMITATION OF ABSTRACT	18. NUMBER OF PAGES	19a. NAME OF RESPONSIBLE PERSON
a. REPORT	b. ABSTRACT	c. THIS PAGE			Mr. Kyle S. Roberts, AFTAC/TTX
U	U	U	SAR	65	19b. TELEPHONE NUMBER *(Include area code)* (321) 494-9471

Reset

Standard Form 298 (Rev. 8/98)
Prescribed by ANSI Std. Z39.18

Abstract (cont.)

funded by the Norwegian Government, with other sponsors acknowledged where appropriate.

The seismic arrays operated by NOR-NDC comprise the Norwegian Seismic Array (NOA), the Arctic Regional Seismic Array (ARCES) and the Spitsbergen Regional Array (SPITS). This report presents statistics for these three arrays as well as for additional seismic stations which through cooperative agreements with institutions in the host countries provide continuous data to NOR-NDC. These additional stations include the Finnish Regional Seismic Array (FINES) and the Hagfors array in Sweden (HFS).

The NOA Detection Processing system has been operated throughout the period with an uptime of 100%. A total of 4,625 seismic events have been reported in the NOA monthly seismic bulletin during the reporting period. On-line detection processing and data recording at the NDC of data from ARCES, FINES, SPITS and HFS data have been conducted throughout the period. Processing statistics for the arrays for the reporting period are given.

A summary of the activities at the NOR-NDC and relating to field installations during the reporting period is provided in Section 4. Norway is now contributing primary station data from two seismic arrays: NOA (PS27) and ARCES (PS28), one auxiliary seismic array SPITS (AS72), and one auxiliary three-component station JMIC (AS73). These data are being provided to the IDC via the global communications infrastructure (GCI). Continuous data from the three arrays are in addition being transmitted to the US NDC. The performance of the data transmission to the US NDC has been satisfactory during the reporting period.

So far among the Norwegian stations, the NOA and the ARCES array (PS27 and PS28 respectively), the radionuclide station at Spitsbergen (RN49) and the auxiliary seismic stations on Spitsbergen (AS72) and Jan Mayen (AS7653) have been certified. Provided that adequate funding continues to be made available (from the CTBTO/PTS and the Norwegian Ministry of Foreign Affairs), we envisage continuing the provision of data from these and other Norwegian IMS- designated stations in accordance with current procedures. As part of NORSAR's obsolescence management, a recapitalization plan for PS27 and PS28 was submitted to CTBTO/PTS in October 2008, in order to prevent severe degradation of the stations due to lack of spare parts. The installation of new equipment started in 2010.

The IMS infrasound station originally planned to be located near Karasjok (IS37) will be established at another site, since the local authorities did not grant the permissions required. Two sites at Bardufoss, both at 69.1^{o} N, 18.6^{o} E, are currently being pursued with landowners and the municipal authorities, with the purpose of selecting one of them for possible installation of IS37. The CTBTO PrepCom has approved a corresponding coordinate change for the station.

Summaries of four scientific and technical contributions presented in Chapter 6 of this report are provided below:

Section 6.1 presents initial results from a project aimed at applying detection probabilities in the IDC global phase association (GA) process. GA is an automated procedure that associates detections by IMS stations in order to form event hypotheses. These hypotheses will later be reviewed by analysts before the Reviewed Event Bulletin (REB) is issued. We have begun investigating ways to improve the GA process for seismic data, in particular by incorporating amplitude data and station detection probabilities in the automatic process. We build on a previous study which has provided regional detection capability estimates for individual primary and auxiliary IMS stations, and use these estimates to develop and test various consistency

measures. The purpose of these measures is to provide a means to assess the validity of seismic events automatically defined in the Standard Event Lists (SEL1, SEL2 and SEL3) and assess the consistency of individual phases associated with such events. By feeding the results of such assessments back into the GA procedure, we anticipate that the results of the global association can be iteratively improved.

A candidate SEL event is a group of automatically associated phases from IMS stations that satisfies certain predefined criteria for defining an event. For each such event an estimated origin time, hypocenter, a list of detecting stations and detected phases, phase arrival times and an average event magnitude as well as individual station magnitudes are given. Our basic approach is to make the hypothetical assumption that each such candidate event is real and correctly located. Using the regionalized station detection thresholds, we have the basis for calculating the station detection probability for events at that location as a function of event magnitude. By taking into consideration the actual pattern of detecting and non-detecting stations for the candidate event as listed in the SEL, we can therefore estimate a maximum-likelihood (MLE) magnitude for the hypothetical event. Based on this magnitude estimate, we then calculate, for each station, its probability of detection. By ranking the stations according to their detection probability, we can assess which stations are likely to detect or not detect this hypothetical event. We can then compare these probabilities to the actually observed phase list for the event as given in the SEL, and identify any inconsistencies.

The single most important criterion for accepting a candidate SEL event is clearly the number of detecting stations that have been associated with the event. If this number is above a certain threshold, the event is accepted, perhaps with a suggestion to the analyst that one or more low probability phases be considered for deletion. Our approach therefore focuses on events with few (typically six or fewer) associated detecting stations. In such cases, we need to carry out several tests, and these tests are still under development. One promising approach is to take as starting point the number of *non-detecting* primary stations which have a higher detection probability than the *n'th best detecting* station (*n=1,2,3…).* For example, if the three primary stations with the highest detection probability are in fact associated with the event, then we would very likely accept the event, with a possible explanatory comment to the analyst. Other supplementary approaches are being considered.

Section 6.2 contains an analysis of the Novaya Zemlya seismic event on 11 October 2010. The event, which had a magnitude of 4.3 (IDC_REB), occurred on the north-west coast of Novaya Zemlya, at 22:48:25.6 (IDC_REB). The event was well recorded globally, and phase readings at 44 IMS stations contributed to the REB location. It has previously been observed that there is very efficient propagation of high-frequency signals for ray-paths crossing the Barents Sea. As a consequence, both the IMS seismic stations on Svalbard (the SPITS array) and in northern Norway (the ARCES array) have been equipped with instruments having sampling rates of 80 Hz and 100Hz, respectively. In addition to an assessment of the reported event locations, we present in this contribution the high-frequency recordings at SPITS and ARCES.

The REB location, 76.2640N; 64.7619E is mainly based on readings at distant stations. Phase picks at stations at regional distances, on Svalbard and in northern Fennoscandia, dominated the input to the initial location reported in NORSAR's regional bulletin. This location, differed significantly, by about 65 km, from the REB. In an attempt to combine phase readings at both regional and teleseismic distances, we relocated the event using a number of re-picked phases. The location was calculated with the HYPOSAT program using a combination of the regional

"barey" model and the global *"AK135"* model. The recalculated location differed by 22 km from the REB location. We conclude that there is a need to improve the regional location models used for routine data analysis of events, and use of existing three-dimensional regional propagation models in this analysis should be encouraged.

The SPITS and the ARCES arrays are located at distances of 1178 and 1451 km, respectively, For the SPITS recordings, the presence of significant energy up to the Nyquist frequency of 40 Hz confirms the documented efficient high-frequency wave propagation from the Novaya Zemlya region to Svalbard, across the Barents Sea. For the ARCES high-frequency element, the spectra show signal energy up to about 25 Hz for the Pn and Sn phases. As compared to the SPITS spectra and the ARCES spectra of an earlier event in the eastern Barents Sea on 11 November 2009, the ARCES spectra for the 2010 event has comparatively less high frequency energy. We attribute this to a longer propagation path, and to signal attenuation when the seismic waves cross the heterogeneous crustal structures of the Novaya Zemlya island. However, we nevertheless consider this as very efficient propagation of high-frequency energy.

Section 6.3 contains an analysis of an earthquake in Hedmark, Southern Norway, which occurred on 21 July 2011 at 02.59 local time. A very preliminary automatic location of the event clearly located the earthquake within the NORSAR array (NOA), between the communities of Elverum and Rena, about 40 - 50 km north of the 7 April 2004 Flisa earthquake. With the 42 seismic sites of the NORSAR array at epicentral distances between about 10 and 60 km from the event and several additional seismic stations in the region, it was possible to perform a high quality determination of the hypocenter.

Although this event was not very large (reported magnitudes are between 3.3 and 3.8), it had been observed at local, regional, and teleseismic distances. With such a large number of close by seismic stations and observations, the GT level of this event will be of interest. Based on the analysis in this paper, the epicenter can be classified as a GT-1 event, located at 60.9642N, 11.5849E. With several NOA sites at epicentral distances of 10 to 20 km and in different azimuthal directions even the depth of the event, estimated at 22.8 km, is well defined with an uncertainty of less than +/-1 km.

We were also able to estimate the fault plane solution of this earthquake. At all stations used to locate the event and at a smaller number of stations at regional distances, P-onset polarities and some SH and SV polarities could be read. In addition, some amplitude ratios between the P and the S (SV and SH) onsets were measured. All these data were inverted for the best fitting double couple solution. The FOCMEC inversion routine was applied to calculate all possible fault planes which are in agreement with the observed data. The assumption for this type of inversion is that one double couple can describe the source mechanism.The presented double couple solution shows a reverse fault with a general NNE - SSW strike. From the observed data it is not possible to decide which of the two possible planes is the actual fault plane. The point of intersection between the two possible fault planes is not very well defined due to station distribution and due to the fact that many stations in the south are located beyond the Teisseyre-Tornquist zone, which is known to block seismic wave propagation. However, systematic search for more polarity data may constrain the solution better.

Section 6.4 is entitled "The International Polar Year (IPY) broadband ocean-bottom seismograph deployment: observations, limitations and integration with the IPY land network". Within the framework of the IPY 2007-2008 project "The Dynamic Continental Margin Between the Mid-Atlantic-Ridge System (Mohns Ridge, Knipovich Ridge) and Bear Island",

several temporary seismic stations were installed in the wider area of the Western Barents Sea margin. Among them was a three-component, broadband ocean-bottom seismometer and hydrophone (OBS/H) deployment, consisting of 12 stations distributed over the area between the Knipovich Ridge and Bear Island. Regarding land stations, the Norwegian National Seismic Network (NNSN) station HOPEN was upgraded with a broadband seismometer, a new broadband station (HSPB) was installed at Hornsund, and a small-aperture seismic array was installed on Bear Island for the summer season of 2008.

This network, together with the permanent stations in the wider region, was used to monitor and locate the seismicity around the continental margin and along the mid-ocean ridge, focusing on the sedimentary wedge between them. The contribution in Section 6.4 mainly deals with a description of the seafloor network, its observations, and its integration with the land-based network in order to locate the seismicity in the target area. Some equipment and data loss took place within the experiment, but most of the stations of the deployment contributed seismic and pressure data for approximately 11 months.

A variety of seismic and acoustic signals were recorded during the project; they included seismicity from different epicentral distance ranges and geodynamic environments, hydroacoustic phases, signals from anthropogenic sources (e.g., airgun shots, boat traffic), weather related phenomena, ocean currents, as well as many unclassified signals. In general, the noise level among the OBS/H stations was rather high, imposing restrictions to the analysis of seismic data. The two deepest stations (OBS09 and OBS06) were the ones with the best SNR, and therefore a strong focus was put on the exploitation of their data.

Unfortunately, the network did not achieve the required resolution to allow the determination of focal depth for the events along the mid-ocean ridge and the sedimentary wedge, which was one of the aims of the project. However, and despite all difficulties, the network had a significant contribution to the monitoring and location of the seismic activity in the region. Comparisons of our knowledge of the seismicity only with the use of the permanent, regional network, and with the use of the IPY stations, show not only a quantitative increase in the number of located events, but a clearly enhanced resolution. This is particularly important for such remote, offshore areas, since it allows us, even if it is only for a relatively short time interval, to obtain accurate images of the spatiotemporal distribution of the seismic activity.

Frode Ringdal

AFTAC Project Authorization	:	T/6110
Purchase Request No.	:	F3KTK85290A1
Name of Contractor	:	Stiftelsen NORSAR
Effective Date of Contract	:	1 March 2006
Contract Expiration Date	:	30 September 2011
Amount of Contract	:	$ 1,003,494.00
Project Manager	:	Frode Ringdal +47 63 80 59 00
Title of Work	:	The Norwegian Seismic Array (NORSAR) Phase 3
Period Covered by Report	:	1 January - 30 June 2011

The operational activities of the seismic field systems and the Norwegian National Data Center (NDC) are currently jointly funded by the Norwegian Government and the CTBTO/PTS, with the understanding that the funding of appropriate IMS-related activities will gradually be transferred to the CTBTO/PTS. Other activities were supported and monitored by AFTAC, Patrick AFB, FL32925, under contract no. FA2521-06-C-8003. Other sponsors are acknowledged where appropriate.

Table of Contents

Page

1 Summary

This report describes activities carried out at NORSAR under Contract No. FA2521-06-C-8003 for the period 1 January - 30 June 2011. In addition, it provides summary information on operation and maintenance (O&M) activities at the Norwegian National Data Center (NOR- NDC) during the same period. The O&M activities, including operation of transmission links within Norway and to Vienna, Austria are being funded jointly by the CTBTO/PTS and the Norwegian Government, with the understanding that the funding of O&M activities for primary stations in the International Monitoring System (IMS) will gradually be transferred to the CTBTO/PTS. The O&M statistics presented in this report are included for the purpose of completeness, and in order to maintain consistency with earlier reporting practice. The cost of transmission of selected data from the Norwegian NDC to the United States NDC is covered by the United States Government. Research activities described in this report are mainly funded by the Norwegian Government, with other sponsors acknowledged where appropriate.

The seismic arrays operated by NOR-NDC comprise the Norwegian Seismic Array (NOA), the Arctic Regional Seismic Array (ARCES) and the Spitsbergen Regional Array (SPITS). This report presents statistics for these three arrays as well as for additional seismic stations which through cooperative agreements with institutions in the host countries provide continuous data to NOR-NDC. These additional stations include the Finnish Regional Seismic Array (FINES) and the Hagfors array in Sweden (HFS).

The NOA Detection Processing system has been operated throughout the period with an uptime of 100%. A total of 4,625 seismic events have been reported in the NOA monthly seismic bulletin during the reporting period. On-line detection processing and data recording at the NDC of data from ARCES, FINES, SPITS and HFS data have been conducted throughout the period. Processing statistics for the arrays for the reporting period are given.

A summary of the activities at the NOR-NDC and relating to field installations during the reporting period is provided in Section 4. Norway is now contributing primary station data from two seismic arrays: NOA (PS27) and ARCES (PS28), one auxiliary seismic array SPITS (AS72), and one auxiliary three-component station JMIC (AS73). These data are being provided to the IDC via the global communications infrastructure (GCI). Continuous data from the three arrays are in addition being transmitted to the US NDC. The performance of the data transmission to the US NDC has been satisfactory during the reporting period.

So far among the Norwegian stations, the NOA and the ARCES array (PS27 and PS28 respectively), the radionuclide station at Spitsbergen (RN49) and the auxiliary seismic stations on Spitsbergen (AS72) and Jan Mayen (AS73) have been certified. Provided that adequate funding continues to be made available (from the CTBTO/PTS and the Norwegian Ministry of Foreign Affairs), we envisage continuing the provision of data from these and other Norwegian IMS- designated stations in accordance with current procedures. As part of NORSAR's obsolescence management, a recapitalization plan for PS27 and PS28 was submitted to CTBTO/ PTS in October 2008, in order to prevent severe degradation of the stations due to lack of spare parts. The installation of new equipment started in 2010.

The IMS infrasound station originally planned to be located near Karasjok (IS37) will be established at another site, since the local authorities did not grant the permissions required. Two sites at Bardufoss, both at 69.1^{o} N, 18.6^{o} E, are currently being pursued with landowners and the municipal authorities, with the purpose of selecting one of them for possible installation of IS37. The CTBTO PrepCom has approved a corresponding coordinate change for the station.

Summaries of four scientific and technical contributions presented in Chapter 6 of this report are provided below:

Section 6.1 presents initial results from a project aimed at applying detection probabilities in the IDC global phase association (GA) process. GA is an automated procedure that associates detections by IMS stations in order to form event hypotheses. These hypotheses will later be reviewed by analysts before the Reviewed Event Bulletin (REB) is issued. We have begun investigating ways to improve the GA process for seismic data, in particular by incorporating amplitude data and station detection probabilities in the automatic process. We build on a previous study which has provided regional detection capability estimates for individual primary and auxiliary IMS stations, and use these estimates to develop and test various consistency measures. The purpose of these measures is to provide a means to assess the validity of seismic events automatically defined in the Standard Event Lists (SEL1, SEL2 and SEL3) and assess the consistency of individual phases associated with such events. By feeding the results of such assessments back into the GA procedure, we anticipate that the results of the global association can be iteratively improved.

A candidate SEL event is a group of automatically associated phases from IMS stations that satisfies certain predefined criteria for defining an event. For each such event an estimated origin time, hypocenter, a list of detecting stations and detected phases, phase arrival times and an average event magnitude as well as individual station magnitudes are given. Our basic approach is to make the hypothetical assumption that each such candidate event is real and correctly located. Using the regionalized station detection thresholds, we have the basis for calculating the station detection probability for events at that location as a function of event magnitude. By taking into consideration the actual pattern of detecting and non-detecting stations for the candidate event as listed in the SEL, we can therefore estimate a maximum-likelihood (MLE) magnitude for the hypothetical event. Based on this magnitude estimate, we then calculate, for each station, its probability of detection. By ranking the stations according to their detection probability, we can assess which stations are likely to detect or not detect this hypothetical event. We can then compare these probabilities to the actually observed phase list for the event as given in the SEL, and identify any inconsistencies.

The single most important criterion for accepting a candidate SEL event is clearly the number of detecting stations that have been associated with the event. If this number is above a certain threshold, the event is accepted, perhaps with a suggestion to the analyst that one or more low probability phases be considered for deletion. Our approach therefore focuses on events with few (typically six or fewer) associated detecting stations. In such cases, we need to carry out several tests, and these tests are still under development. One promising approach is to take as starting point the number of *non-detecting* primary stations which have a higher detection probability than the *n'th best detecting* station (*n=1,2,3…).* For example, if the three primary stations with the highest detection probability are in fact associated with the event, then we would very likely accept the event, with a possible explanatory comment to the analyst. Other supplementary approaches are being considered.

Section 6.2 contains an analysis of the Novaya Zemlya seismic event on 11 October 2010. The event, which had a magnitude of 4.3 (IDC_REB), occurred on the north-west coast of Novaya Zemlya, at 22:48:25.6 (IDC_REB). The event was well recorded globally, and phase readings at 44 IMS stations contributed to the REB location. It has previously been observed that there is very efficient propagation of high-frequency signals for ray-paths crossing the Barents Sea.

As a consequence, both the IMS seismic stations on Svalbard (the SPITS array) and in northern Norway (the ARCES array) have been equipped with instruments having sampling rates of 80 Hz and 100Hz, respectively. In addition to an assessment of the reported event locations, we present in this contribution the high-frequency recordings at SPITS and ARCES.

The REB location, 76.2640N; 64.7619E is mainly based on readings at distant stations. Phase picks at stations at regional distances, on Svalbard and in northern Fennoscandia, dominated the input to the initial location reported in NORSAR's regional bulletin. This location, differed significantly, by about 65 km, from the REB. In an attempt to combine phase readings at both regional and teleseismic distances, we relocated the event using a number of re-picked phases. The location was calculated with the HYPOSAT program using a combination of the regional *"barey"* model and the global *"AK135"* model. The recalculated location differed by 22 km from the REB location. We conclude that there is a need to improve the regional location models used for routine data analysis of events, and use of existing three-dimensional regional propagation models in this analysis should be encouraged.

The SPITS and the ARCES arrays are located at distances of 1178 and 1451 km, respectively, For the SPITS recordings, the presence of significant energy up to the Nyquist frequency of 40 Hz confirms the documented efficient high-frequency wave propagation from the Novaya Zemlya region to Svalbard, across the Barents Sea. For the ARCES high-frequency element, the spectra show signal energy up to about 25 Hz for the Pn and Sn phases. As compared to the SPITS spectra and the ARCES spectra of an earlier event in the eastern Barents Sea on 11 November 2009, the ARCES spectra for the 2010 event has comparatively less high frequency energy. We attribute this to a longer propagation path, and to signal attenuation when the seismic waves cross the heterogeneous crustal structures of the Novaya Zemlya island. However, we nevertheless consider this as very efficient propagation of high-frequency energy.

Section 6.3 contains an analysis of an earthquake in Hedmark, Southern Norway, which occurred on 21 July 2011 at 02.59 local time. A very preliminary automatic location of the event clearly located the earthquake within the NORSAR array (NOA), between the communities of Elverum and Rena, about 40 - 50 km north of the 7 April 2004 Flisa earthquake. With the 42 seismic sites of the NORSAR array at epicentral distances between about 10 and 60 km from the event and several additional seismic stations in the region, it was possible to perform a high quality determination of the hypocenter.

Although this event was not very large (reported magnitudes are between 3.3 and 3.8), it had been observed at local, regional, and teleseismic distances. With such a large number of close by seismic stations and observations, the GT level of this event will be of interest. Based on the analysis in this paper, the epicenter can be classified as a GT-1 event, located at 60.9642N, 11.5849E. With several NOA sites at epicentral distances of 10 to 20 km and in different azimuthal directions even the depth of the event, estimated at 22.8 km, is well defined with an uncertainty of less than +/-1 km.

We were also able to estimate the fault plane solution of this earthquake. At all stations used to locate the event and at a smaller number of stations at regional distances, P-onset polarities and some SH and SV polarities could be read. In addition, some amplitude ratios between the P and the S (SV and SH) onsets were measured. All these data were inverted for the best fitting double couple solution. The FOCMEC inversion routine was applied to calculate all possible fault planes which are in agreement with the observed data. The assumption for this type of inversion is that one double couple can describe the source mechanism.The presented double couple

solution shows a reverse fault with a general NNE - SSW strike. From the observed data it is not possible to decide which of the two possible planes is the actual fault plane. The point of intersection between the two possible fault planes is not very well defined due to station distribution and due to the fact that many stations in the south are located beyond the Teisseyre-Tornquist zone, which is known to block seismic wave propagation. However, systematic search for more polarity data may constrain the solution better.

Section 6.4 is entitled "The International Polar Year (IPY) broadband ocean-bottom seismograph deployment: observations, limitations and integration with the IPY land network". Within the framework of the IPY 2007-2008 project "The Dynamic Continental Margin Between the Mid-Atlantic-Ridge System (Mohns Ridge, Knipovich Ridge) and Bear Island", several temporary seismic stations were installed in the wider area of the Western Barents Sea margin. Among them was a three-component, broadband ocean-bottom seismometer and hydrophone (OBS/H) deployment, consisting of 12 stations distributed over the area between the Knipovich Ridge and Bear Island. Regarding land stations, the Norwegian National Seismic Network (NNSN) station HOPEN was upgraded with a broadband seismometer, a new broadband station (HSPB) was installed at Hornsund, and a small-aperture seismic array was installed on Bear Island for the summer season of 2008.

This network, together with the permanent stations in the wider region, was used to monitor and locate the seismicity around the continental margin and along the mid-ocean ridge, focusing on the sedimentary wedge between them. The contribution in Section 6.4 mainly deals with a description of the seafloor network, its observations, and its integration with the land-based network in order to locate the seismicity in the target area. Some equipment and data loss took place within the experiment, but most of the stations of the deployment contributed seismic and pressure data for approximately 11 months.

A variety of seismic and acoustic signals were recorded during the project; they included seismicity from different epicentral distance ranges and geodynamic environments, hydroacoustic phases, signals from anthropogenic sources (e.g., airgun shots, boat traffic), weather related phenomena, ocean currents, as well as many unclassified signals. In general, the noise level among the OBS/H stations was rather high, imposing restrictions to the analysis of seismic data. The two deepest stations (OBS09 and OBS06) were the ones with the best SNR, and therefore a strong focus was put on the exploitation of their data.

Unfortunately, the network did not achieve the required resolution to allow the determination of focal depth for the events along the mid-ocean ridge and the sedimentary wedge, which was one of the aims of the project. However, and despite all difficulties, the network had a significant contribution to the monitoring and location of the seismic activity in the region. Comparisons of our knowledge of the seismicity only with the use of the permanent, regional network, and with the use of the IPY stations, show not only a quantitative increase in the number of located events, but a clearly enhanced resolution. This is particularly important for such remote, offshore areas, since it allows us, even if it is only for a relatively short time interval, to obtain accurate images of the spatiotemporal distribution of the seismic activity.

Frode Ringdal

2 Operation of International Monitoring System (IMS) Stations in Norway

2.1 PS27 — Primary Seismic Station NOA

The mission-capable data statistics were 99.997%, as compared to 100% for the previous reporting period. The net instrument availability was 95.908%.

There were no outages of all subarrays at the same time in the reporting period.

Monthly uptimes for the NORSAR on-line data recording task, taking into account all factors (field installations, transmissions line, data center operation) affecting this task were as follows:

2011		Mission Capable	Net instrument availability
January	:	100%	96.801%
February	:	99.994%	96.808%
March	:	99.997%	96.614%
April	:	100%	96.800%
May	:	100%	95.348%
June	:	99.992%	93.076%

B. Paulsen

NOA Event Detection Operation

In Table 2.1.1 some monthly statistics of the Detection and Event Processor operation are given. The table lists the total number of detections (DPX) triggered by the on-line detector, the total number of detections processed by the automatic event processor (EPX) and the total number of events accepted after analyst review (teleseismic phases, core phases and total).

	Total DPX	Total EPX	Accepted Events		Sum	Daily
			P-phases	Core Phases		
Jan	12,341	1,122	244	65	309	10.0
Feb	11,568	1,015	225	74	299	10.7
Mar	19,196	3,210	2,085	58	2,143	69.1
Apr	9,690	1,589	735	78	813	27.1
May	7,972	1,179	488	80	568	18.3
Jun	5,590	956	416	77	493	16.4
	66,357	9,071	4,193	432	4,625	25,3

Table 2.1.1. *Detection and Event Processor statistics, 1 January - 30 June 2011.*

NOA detections

The number of detections (phases) reported by the NORSAR detector during day 001, 2011, through day 181, 2011, was 66,357, giving an average of 367 detections per processed day (181 days processed).

B. Paulsen
U. Baadshaug

2.2 PS28 — Primary Seismic Station ARCES

The mission-capable data statistics were 99.997%, the same as for the previous reporting period. The net instrument availability was 99.181%.

There were no outages of all subarrays at the same time in the reporting period.

Monthly uptimes for the ARCES on-line data recording task, taking into account all factors (field installations, transmission lines, data center operation) affecting this task were as follows:

2011		Mission Capable	Net instrument availability
January	:	99.999%	99.901%
February	:	99.994%	98.591%
March	:	99.997%	96.614%
April	:	100%	99.988%
May	:	99.997%	99.997%
June	:	99.996%	99.993%

B. Paulsen

Event Detection Operation

ARCES detections

The number of detections (phases) reported during day 001, 2011, through day 181, 2011, was 186,921, giving an average of 1033 detections per processed day (181 days processed).

Events automatically located by ARCES

During days 001, 2011, through 181, 2011, 9,569 local and regional events were located by ARCES, based on automatic association of P- and S-type arrivals. This gives an average of 52.9 events per processed day (181 days processed). 76% of these events are within 300 km, and 92 % of these events are within 1000 km.

U. Baadshaug

2.3 AS72 — Auxiliary Seismic Station Spitsbergen

The mission-capable data for the period were 99.989%, as compared to 98.001% for the previous reporting period. The net instrument availability was 99.964%.

There were no outages of all subarrays at the same time in the reporting period.

Monthly uptimes for the Spitsbergen on-line data recording task, taking into account all factors (field installations, transmissions line, data center operation) affecting this task were as follows:

2011		Mission Capable	Net instrument availability
January	:	99.997%	99.871%
February	:	100%	99.990%
March	:	99.998%	99.995%
April	:	99.943%	99.940%
May	:	99.997%	99.994%
June	:	99.996%	99.994%

B. Paulsen

Event Detection Operation

Spitsbergen array detections

The number of detections (phases) reported from day 001, 2011, through day 181, 2011, was 342,747, giving an average of 1,894 detections per processed day (181 days processed).

Events automatically located by the Spitsbergen array

During days 001, 2011 through 181, 2011, 29,883 local and regional events were located by the Spitsbergen array, based on automatic association of P- and S-type arrivals. This gives an average of 165.1 events per processed day (181 days processed). 78% of these events are within 300 km, and 91% of these events are within 1000 km.

U. Baadshaug

2.4 AS73 — Auxiliary Seismic Station at Jan Mayen

The IMS auxiliary seismic network includes a three-component station on the Norwegian island of Jan Mayen. The station location given in the protocol to the Comprehensive Nuclear-Test-Ban Treaty is 70.9°N, 8.7°W.

The University of Bergen has operated a seismic station at this location since 1970. A so-called Parent Network Station Assessment for AS73 was completed in April 2002. A vault at a new location (71.0^{o}N, 8.5^{o}W) was prepared in early 2003, after its location had been approved by the PrepCom. New equipment was installed in this vault in October 2003, as a cooperative

effort between NORSAR and the CTBTO/PTS. Continuous data from this station are being transmitted to the NDC at Kjeller via a satellite link installed in April 2000. Data are also made available to the University of Bergen.

The station was certified by the CTBTO/PTS on 12 June 2006.

J. Fyen

2.5 IS37 — Infrasound Station at Karasjok

The IMS infrasound network will, according to the protocol of the CTBT, include a station at Karasjok in northern Norway. The coordinates given for this station are 69.5°N, 25.5°E. These coordinates coincide with those of the primary seismic station PS28.

It has, however, proved very difficult to obtain the necessary permits for use of land for an infrasound station in Karasjok. Various alternatives for locating the station in Karasjok were prepared, but all applications to the local authorities to obtain the permissions needed to establish the station were turned down by the local governing council in June 2007.

In 2008, investigations were initiated to identify an alternative site for IS37 outside Karasjok. Two sites at Bardufoss, both at 69.1^{o} N, 18.6^{o} E, are currently being pursued with landowners and the municipal authorities, with the purpose of selecting one of them for possible installation of IS37. The CTBTO PrepCom has approved a corresponding coordinate change for the station.

J. Fyen

2.6 RN49 — Radionuclide Station on Spitsbergen

The IMS radionuclide network includes a station on the island of Spitsbergen. This station has been selected to be among those IMS radionuclide stations that will monitor for the presence of relevant noble gases upon entry into force of the CTBT.

A site survey for this station was carried out in August of 1999 by NORSAR, in cooperation with the Norwegian Radiation Protection Authority. The site survey report to the PTS contained a recommendation to establish this station at Platåberget, near Longyearbyen. The infrastructure for housing the station equipment was established in early 2001, and a noble gas detection system, based on the Swedish “SAUNA” design, was installed at this site in May 2001, as part of PrepCom’s noble gas experiment. A particulate station (“ARAME” design) was installed at the same location in September 2001. A certification visit to the particulate station took place in October 2002, and the particulate station was certified on 10 June 2003. Both systems underwent substantial upgrading in May/June 2006. The equipment at RN49 is being maintained and operated under a contract with the CTBTO/PTS.

S. Mykkeltveit

3 Contributing Regional Seismic Arrays

3.1 NORES

NORES has been out of operation since lightning destroyed the station electronics on 11 June 2002.

B. Paulsen

3.2 Hagfors (IMS Station AS101)

Data from the Hagfors array are made available continuously to NORSAR through a cooperative agreement with Swedish authorities.

The mission-capable data statistics were 99.182%, as compared to 99.999% for the previous reporting period. The net instrument availability was 99.462%.

The main outages in the period are presented in Table 3.3.1.

Day	Period
03 May	21.59-00.00
04 May	00.00-02.52
28 Jun	13.44-13.49
29 Jun	12.43-12.51
29 Jun	12.52-12.59
29 Jun	13.08-14.04
29 Jun	14.06-16.45
29 Jun	16.49-17.28
29 Jun	17.31-17.53
29 Jun	17.56-18.03
29 Jun	18.09-18.31
29 Jun	18.36-18.44
29 Jun	18.50-18-57
29 Jun	19.00-19.02
29 Jun	19.08-19.13
29 Jun	19.17-19.19
29 Jun	19.52-19.55
30 Jun	11.37-11.44
30 Jun	11.52-12.09
30 Jun	12.15-14.55
30 Jun	15.06-15.14

Table 3.2.1. *The main interruptions in recording of Hagfors data at NDPC, 1 January - 30 June 2011.*

Monthly uptimes for the Hagfors on-line data recording task, taking into account all factors (field installations, transmissions line, data center operation) affecting this task were as follows:

2011		Mission Capable	Net instrument availability
January	:	100%	100%
February	:	100%	100%
March	:	100%	100%
April	:	100%	100%
May	:	96.384%	98.048%
June	:	98.710%	98.722%

B. Paulsen

Hagfors Event Detection Operation

Hagfors array detections

The number of detections (phases) reported from day 001, 2011, through day 181, 2011, was 114,733, giving an average of 637 detections per processed day (180 days processed).

Events automatically located by the Hagfors array

During days 001, 2011, through 181, 2011, 3,421 local and regional events were located by the Hagfors array, based on automatic association of P- and S-type arrivals. This gives an average of 19.0 events per processed day (180 days processed). 74% of these events are within 300 km, and 92% of these events are within 1000 km.

U. Baadshaug

3.3 FINES (IMS station PS17)

Data from the FINES array are made available continuously to NORSAR through a cooperative agreement with Finnish authorities.

The mission-capable data statistics were 99.454%, as compared to 94.662% for the previous reporting period. The net instrument availability was 99.692%.

The main outages in the period are presented in Table 3.3.1.

Day	Period
27 Jan	03.17-10.15
12 Jun	13.49-00.00
13 Jun	00.00-06.25

Table 3.3.1. *The main interruptions in recording of FINES data at NDPC, 1 January - 30 June 2011.*

Monthly uptimes for the FINES on-line data recording task, taking into account all factors (field installations, transmissions line, data center operation) affecting this task were as follows:

2011		Mission Capable	Net instrument availability
January	:	99.037%	99.037%
February	:	99.995%	99.995%
March	:	100%	100%
April	:	100%	100%
May	:	100%	100%
June	:	97.692%	99.120%

B. Paulsen

FINES Event Detection Operation

FINES detections

The number of detections (phases) reported during day 001, 2011, through day 181, 2011, was 42,841, giving an average of 237 detections per processed day (181 days processed).

Events automatically located by FINES

During days 001, 2011, through 181, 2011, 2,261 local and regional events were located by FINES, based on automatic association of P- and S-type arrivals. This gives an average of 12.5 events per processed day (181 days processed). 89% of these events are within 300 km, and 95% of these events are within 1000 km.

U. Baadshaug

3.4 Regional Monitoring System Operation and Analysis

The Regional Monitoring System (RMS) was installed at NORSAR in December 1989 and has been operated at NORSAR from 1 January 1990 for automatic processing of data from ARCES and NORES. A second version of RMS that accepts data from an arbitrary number of arrays and single 3-component stations was installed at NORSAR in October 1991, and regular operation of the system comprising analysis of data from the 4 arrays ARCES, NORES, FINES and GERES started on 15 October 1991. As opposed to the first version of RMS, the one in current operation also has the capability of locating events at teleseismic distances.

Data from the Apatity array was included on 14 December 1992, and from the Spitsbergen array on 12 January 1994. Detections from the Hagfors array were available to the analysts and could be added manually during analysis from 6 December 1994. After 2 February 1995, Hagfors detections were also used in the automatic phase association.

Since 24 April 1999, RMS has processed data from all the seven regional arrays ARCES, NORES, FINES, GERES (until January 2000), Apatity, Spitsbergen, and Hagfors. Starting 19 September 1999, waveforms and detections from the NORSAR array have also been available to the analyst.

Phase and event statistics

Table 3.5.1 gives a summary of phase detections and events declared by RMS. From top to bottom the table gives the total number of detections by the RMS, the number of detections that are associated with events automatically declared by the RMS, the number of detections that are not associated with any events, the number of events automatically declared by the RMS, and finally the total number of events worked on interactively (in accordance with criteria that vary over time; see below) and defined by the analyst.

New criteria for interactive event analysis were introduced from 1 January 1994. Since that date, only regional events in areas of special interest (e.g, Spitsbergen, since it is necessary to acquire new knowledge in this region) or other significant events (e.g, felt earthquakes and large industrial explosions) were thoroughly analyzed. Teleseismic events of special interest are also analyzed.

To further reduce the workload on the analysts and to focus on regional events in preparation for Gamma-data submission during GSETT-3, a new processing scheme was introduced on 2 February 1995. The GBF (Generalized Beamforming) program is used as a pre-processor to RMS, and only phases associated with selected events in northern Europe are considered in the automatic RMS phase association. All detections, however, are still available to the analysts and can be added manually during analysis.

	Jan 11	Feb 11	Mar 11	Apr 11	May 11	Jun 11	Total
Phase detections	160,379	122,100	153,146	127,385	145,738	122,652	831,400
- Associated phases	6,726	5,008	6,867	5,315	5,797	5,012	34,725
- Unassociated phases	153,653	117,092	146,279	122,070	139,941	117,640	796,675
Events automatically declared by RMS	1153	883	1,234	966	1,077	991	6,304
No. of events defined by the analyst	94	53	88	57	65	53	410

Table 3.5.1. RMS phase detections and event summary 1 January - 30 June 2011.

U. Baadshaug
B. Paulsen

4 NDC and Field Activities

4.1 NDC Activitities

NORSAR functions as the Norwegian National Data Center (NDC) for CTBT verification. Six monitoring stations, comprising altogether 132 field sensors plus radionuclide monitoring equipment, will be located on Norwegian territory as part of the future IMS as described elsewhere in this report. The four seismic IMS stations are all in operation today, and all of them are currently providing data to the CTBTO on a regular basis. PS27, PS28, AS72, AS73 and RN49 are all certified. Data recorded by the Norwegian stations is being transmitted in real time to the Norwegian NDC, and provided to the IDC through the Global Communications Infrastructure (GCI). Norway is connected to the GCI with a frame relay link to Vienna.

Operating the Norwegian IMS stations continues to require significant efforts by personnel both at the NDC and in the field. Strictly defined procedures as well as increased emphasis on regularity of data recording and timely data transmission to the IDC in Vienna have led to increased reporting activities and implementation of new procedures for the NDC. The NDC carries out all the technical tasks required in support of Norway's treaty obligations. NORSAR will also carry out assessments of events of special interest, and advise the Norwegian authorities in technical matters relating to treaty compliance. A challenge for the NDC is to carry 40 years' experience over to the next generation of personnel.

Verification functions; information received from the IDC

After the CTBT enters into force, the IDC will provide data for a large number of events each day, but will not assess whether any of them are likely to be nuclear explosions. Such assessments will be the task of the States Parties, and it is important to develop the necessary national expertise in the participating countries. An important task for the Norwegian NDC will thus be to make independent assessments of events of particular interest to Norway, and to communicate the results of these analyses to the Norwegian Ministry of Foreign Affairs.

Monitoring the Arctic region

Norway will have monitoring stations of key importance for covering the Arctic, including Novaya Zemlya, and Norwegian experts have a unique competence in assessing events in this region. On several occasions in the past, seismic events near Novaya Zemlya have caused political concern, and NORSAR specialists have contributed to clarifying these issues.

International cooperation

After entry into force of the treaty, a number of countries are expected to establish national expertise to contribute to the treaty verification on a global basis. Norwegian experts have been in contact with experts from several countries with the aim of establishing bilateral or multilateral cooperation in this field. One interesting possibility for the future is to establish NORSAR as a regional center for European cooperation in the CTBT verification activities.

NORSAR event processing

The automatic routine processing of NORSAR events as described in NORSAR Sci. Rep. No. 2-93/94, has been running satisfactorily. The analyst tools for reviewing and updating the solu-

tions have been continually modified to simplify operations and improve results. NORSAR is currently applying teleseismic detection and event processing using the large-aperture NOA array as well as regional monitoring using the network of small-aperture arrays in Fennoscandia and adjacent areas.

Communication topology

Norway has implemented an independent subnetwork, which connects the IMS stations AS72, AS73, PS28, and RN49 operated by NORSAR to the GCI at NOR_NDC. A contract has been concluded and VSAT antennas have been installed at each station in the network. Under the same contract, VSAT antennas for 6 of the PS27 subarrays have been installed for intra-array communication. The seventh subarray is connected to the central recording facility via a leased land line. The central recording facility for PS27 is connected directly to the GCI (Basic Topology). All the VSAT communication is functioning satisfactorily. As of 10 June 2005, AS72 and RN49 are connected to NOR_NDC through a VPN link.

Jan Fyen

4.2 Status Report: Provision of data from Norwegian seismic IMS stations to the IDC

Introduction

This contribution is a report for the period January - June 2011 on activities associated with provision of data from Norwegian seismic IMS stations to the International Data Centre (IDC) in Vienna. This report represents an update of contributions that can be found in previous editions of NORSAR's Semiannual Technical Summary. All four Norwegian seismic stations providing data to the IDC have now been formally certified.

Norwegian IMS stations and communications arrangements

During the reporting interval, Norway has provided data to the IDC from the four seismic stations shown in Fig. 4.2.1. PS27 —NOA is a 60 km aperture teleseismic array, comprised of 7 subarrays, each containing six vertical short period sensors and a three-component broadband instrument. PS28 — ARCES is a 25-element regional array with an aperture of 3 km, whereas AS72 — Spitsbergen array (station code SPITS) has 9 elements within a 1-km aperture. AS73 — JMIC has a single three-component broadband instrument.

The intra-array communication for NOA utilizes a land line for subarray NC6 and VSAT links based on TDMA technology for the other 6 subarrays. The central recording facility for NOA is located at the Norwegian National Data Center (NOR_NDC).

Continuous ARCES data are transmitted from the ARCES site to NOR_NDC using a 64 kbits/s VSAT satellite link, based on BOD technology.

Continuous SPITS data were transmitted to NOR_NDC via a VSAT terminal located at Platåberget in Longyearbyen (which is the site of the IMS radionuclide monitoring station RN49 installed during 2001) up to 10 June 2005. The central recording facility (CRF) for the SPITS array has been moved to the University of Spitsbergen (UNIS). A 512 bps SHDSL link has been established between UNIS and NOR_NDC. Data from the array elements to the CRF are

transmitted via a 2.4 Ghz radio link (Wilan VIP-110). Both AS72 and RN49 data are now transmitted to NOR_NDC over this link using VPN technology.

A minimum of seven-day station buffers have been established at the ARCES and SPITS sites and at all NOA subarray sites, as well as at the NOR_NDC for ARCES, SPITS and NOA. In addition, each individual site of the SPITS array has a 14-day buffer.

The NOA and ARCES arrays are primary stations in the IMS network, which implies that data from these stations is transmitted continuously to the receiving international data center. Since October 1999, this data has been transmitted (from NOR_NDC) via the Global Communications Infrastructure (GCI) to the IDC in Vienna. Data from the auxiliary array station SPITS — AS72 have been sent in continuous mode to the IDC during the reporting period. AS73 — JMIC is an auxiliary station in the IMS, and the JMIC data have been available to the IDC throughout the reporting period on a request basis via use of the AutoDRM protocol (Kradolfer, 1993; Kradolfer, 1996). In addition, continuous data from all three arrays is transmitted to the US_NDC.

Uptimes and data availability

Figs. 4.2.2 and 4.2.3 show the monthly uptimes for the Norwegian IMS primary stations ARCES and NOA, respectively, for the reporting period given as the hatched (taller) bars in these figures. These barplots reflect the percentage of the waveform data that is available in the NOR_NDC data archives for these two arrays. The downtimes inferred from these figures thus represent the cumulative effect of field equipment outages, station site to NOR_NDC communication outage, and NOR_NDC data acquisition outages.

Figs. 4.2.2 and 4.2.3 also give the data availability for these two stations as reported by the IDC in the IDC Station Status reports. The main reason for the discrepancies between the NOR_NDC and IDC data availabilities as observed from these figures is the difference in the ways the two data centers report data availability for arrays: Whereas NOR_NDC reports an array station to be up and available if at least one channel produces useful data, the IDC uses weights where the reported availability (capability) is based on the number of actually operating channels.

Use of the AutoDRM protocol

NOR_NDC's AutoDRM has been operational since November 1995 (Mykkeltveit & Baadshaug, 1996). The monthly number of requests by the IDC for JMIC data for the period January - June 2011 is shown in Fig. 4.2.4.

NDC automatic processing and data analysis

These tasks have proceeded in accordance with the descriptions given in Mykkeltveit and Baadshaug (1996). For the reporting period NOR_NDC derived information on 410 supplementary events in northern Europe and submitted this information to the Finnish NDC as the NOR_NDC contribution to the joint Nordic Supplementary (Gamma) Bulletin, which in turn is forwarded to the IDC. These events are plotted in Fig. 4.2.5.

Data access for the station NIL at Nilore, Pakistan

NOR_NDC has for many years provided access to the seismic station NIL at Nilore, Pakistan, through a VSAT satellite link between NOR_NDC and Nilore. In late July 2009, the VSAT ground station equipment at Nilore failed, and it turned out that this equipment is obsolete and cannot be repaired. The service provider has proposed the installation of new equipment. Following some technical clarifications, NORSAR submitted a proposal to AFTAC on 9 February 2011for a new satellite communications system between NOR_NDC and Nilore. NORSAR and AFTAC have later agreed to put this proposal on hold until the seismic station at Nilore has been reestablished.

Current developments and future plans

NOR_NDC is continuing the efforts towards improving and hardening all critical data acquisition and data forwarding hardware and software components, so as to meet the requirements related to operation of IMS stations.

The NOA array was formally certified by the PTS on 28 July 2000, and a contract with the PTS in Vienna currently provides partial funding for operation and maintenance of this station. The ARCES array was formally certified by the PTS on 8 November 2001, and a contract with the PTS is in place which also provides for partial funding of the operation and maintenance of this station. The operation of the two IMS auxiliary seismic stations on Norwegian territory (Spitsbergen and Jan Mayen) is funded by the Norwegian Ministry of Foreign Affairs. Provided that adequate funding continues to be made available (from the PTS and the Norwegian Ministry of Foreign Affairs), we envisage continuing the provision of data from all Norwegian seismic IMS stations without interruption to the IDC in Vienna.

The two stations PS27 and PS28 are both suffering from lack of spare parts. The PS27 NOA equipment was acquired in 1995 and it is now impossible to get spare GPS receivers. The PS28 ARCES equipment was acquired in 1999, and it is no longer possible to get spare digitizers. A recapitilization plan for both arrays was submitted to the PTS in October 2008, and installation of new equipment started in 2010.

U. Baadshaug
S. Mykkeltveit
J. Fyen

References

Kradolfer, U. (1993): Automating the exchange of earthquake information. *EOS, Trans., AGU*, 74, 442.

Kradolfer, U. (1996): AutoDRM — The first five years, *Seism. Res. Lett.*, 67, 4, 30-33.

Mykkeltveit, S. & U. Baadshaug (1996): Norway's NDC: Experience from the first eighteen months of the full-scale phase of GSETT-3. *Semiann. Tech. Summ., 1 October 1995 - 31 March 1996*, NORSAR Sci. Rep. No. 2-95/96, Kjeller, Norway.

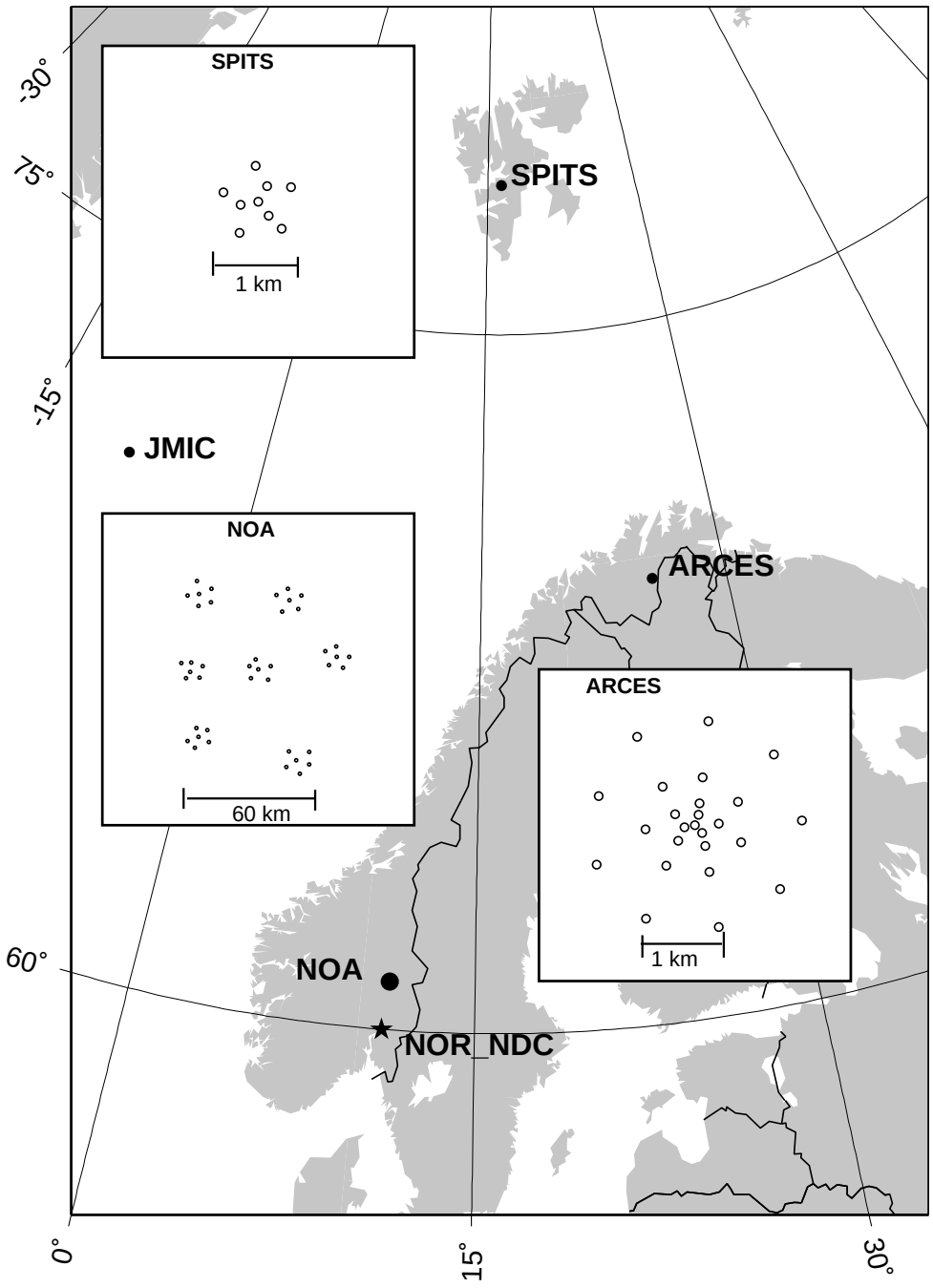

Fig. 4.2.1. The figure shows the locations and configurations of the three Norwegian seismic IMS array stations that provided data to the IDC during the period January - June 2011 The data from these stations and the JMIC three-component station are transmitted continuously and in real time to the Norwegian NDC (NOR_NDC). The stations NOA and ARCES are primary IMS stations, whereas SPITS and JMIC are auxiliary IMS stations.

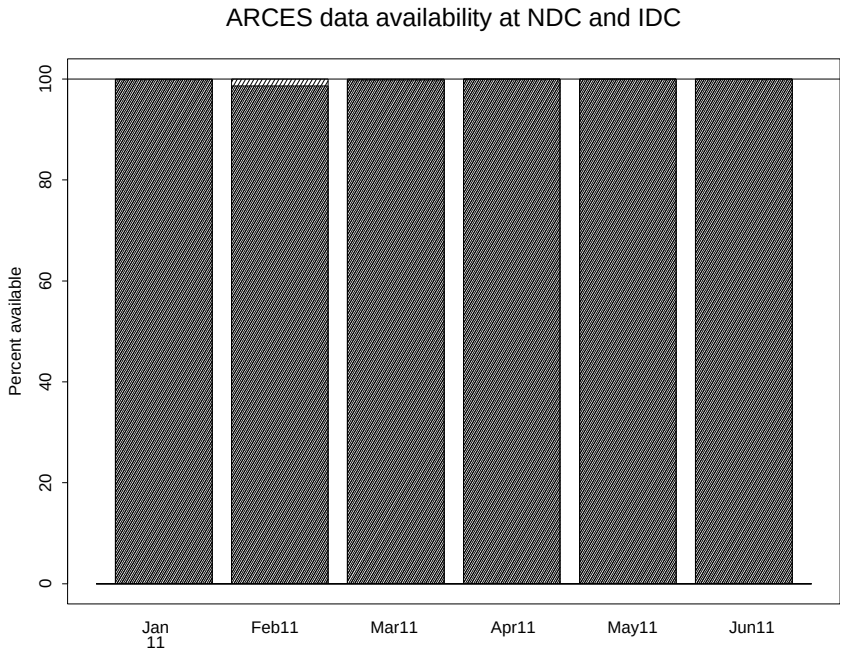

Fig. 4.2.2. The figure shows the monthly availability of ARCES array data for the period January - June 2011at NOR_NDC and the IDC. See the text for explanation of differences in definition of the term "data availability" between the two centers. The higher values (hatched bars) represent the NOR_NDC data availability.

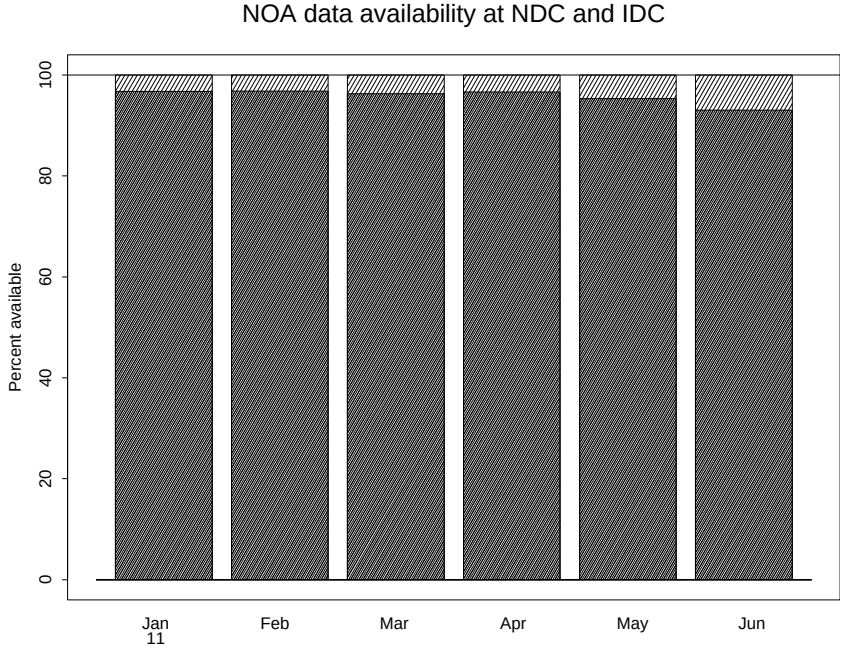

Fig. 4.2.3. The figure shows the monthly availability of NORSAR array data for the period January - June 2011 at NOR_NDC and the IDC. See the text for explanation of differences in definition of the term "data availability" between the two centers. The higher values (hatched bars) represent the NOR_NDC data availability.

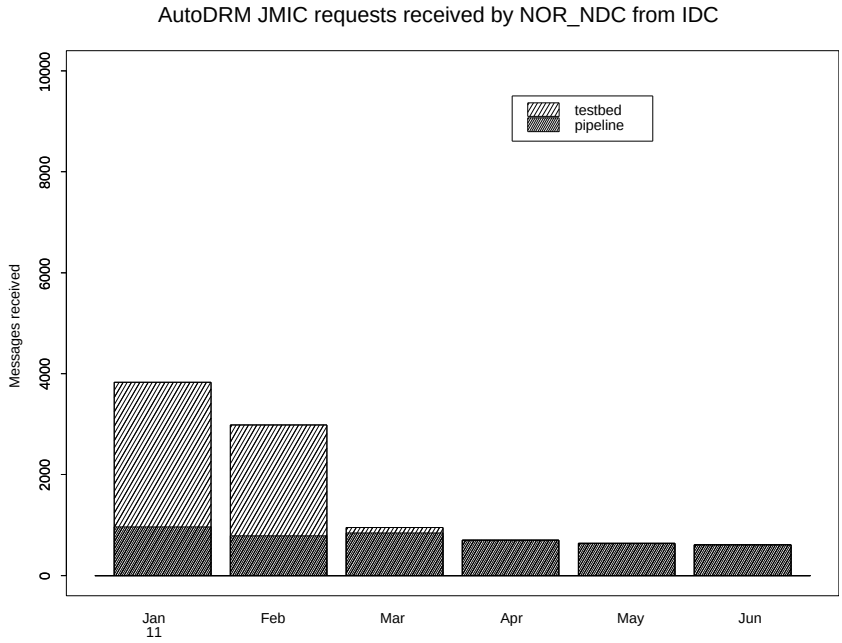

Fig. 4.2.4. The figure shows the monthly number of requests received by NOR_NDC from the IDC for JMIC waveform segments during January - June 2011.

Fig. 4.2.5. The map shows the 410 events in and around Norway contributed by NOR_NDC during January - June 2011 as supplementary (Gamma) events to the IDC, as part of the Nordic supplementary data compiled by the Finnish NDC. The map also shows the main seismic stations used in the data analysis to define these events.

4.3 Field Activities

The activities at the NORSAR Maintenance Center (NMC) at Hamar currently include work related to operation and maintenance of the following IMS seismic stations: the NOA teleseismic array (PS27), the ARCES array (PS28) and the Spitsbergen array (AS72). Some work has also been carried out in connection with the seismic station on Jan Mayen (AS73), the radionuclide station at Spitsbergen (RN49), and preparations for the infrasound station at IS37. NORSAR also acts as a consultant for the operation and maintenance of the Hagfors array in Sweden (AS101).

NORSAR carries out the field activities relating to IMS stations in a manner generally consistent with the requirements specified in the appropriate IMS Operational Manuals, which are currently being developed by Working Group B of the Preparatory Commission. For seismic stations these specifications are contained in the Operational Manual for Seismological Monitoring and the International Exchange of Seismological Data (CTBT/WGB/TL-11/2), currently available in a draft version.

All regular maintenance on the NORSAR field systems is conducted on a one-shift-per-day, five-day-per-week basis. The maintenance tasks include:

- Operating and maintaining the seismic sensors and the associated digitizers, authentication devices and other electronics components.
- Maintaining the power supply to the field sites as well as backup power supplies.
- Operating and maintaining the VSATs, the data acquisition systems and the intra-array data transmission systems.
- Assisting the NDC in evaluating the data quality and making the necessary changes in gain settings, frequency response and other operating characteristics as required.
- Carrying out preventive, routine and emergency maintenance to ensure that all field systems operate properly.
- Maintaining a computerized record of the utilization, status, and maintenance history of all site equipment.
- Providing appropriate security measures to protect against incidents such as intrusion, theft and vandalism at the field installations.

Details of the daily maintenance activities are kept locally. As part of its contract with CTBTO/PTS NORSAR submits, when applicable, problem reports, outage notification reports and equipment status reports. The contents of these reports and the circumstances under which they will be submitted are specified in the draft Operational Manual.

P.W. Larsen
K.A. Løken

5 Documentation Developed

Borleanu, F., M. Popa, M. Radulian & J. Schweitzer (2011): Slowness and azimuth determination for Bucovina array (BURAR) applying multiple signal techniques. J. of Seismolgoy., 15/3, 431-442, doi: 10.1007/s10950-011-9228-9.

Czuba, W., M. Grad, R. Mjelde, A. Guterch, A. Libak, F. Krüger, Y. Murai, J. Schweitzer & the IPY Project Group (2011): Continent-ocean-transition across a trans-tensional margin segment: Off Bear Island, Barents Sea. Geophys. J. Inter., 184/2, 541-554. doi: 10.1111/j.1365-246X.2010.04873.x.

Evers, L.G. & J. Schweitzer (2011): A climatology of infrasound detections in northern Norway at the experimental ARCI array. J. of Seismology, 15/3, 473-486. doi: 10.1007/s10950-011-9237-8.

Hauser, J., K.M. Dyer, M.E. Pasyanos, H. Bungum, J.E. Faleide, S.A. Clark & J. Schweitzer (2011): A probabilistic seismic model for the European Arctic. J. of Geophys. Res., 116, B01303, 17pp. doi: 10.1029/2010JB007889.

Kværna, T. & S. Gibbons (2011): The Novaya Zemlya event on 11 October 2011. In: Semiannual Technical Summary, 1 January - 30 June 2011, NORSAR, Kjeller, Norway.

Kværna, T., F. Ringdal & J. Given (2011): Application of detection probabilities in the IDC global phase association process. In: Semiannual Technical Summary, 1 January - 30 June 2011, NORSAR, Kjeller, Norway.

Pirli, M., S.J. Gibbons & J. Schweitzer (2011): Application of array-based waveform cross-correlation techniques to aftershock sequences: The 2003 Lefkada Island, Greece, case. J. of Seismology, 15/3, 533-544. doi: 10.1007/s10950-010-9216-5.

Pirli, M., J. Schweitzer & The IPY Project Consortium (2011): The International Polar Year (IPY) broadband ocean-bottom seismograph deployment: observations, limitations and integration with the IPY land network. In: Semiannual Technical Summary, 1 January - 30 June 2011, NORSAR, Kjeller, Norway.

Schweitzer, J. (2011): The 21 July 2011 earthquake in Hedmark, Southern Norway. In: Semiannual Technical Summary, 1 January - 30 June 2011, NORSAR, Kjeller, Norway.

Schweitzer, J. (2011). Den dynamiske kontinental marginen mellom den midtartlantiske ryggen og Bjørnøya. Orheim, O. & K. Ulstein (red.) (2011): Det norske bidraget (Polaråret 2007-2009), 168-172, Norges forskningsråd, Oslo, 192 pp. ISBN: 978-82-12-02902-6.

Schweitzer, J. (2011): The dynamic continental margine between the Mid-Atlantic Ridge and Bjørnøya (Bear Island). In: Orheim, O. & K. Ulstein (Ed.): The Norwegian Contribution (International Polar Year 2007-2008), The Research Council of Norway, 192 pp. ISBN: 978-82-12-02901-9 (PDF version: ISBN 978-82-12-02934-7), 168-172.

Schweitzer, J. (2011): NORSAR's Data Center Network Report. FDSN Meeting, IASPEI, June/July 2011, Melbourne, Australia.

Schweitzer, J. & F. Krüger (2011): Foreword (special issue "Array Seismology in Europe: Recent developments and Applications") J. of Seismology, 15/3, 429-430. doi: 10.1007/s10950-011-9241-z.

Storchak, D.A., J. Schweitzer & P. Bormann (2011): Seismic phase names: IASPEI standard. In: Gupta, H.K. (ed.): Encyclopedia of Solid Earth Geophysics (Encyclopedia of Earth Sciences series), ISBN: 978-1-4020-8702-0, Springer, Dordrecht, xxxvii + 1539 pp. 1162-1173 (also available under Electronic publication ISBN 978-90-481-8702-7 and print and electronic bundle ISBN 978-90-481-8732-4). doi: 10.1007/978-90-481-8702-7_11.

6 Summary of Technical Reports / Papers Published

6.1 Application of detection probabilities in the IDC global phase association process

Sponsored by the Comprehensive Nuclear-Test-Ban Treaty Organization

ABSTRACT

The Global Association (GA) process at the International Data Centre (IDC) is an automated procedure that associates detections by stations in the International Monitoring System (IMS) in order to form event hypotheses. These hypotheses will later be reviewed by analysts before the Reviewed Event Bulletin (REB) is issued. We have begun investigating ways to improve the GA process for seismic data, in particular by incorporating amplitude data and station detection probabilities in the automatic process. We build on a previous study which has provided regional detection capability estimates for individual primary and auxiliary IMS stations, and use these estimates to develop and test various consistency measures. The purpose of these measures is to provide a means to assess the validity of seismic events automatically defined in the Standard Event Lists (SEL1, SEL2 and SEL3) and assess the consistency of individual phases associated with such events. By feeding the results of such assessments back into the GA procedure, we anticipate that the results of the global association can be iteratively improved.

A candidate SEL event is a group of automatically associated phases from IMS stations that satisfies certain predefined criteria for defining an event. For each such event an estimated origin time, hypocenter, a list of detecting stations and detected phases, phase arrival times and an average event magnitude as well as individual station magnitudes are given. Our basic approach is to make the hypothetical assumption that each such candidate event is real and correctly located. Using the regionalized station detection thresholds, we have the basis for calculating the station detection probability for events at that location as a function of event magnitude. By taking into consideration the actual pattern of detecting and non-detecting stations for the candidate event as listed in the SEL, we can therefore estimate a maximum-likelihood (MLE) magnitude for the hypothetical event. Based on this magnitude estimate, we then calculate, for each station, its probability of detection. By ranking the stations according to their detection probability, we can assess which stations are likely to detect or not detect this hypothetical event. We can then compare these probabilities to the actually observed phase list for the event as given in the SEL, and identify any inconsistencies

The single most important criterion for accepting a candidate SEL event is clearly the number of detecting stations that have been associated with the event. If this number is above a certain threshold, the event is accepted, perhaps with a suggestion to the analyst that one or more low probability phases be considered for deletion. Our approach therefore focuses on events with few (typically six or fewer) associated detecting stations. In such cases, we need to carry out several tests, and these tests are still under development. One promising approach is to take as starting point the number of *non-detecting* primary stations which have a higher detection probability than the *n'th best detecting* station (*n=1,2,3…).* For example, if the three primary

stations with the highest detection probability are in fact associated with the event, then we would very likely accept the event, with a possible explanatory comment to the analyst. Other supplementary approaches are being considered.

An important consideration is to be able to identify whether or not a non-detecting station has actually been in operation at the expected time of detection. We accomplish this by making use of the continuous threshold monitoring (TM) system which is in operation at the IDC. The TM system calculates a threshold for each primary station at any point in time where data from that station is available, and therefore provides a reliable indication of the station's operational status. This paper presents some case studies illustrating various aspects of our approach.

OBJECTIVE

The objective of this project is to investigate various approaches to assessing the validity of seismic events defined through automatic phase association at the IDC. This includes the following:

- Develop and test various consistency measures for individual phases associated with a seismic event, using in particular the dynamic phase information (i.e., amplitudes or magnitudes).
- Define 'consistency indices' for each associated phase, and determine empirically a threshold for these indices in order to accept or reject a phase in the event definition.
- In this process, make use of the detection parameters of each station associated with the event as well as the information from non-detecting stations (i.e., stations not listed as associated with the event).

Our approach focuses on how to check individual phases of associated events after GA has been performed and magnitudes have been calculated (e.g., after SEL3). However, in principle such checks could be applied at any point in the phase association procedure, with feedback to GA for reprocessing as appropriate.

The study presented here is a first attempt to develop and test various consistency measures. They can be used individually or in combination. One important application is to provide the analyst with a summary of the consistency measurements for each individual event candidate. This would help in determining the most likely phases to delete or add in a possible revised solution.

RESEARCH ACCOMPLISHED

Estimating regionalized detection thresholds

The database for this study comprises automatic and reviewed event lists produced by the IDC from 1999 to present. The automatic event lists comprise SEL1, SEL2 and SEL3. The reviewed event lists comprise the REB and the late event bulletin (LEB). The LEB contains the REB events plus reviewed events that are real, but do not fulfil the formal event definition criteria. The work described in the following is an extension of the work by Kværna et al. (2009).

The event lists referenced above are based mainly on data from the primary and auxiliary seismic stations. However, observations from hydroacoustic and infrasonic stations are associated

with some of the events. Although these two technologies are important components of the monitoring systems, the present project does not cover the analysis of hydroacoustic and infra-sound data.

In order to obtain regionalized detection thresholds, we divide the events into a binned global grid system and investigate various ways to estimate the station detection threshold for each IMS station within each geographical bin. Clearly, there is a tradeoff between the grid density and the accuracy with which we can estimate the thresholds. In many bins, there will be few or none events, and in such cases a generic (average) threshold will be applied. It is important to make use of all available information, and for this reason, we have investigated three different estimation algorithms applied to each specific target area.

In the following discussion, we will illustrate the procedure for estimating station detection thresholds by presenting a specific example of a station/source region combination. As shown in Figure 6.1.1, we consider one station (ARCES) and a specific source area, in this example in China (the region within 1.5 degrees of 32^{o}N, 104^{o}E). Our purpose is to estimate the station detection threshold for events from this limited source area. From the REB, we obtain a large number of events, some detected by ARCES, some not detected by this station. Each event has reference network body-wave magnitudes, both conventional so-called generalized $m_b$values (Murphy and Barker, 2003) which we denote mb1, and MLE estimates. We have used the MLE magnitudes (mb1MLE) reported in the REB for reference event body-wave magnitude in this study.

Method 1

A commonly used method for threshold estimation is the approach described by Ringdal (1975). We will denote this approach *Method 1.* In this approach, the number of detections and non-detections in each magnitude bin is counted, and a cumulative Gaussian distribution curve is then fitted to the ensemble of observed detection percentages by maximum likelihood. The detection threshold m_t is considered to be a normally distributed random variable.

The probability *P(m)* of detecting an event of magnitude m at an individual station can be written as:

$$P(m) = \Phi\left(\frac{m-\mu}{\sigma}\right) \qquad (1)$$

Here Φ is the cumulative distribution function of the standard normal distribution. The parameters μ is the 50% incremental detection threshold and σ is the standard deviation of the detection curve.

Denoting by D the ensemble of REB events of magnitudes m_i in this region detected by ARCES, we have the following likelihood function (Ringdal, 1975):

$$L(\mu, \sigma) = \prod_{i \in D} \Phi\left(\frac{m_i-\mu}{\sigma}\right) \prod_{i \notin D} \left(1 - \Phi\left(\frac{m_i-\mu}{\sigma}\right)\right) \qquad (2)$$

Here, the m_i are the network magnitudes of the events in the data set. The symbol μ is the ARCES 50% detection threshold for this region which will be estimated together with σ as the value which maximizes the likelihood function (2). We choose to restrict σ to be within the

range 0.10 - 0.60, since the estimation of this parameter can become unstable when the number of reference events is small. Figure 6.1.2 (top two panels) shows an example of application of *Method 1*.

Fig. 6.1.1 The source region selected for the case study presented here is centered on 32°N 104°E in China, having a radius of 1.5°, as shown by the open circle. The red curve shows the great circle path to the ARCES array in northern Norway, located at a distance of 56.4° from the center of the source region.

Method 1 does not make use of some of the additional information provided by the IDC. This information includes the signal-to-noise (SNR) values for the detected phases, as well as noise levels for the non-detections (in certain cases). We now wish to use this additional information in order to estimate regional detection thresholds.

Method 2

We denote by *Method 2* the following approach, again using the ARCES case study as an illustration: For each REB event in this source area detected by ARCES, we scale down the network magnitude values by the log(SNR), to arrive at an instantaneous "noise magnitude". We then add 0.5 m_b units (corresponding to SNR=3) to obtain an estimate of the instantaneous ARCES detection threshold. By carrying out the procedure described above for all the detected events, we obtain a set of instantaneous thresholds, as shown as a function of SNR in Figure 6.1.2 (third panel from the top). We can calculate the mean and standard deviation of these values to obtain an estimate of the regional 50% threshold.

The instantaneous ARCES detection threshold a_i for the *i'th* detected event is thus:

$$a_i = m_i - \log(SNR_i) + 0{,}5 \qquad (3)$$

If the number of detected events is *ND*, the estimate by *Method 2* then becomes:

$$\mu = \frac{1}{ND}\left(\sum_{i \in D} a_i \right) \tag{4}$$

A problem with this approach is that the instantaneous thresholds a_i estimated in this way turn out to be magnitude dependent. This is because of the influence of non-detections at low magnitudes. As can be seen from Figure 6.1.2 (top panel), the percentage of non-detections increases dramatically below magnitude 4.0. As a consequence, only those events with particularly favorable path focusing effects or unusually low noise levels at the time of the event would be detected, and thus estimating the thresholds solely on the basis of these events as done in *Method 2* would cause a systematic bias.

Method 3

The problems mentioned for *Method 2* lead us to *Method 3*, which we summarize as follows. For each undetected event we have the additional information that the instantaneous ARCES detection threshold must be higher than the corresponding magnitude value m_i of the reference network . We are thus faced with a classical maximum likelihood estimation framework (Ringdal, 1976). Specifically, we have a number of point estimates of the instantaneous ARCES detection threshold (for those events detected by ARCES), and a number of lower bounds (corresponding to the ARCES non-detections).

Thus, for $i \in D$ we have that

$$a_i < m_t < a_i + da_i \tag{5}$$

$$P(a_i < m_t < a_i + da_i) = \frac{1}{\sigma}\phi\left(\frac{a_i - \mu}{\sigma}\right) da_i \tag{6}$$

Here, ϕ is the density function of the standard normal distribution and *P* denotes probability.Correspondingly, for $i \notin D$ we have that

$$m_t > m_i \tag{7}$$

$$P(m_t > m_i) = 1 - \Phi\left(\frac{m_i - \mu}{\sigma}\right) \tag{8}$$

We can then easily derive the likelihood function for *Method 3,* which becomes:

$$L(\mu, \sigma) = \prod_{i \in D} \frac{1}{\sigma}\phi\left(\frac{a_i - \mu}{\sigma}\right) \prod_{i \notin D} \left(1 - \Phi\left(\frac{m_i - \mu}{\sigma}\right)\right) \tag{9}$$

The symbol μ is the ARCES detection threshold which will be estimated together with σ as the value which maximizes the likelihood function (9). As with *Method 1*, we choose to restrict σ to be in the interval 0.10-0.60.

We note in passing that the likelihood function (9) is similar to the one developed by Ringdal (1976), with the important difference that the non-detections here provide *lower bounds* rather than the *upper bounds* presented in that paper. Following the procedure described in that paper, we can derive an approximation of the standard deviation associated with the estimate of μ in (9). Assuming that σ is known, the variance Var (μ), (i.e. the square of the standard deviation) becomes:

$$Var(\mu) = \sigma^2 \left[\sum_i \left(-y_i \phi(y_i) + \Phi(y_i) + \frac{[\Phi(y_i)^2]}{1 - \Phi(y_i)} \right) \right]^{(-1)} \qquad (10)$$

where $y_i = (a_i - \mu)/\sigma$ for $i \in D$ and $y_i = (m_i - \mu)/\sigma$ for $i \notin D$.

Figure 6.1.2 (bottom panel) shows the scaled-down thresholds for detected events as well as the lower limits for the non-detected events for the ARCES case study. Based on this information, we can estimate the overall ARCES detection threshold for the target site, using equation (9) which takes into account detections as well as
non-detections. We obtain a threshold of 3.81, which is slightly higher than the threshold of 3.69 obtained by *Method 2*.

We note that for the case study discussed in this section, the three methods produce very similar threshold estimates (see Figure 6.1.2). The situation may be quite different in cases where fewer events are available for the estimation. A comparison of the three methods will be presented in the following.

Comparison of the estimation procedures

We proceed to compare the three methods for an extended dataset, comprising a large number of source regions, and we begin by comparing *Method 1* (Direct estimation using detection/no detection information only) and *Method 3* (MLE using scaled network magnitudes). Figure 6.1.3 (left panel) shows the results of such a comparison for the ARCES array, displaying the results for all the bins with at least 5 detected events and 5 undetected events, and where the standard deviation using *Method 1* is less than 0.4. The results are quite consistent, which is encouraging. We note that in cases when there are sufficient observations (like the case presented in the figure), *Method 1* and *Method 3* provide consistent results. We also note that *Method 3* uses more information and is therefore expected to be more stable when there are few observations.

We next compare *Method 2* and *Method 3*. Figure 6.1.3 (two right panels) shows the results for the ARCES array, again plotting all the bins with a sufficient number of observations. We note that the results are not as consistent as between *Method 1* and *Method 3*, but that it is possible to improve the consistency by estimating and removing a linear trend.

We will use *Method 3* when the LEB contains information about non-detecting stations. For primary stations, such information is provided for distance range 20-100 degrees. Outside this distance range, we will use *Method 2*. For auxiliary stations, the LEB does not contain any information about non-detections before 2008, and in order to obtain consistency, we therefore chose to use *Method 2* for all auxiliary stations at all distance ranges.

Station detection capabilities

For the regionalized threshold estimates in this study, we make the following choices: For IMS primary stations, we use the maximum-likelihood estimate of the event detection thresholds *(Method 3*) in the distance range 20-100 degrees. Outside the 20-100 degree distance range we use the average scaled-down estimates *(Method 2*), but in addition, for each station, we calculate a regression line in order to estimate an average trend in a way similar to that illustrated in Figure 6.1.3 (upper right panel), and then compensate for this trend. For IMS auxiliary stations, we use *Method 2*, and compensate for a trend representing an average of those applied to the primary stations.

In Figures 6.1.4 and 6.1.5 we show, as an illustration, the results from applying this estimation procedure to primary station AKASG in Ukraine. In this study, we have applied the similar procedures to all available IMS primary and auxiliary stations, and the results form the basis for our application of dynamic phase information to assess the automatic IDC event lists.

Application to SEL event lists

We have developed a procedure for automatic application of the regionalized detection thresholds to assess the validity of individual candidate events in the SEL event lists as well as assess the consistency of individual phases associated with such events. We have applied this procedure to a large number of events, and for illustration we present an example of such application in Figure 6.1.6. The candidate event shown in this figure is typical of many of the false associations in SEL3, but it should be noted that the majority of the candidate events in SEL3 are real, and many of them have a remarkably accurate set of automatically associated seismic phases. Nevertheless, there is a clear need for improvement, and this project aims at providing a significant contribution in this regard.

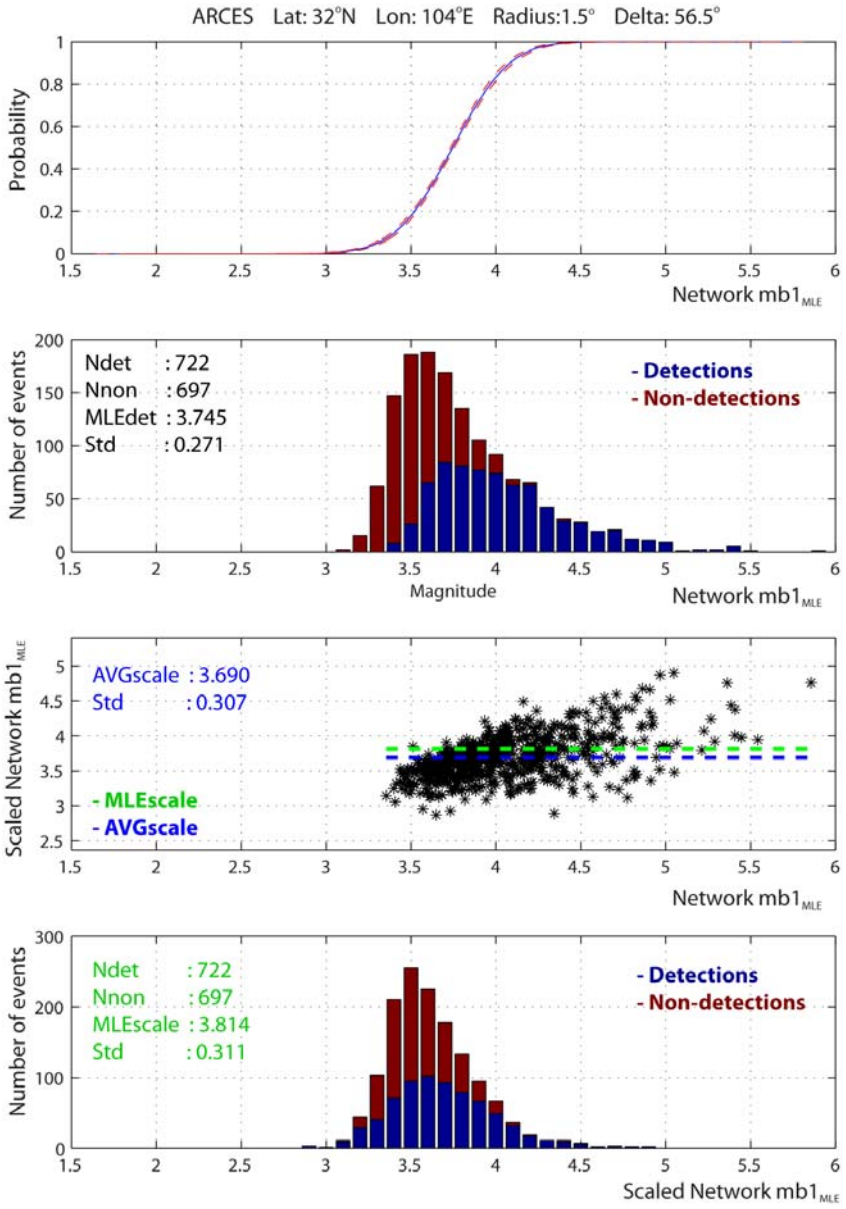

Fig. 6.1.2 The three estimation methods, as applied to ARCES for the source region shown in Figure 6.1.1 all give similar results, as shown in this figure:

- *Method 1 is illustrated in the top two panels. The station detection threshold (MLEdet) is given by the 50% level of the probability curve shown in the top panel. The information about event magnitudes, station magnitudes and noise magnitudes of non-detecting stations are shown in the second panel from the top.*
- *Method 2 is illustrated in the third panel from the top, and shows the scaled-down thresholds for detected events (blue) as well as their average value (AVGscale, also in blue). For comparison, the results of Method 3 (MLEscale) are shown in green color.*
- *Method 3 is illustrated in the bottom panel, and shows the scaled-down thresholds for detected events (blue) as well as lower limits for the non-detected events (red) for the ARCES case study. By maximizing the formula (9) we obtain a mean (MLEscale) and standard deviation of the detection threshold as indicated on the figure.*

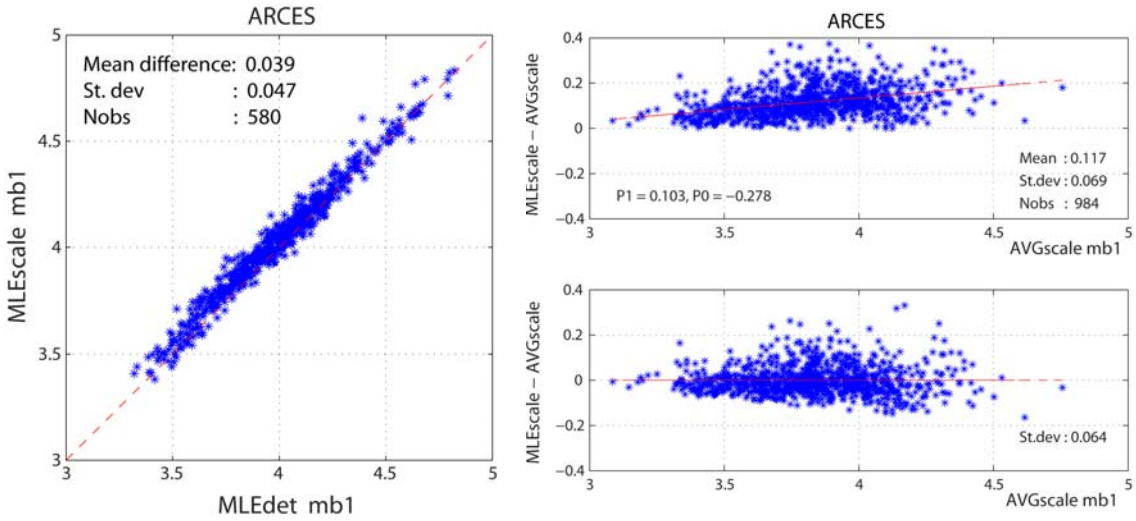

Fig. 6.1.3 Comparison of the three estimation methods of event detection thresholds for IMS primary station ARCES:

- *Left panel: Correspondence between Method 1 and Method 3 estimates. The data represent 580 bins in the teleseismic distance range. The points on the plot represent all the bins (in a 2 by 2 degree grid) for which there are at least 5 detected events and 5 undetected events, and where the standard deviation of the detection curve using Method 1 is less than 0.4. Results by Method 1 (Direct estimation) are along the horizontal axis (MLEdet), while results by Method 3 (MLE using scaled network magnitudes) are along the vertical axis (MLEscale).*
- *Right panels: Correspondence between Method 2 and Method 3 estimates. The x-axis represents the event detection thresholds for different 2x2 degree bins using the average scaled-down magnitudes of events detected at ARCES. The y-axis shows the difference between the maximum-likelihood estimate (also taking into account non-detected events) and the scaled-down estimate. The top panel has a linear trend which is removed in the bottom panel.*

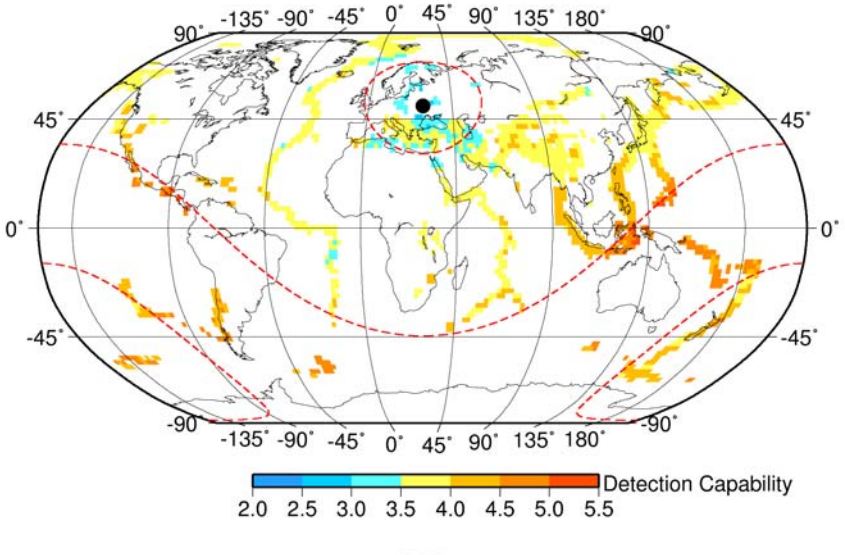

Fig. 6.1.4 Maps showing the estimated regional event detection thresholds for IMS primary station AKASG. For each of the 2x2 degree bins, a minimum of 5 events are required for calculation of the detection threshold. The upper map shows a global projection, and distances of 20, 95 and 144 degrees from AKASG are illustrated by red dashed lines. The lower map shows an azimuthal projection, and the red dashed circle shows a distance of 20 degrees from AKASG.

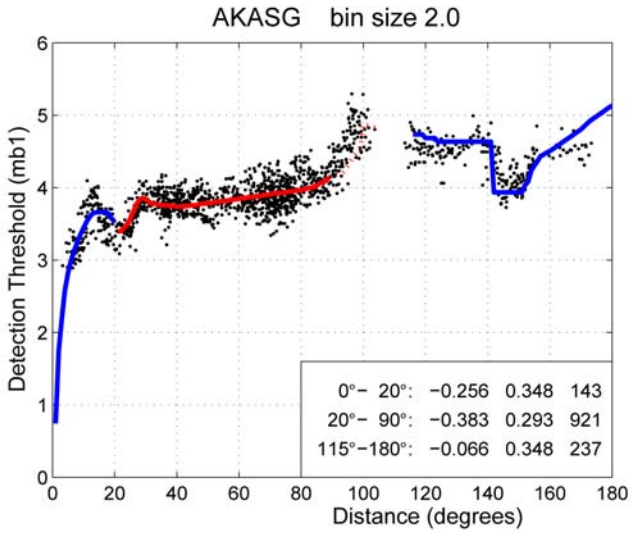

Fig. 6.1.5 The black dots show the estimated regional event detection thresholds for IMS primary station AKASG plotted versus epicentral distance. For each of the distance ranges 0-20 degrees, 20-90 degrees, and 115-180 degrees, the mb1 amplitude-distance curve is fitted to the data. The numbers for each of the distance ranges, given in the lower right box, are:

1. *the constant offset level of the mb1 amplitude-distance curve,*
2. *the standard deviation, and*
3. *the number of bins.*

In general, the lower the constant offset level, the better is the overall station detection capability.

Northwest Africa										Event only in SEL3				
Event id	Year	Mo	Dy	Hr	Min	Sec	Lat	Lon	Depth	REB Lat	REB Lon	REB-SEL3 loc. diff	SEL3 mb	New mb_{MLE}
6828087	2010	11	10	03	24	24.400	7.17	-6.10	0.0f	-	-	-	4.23	3.54

Detecting stations							
Station	Phase	Delta	Event magnitude	Detection threshold	Sigma	Detection probability	Station magnitude
DBIC	Pg	1.33	3.5363	1.1059	0.4320	1.000000	-
PLCA	P	75.84	3.5363	4.3974	0.3000	0.002051	4.30
ULM	P	84.40	3.5363	4.4208	0.3090	0.002102	4.50
TXAR	P	93.08	3.5363	4.0911	0.3220	0.042467	3.90
Third highest detection probability						0.002102	
Lowest detection probability						0.002051	

Non-detecting operational IMS primary stations					
Station	Delta	Event magnitude	Detection threshold	Sigma	Detection probability
TORD	9.70	3.5363	2.9086	0.3000	0.981800
MKAR	83.73	3.5363	3.7313	0.3300	0.277324
FINES	59.18	3.5363	3.8318	0.3370	0.190282
BRTR	48.14	3.5363	3.8190	0.3000	0.173042
AKASG	52.37	3.5363	3.8287	0.3000	0.164861
GERES	44.78	3.5363	3.8528	0.3070	0.151312
YKA	92.09	3.5363	4.0508	0.4260	0.113574
ARCES	65.59	3.5363	4.0040	0.3740	0.105570
ZALV	84.80	3.5363	3.9853	0.3360	0.090752
LPAZ	65.64	3.5363	4.0100	0.3410	0.082410
ESDC	32.42	3.5363	3.9990	0.3120	0.069051
NOA	55.29	3.5363	4.0030	0.3000	0.059908
KBZ	56.13	3.5363	4.0293	0.3160	0.059384
WRA	139.62	3.5363	4.1460	0.3800	0.054315
ASAR	138.29	3.5363	4.1330	0.3620	0.049652
BOSA	46.69	3.5363	4.0929	0.3150	0.038626
GEYT	65.34	3.5363	4.0750	0.3000	0.036284
KEST	31.76	3.5363	4.2390	0.3460	0.021141
CPUP	59.80	3.5363	4.2120	0.3200	0.017361
BDFB	47.30	3.5363	4.1760	0.3000	0.016499
KMBO	44.03	3.5363	4.3623	0.3360	0.006981
SCHQ	67.56	3.5363	4.3396	0.3150	0.005388
MAW	88.74	3.5363	4.6437	0.3850	0.002011
ROSC	67.83	3.5363	4.5593	0.3340	0.001096
ILAR	102.56	3.5363	4.6168	0.3480	0.000952
KSRS	118.26	3.5363	4.8590	0.3970	0.000432
SONM	99.45	3.5363	4.6297	0.3160	0.000270
MJAR	125.17	3.5363	4.9410	0.3550	0.000038
CMAR	101.86	3.5363	4.9074	0.3420	0.000030
PETK	118.40	3.5363	5.0220	0.3650	0.000023
VNDA	109.40	3.5363	5.3630	0.4290	0.000010
NVAR	102.58	3.5363	4.9104	0.3000	0.000002
USRK	116.42	3.5363	5.1440	0.3370	0.000001
PPT	142.92	3.5363	5.5010	0.3000	0.000000
Number of primary non-detections:					34
Number of stations exceeding third detection probability					22
Number of stations exceeding lowest detection probability					22

Fig. 6.1.6 This figure is an example of the type of processing results that we have obtained and analyzed for a large number of seismic events in SEL3. This particular example shows processing results from a candidate SEL3 event in Northwest Africa which has not been accepted in the LEB or REB. Three of the four detecting stations have a detection probability near zero. One non-detecting station (TORD) has a detection probability as high as 0.98. As many as 22 stations have better detection probability than the third best detecting stations. This event is clearly false, and can be discarded.

CONCLUSIONS AND RECOMMENDATIONS

We have developed a scheme to automatically process the individual candidate events in either SEL1, SEL2 or SEL3. For each event a set of consistency measures is calculated, as shown in the example in Figure 6.1.6. The consistency measures can be used individually or in combination. The most effective scheme is still to be developed.

In addition to calculating consistency measures based exclusively on SEL3 bulletin data, we have also during the developmental phase correlated the candidate events with the events actually accepted in the REB (or LEB). This provides a possibility to evaluate the consistency measures against the decision of the analyst.

In practical operation, it is intended to apply this processing scheme automatically, using the information from the SEL bulletins, the regionalized detection thresholds of the IMS stations, and the Threshold Monitoring (TM) results which are automatically computed at the IDC (see Kværna and Ringdal, 1999). We are already using the TM results to determine if any given station is actually in operation at a given time. Candidate events could be either accepted or rejected, or in some cases returned to the GA process for reanalysis, with one or more phases excluded from consideration.

Besides producing improved SEL lists, this processing scheme could also be applied in an interactive mode to provide the analyst with an assessment of the quality of the candidate event with respect to the pattern of detections/non-detections in view of the individual station capabilities.

REFERENCES

Kværna, T. and F. Ringdal (1999). Seismic Threshold Monitoring for Continuous Assessment of Global Detection Capability, *Bull. Seismol. Soc. Am*. 89: 946–959.

Kværna, T., F. Ringdal and U. Baadshaug (2009). Detection Capability of IMS Primary and Auxiliary Seimic Stations. *in* Semiannual Technical Summary, January-June 2009, *NORSAR Sci. Rep*. 2-2009, Kjeller, Norway.

Murphy, J. R. and B. W. Barker (2003). Revised Distance and Depth Corrections for Use in the Estimation of Short-Period P-Wave Magnitudes, *Bull. Seism. Soc. Am*. 93: 1746–1764.

Ringdal, F. (1975). On the estimation of seismic detection thresholds, *Bull. Seismol. Soc. Am*. 65: 1631–1642.

Ringdal, F. (1976). Maximum likelihood estimation of seismic magnitude, *Bull. Seismol. Soc. Am*. 66: 789–802.

Tormod Kværna
Frode Ringdal
Jeffrey Given, CTBTO

6.2 The Novaya Zemlya event on 11 October 2010

6.2.1 Introduction

The area around the archipelago of Novaya Zemlya is considered to be relatively aseismic. However, since Novaya Zemlya was the site of many years of extensive nuclear testing by the former Soviet Union, there has been a considerable interest in analysis and classification of all seismic events occurring in this region. Apart from the large explosions at the known test sites, there have during the last decades only been two events with magnitudes larger than 4. An analysis of the m_b 4.7 event on 1 August 1986, located on the east coast of the island (see Figure 6.2.1), was published by Marshall et. al, 1989.

On 11 October 2010, at 22:48:25.6 (IDC_REB), an event with magnitude 4.3 (IDC_REB) occurred on the north-west coast of Novaya Zemlya. The event was well recorded globally, and phase readings at 44 IMS stations contributed to the REB location. It has previously been observed that there is very efficient propagation of high-frequency signals for ray-paths crossing the Barents Sea (Ringdal et. al, 2008). As a consequence, both the IMS seismic stations on Svalbard (the SPITS array) and in northern Norway (the ARCES array) have been equipped with instruments having sampling rates of 80 Hz and 100Hz, respectively. In addition to an assessment of the reported event locations, we will in this contribution present the high-frequency recordings at SPITS and ARCES.

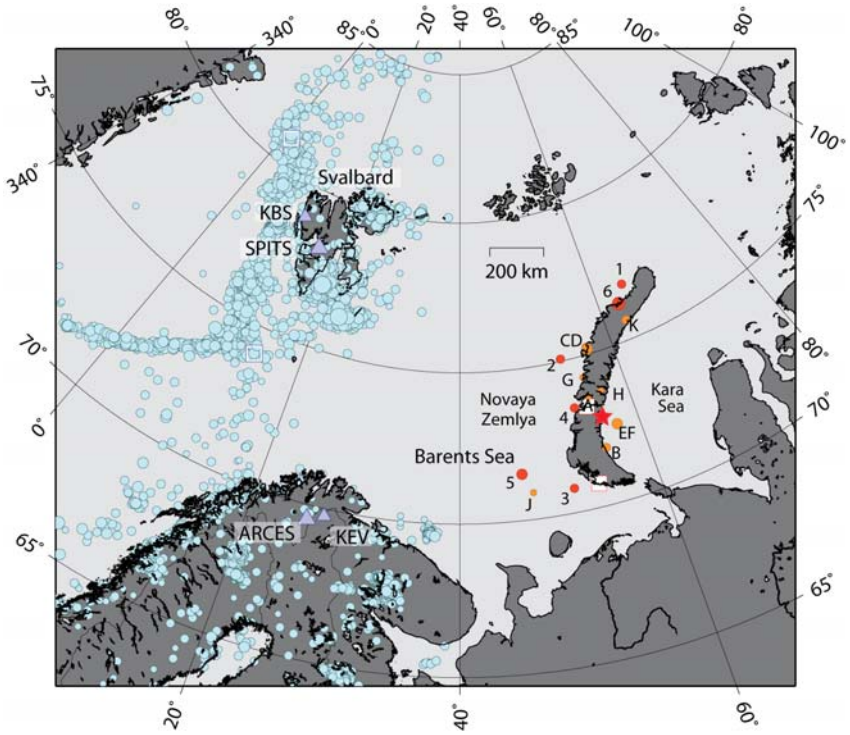

Fig. 6.2.1. Map showing the location of the SPITS and ARCES array, seismic events near Novaya Zemlya since 1992 (red/orange filled circles), and the seismicity of the region as reported in NORSAR's monthly seismic bulletin 1998-2008 (blue filled circles). The 1 August 1986 event is marked by a red star, and the 11 October 2011 event is labelled by the number 6. The figure is adapted from Gibbons et. al, 2011.

6.2.2 Location estimates

The IDC reviewed event bulletin (REB) reports the following hypcenter information for the 11 October 2010 event:

Origin time (UTC)	2010/10/11 22:48:25.62
Location	76.2640N; 64.7619E
Location errors (km)	Smaj10.6; Smin 8.6; Az 160
Depth	0 (Fixed)
Magnitude	$mb1_{mx}$ 4.3; $ms1_{mx}$ 3.2

The REB location and the associated error ellipse is shown red in Figure 6.2.2. The NEIC location is shown by a green symbol. The REB location is mainly based on readings at distant stations. ARCES is the only station within 2000 km of the event that contributed to the REB location, and surprisingly the high-quality recordings at the SPITS array were not used in the REB.

Phase picks at regional distance stations, on Svalbard and in northern Fennoscandia, dominated the input to the initial location reported in NORSAR's regional bulletin. This location, differed significantly, by about 65 km, from the REB location (see black symbol in Figure 6.2.2). In an attempt to combine phase readings at both regional and teleseismic distances, we relocated the event using the re-picked phases listed in Table 6.2.1. The location was calculated with the HYPOSAT program of Schweitzer, 2001, using a combination of the regional *"barey"* model (Schweitzer and Kennett, 2007) and the global *"AK135"* model. The recalculated location differed by 22 km from the REB location (see blue symbol in Figure 6.2.2). The following hypocentral parameters were obtained:

Origin time (UTC)	2010/10/11 22:48:27.725
Location	76.2999N; 63.9627E
Location errors (km)	Smaj6.3; Smin 5.6; Az 39
Depth	0 (Fixed)

The distances to the stations used for the event relocation were all exceeding 900 km from the event epicenter. The stations at regional distances (within 2000 km) cover a very narrow azimuth range (240-310 degrees) in the westerly direction from the event (see Table 6.2.1). As a result, a small error in the propagation velocities of the one-dimensional location model may cause in a significantly biased location. This is particularly apparent for NORSAR's initial event location, shown by the black symbol of Figure 6.2.1. We conclude that there is a need to improve the regional location models used for routine data analysis of events, and use of existing three-dimensional regional propagation models in this analysis should be encouraged.

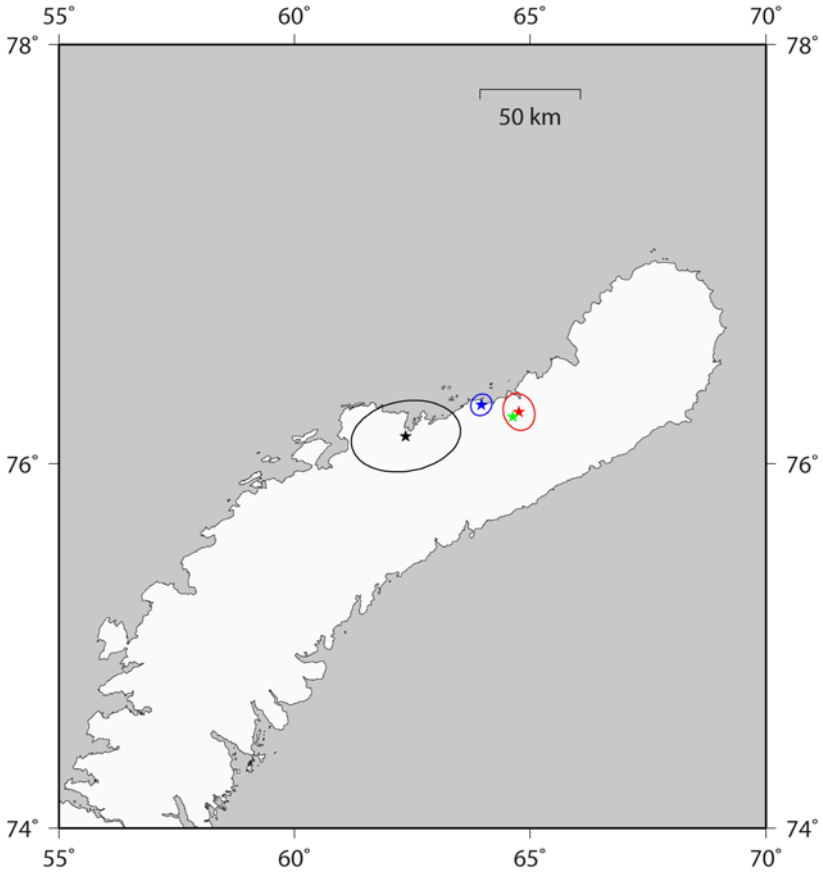

Fig. 6.2.2. Location estimates of the 11 October 2010 event.
Red: IDC Reviewed Event Bulletin
Green: NEIC
Black: NORSAR's regional reviewed bulletin
Blue: NORSAR's relocation using a combination of regional and teleseismic data

Table 6.2.1. Phase readings used for relocating the 10 October 2010 event

Stat	Delta	Azi	Phase	[used]	Onset time	Res	Baz	Res	Rayp	Res	Used
HOPEN	9.050	290.22	Sn		22 52 13.088	-2.433					T
SPITS	10.437	302.81	Pn		22 50 56.091	1.051	70.89	-5.39	14.46	1.12	T D
SPITS	10.437	302.81	Sn		22 52 47.634	-0.704	90.70	14.42	24.82	1.19	T D
HSPB	10.957	297.00	P1	Pn	22 51 1.474	-0.435					T D
HSPB	10.957	297.00	S1	Sn	22 52 57.697	-2.808					T D
TER	10.984	244.78	Pn		22 51 2.815	0.524	13.11	-24.03	9.14	-4.19	T D
TER	10.984	244.78	Sn		22 52 57.835	-3.348					T D
KBS	11.123	307.82	Pn		22 51 5.333	1.198	99.58	22.72	2.90	-10.43	T D
KBS	11.123	307.82	Sn		22 53 4.249	-0.197					T D
LVZ	12.149	241.68	Pn		22 51 18.810	0.918					T
LVZ	12.149	241.68	Sn		22 53 25.349	-3.447					T
KEV	12.381	257.42	P1	Pn	22 51 21.451	0.568	45.64	3.70	12.81	-0.50	TASD
KEV	12.381	257.42	S1	Sn	22 53 31.542	-2.555					T D
ARA0	12.896	258.54	P1	Pn	22 51 28.074	0.298	54.09	12.47	11.51	-1.80	T D
ARA0	12.896	258.54	S1	Sn	22 53 43.107	-3.184	50.72	9.10	17.71	-5.84	T D
VRF	13.363	248.42	Pn		22 51 34.783	0.813	30.83	-4.76	10.55	-2.75	TA D
VRF	13.363	248.42	Sn		22 53 55.670	-1.582					T D
HEF	14.191	257.57	Pn		22 51 45.080	0.114	34.53	-4.43	8.63	-4.66	TA D
HEF	14.191	257.57	Sn		22 54 14.382	-2.321					T D
KIF	14.372	262.48	Pn		22 51 48.278	0.897	43.18	2.12	11.03	-2.26	TA D
KIF	14.372	262.48	Sn		22 54 19.118	-1.856					T D
TRO	14.380	266.10	Pn		22 51 49.359	1.953	16.85	-25.94	11.01	-2.28	T
TRO	14.380	266.10	Sn		22 54 16.682	-4.341					T
KU6	14.743	244.10	Pn		22 51 53.484	1.203	42.93	11.28	12.92	-0.36	T SD
KU6	14.743	244.10	Sn		22 54 28.673	-0.972					T D
LANU	14.862	258.62	Pn		22 51 54.065	0.184	10.89	-27.53	5.83	-7.45	T D
LANU	14.862	258.62	Sn		22 54 32.148	-0.325					T D
MSF	15.024	245.02	Pn		22 51 57.138	1.123	35.06	3.30	11.60	-1.68	TA
DAG	17.822	311.71	P1	Pn	22 52 33.727	0.801	53.72	3.14	13.68	0.46	TAS
DAG	17.822	311.71	S1	Sn	22 55 32.510	-9.044					
FINES	19.592	241.64	P1	P	22 52 55.090	0.661	22.18	-3.70	12.80	1.85	TA
ARU	20.057	188.77	P		22 53 0.194	0.639	353.07	-10.68	13.27	2.35	T
CHKZ	22.860	169.78	P		22 53 29.348	-0.379	359.49	3.57	10.64	0.02	TASD
CHKZ	22.860	169.78	S		22 57 33.147	-1.212					T D
NC400	23.123	258.13	P		22 53 34.966	2.437	17.95	-10.73	6.34	-4.24	T
NB200	23.276	258.63	P		22 53 36.194	2.024	29.98	1.29	9.53	-1.03	TA
NBO00	23.386	259.09	P		22 53 37.160	1.860	30.06	1.33	8.38	-2.17	TA
NC600	23.477	258.01	P		22 53 37.806	1.583	20.52	-7.82	8.67	-1.87	T
BVAR	23.502	170.24	P		22 53 35.720	-0.838	5.31	9.15	7.75	-2.78	T
ZRNK	23.526	172.34	P		22 53 36.321	-0.483					T D
ZRNK	23.526	172.34	S		22 57 48.312	1.615					T D
NAO00	23.555	258.78	P		22 53 38.402	1.343	24.34	-4.16	9.24	-1.28	TA
ZALV	23.793	148.56	P		22 53 37.908	-1.604	341.33	-6.53	8.78	-0.37	T S
VOS	23.828	169.40	P1	P	22 53 38.917	-0.933	10.94	15.07	12.36	3.21	T
AKTO	26.073	188.67	P1	P	22 54 0.276	-0.012					T
KURK	26.329	158.73	P1	P	22 54 2.644	0.060	356.42	4.24	8.31	-0.74	TAS
ABKAR	27.194	185.77	P		22 54 10.768	0.376	343.61	-18.49	9.39	0.39	T S
AKASG	29.076	228.25	P1	P	22 54 27.109	-0.053	18.63	2.40	9.55	0.67	TAS
MKAR	30.559	154.85	P		22 54 39.405	-0.994	352.76	1.24	7.69	-1.15	TA
EKA	31.817	267.81	P1	P	22 54 52.885	1.545	25.57	0.95	8.93	0.13	TAS
BURAR	32.763	231.49	P1	P	22 55 1.064	1.201	4.61	-11.39	7.64	-1.12	T
SONM	33.260	124.02	P1	P	22 55 3.580	-0.674	334.54	-8.41	8.69	-0.05	T S
KKAR	33.418	171.28	P1	P	22 55 6.158	0.637					T
USP	33.443	165.97	P1	P	22 55 6.349	0.578	343.10	-12.36	5.72	-3.01	T
CHM	33.725	165.68	P1	P	22 55 9.289	1.074	358.40	3.01	7.31	-1.40	TA
GERES	33.934	245.52	P1	P	22 55 12.175	2.132	29.72	10.55	9.02	0.32	T S
EKS2	34.006	167.01	P1	P	22 55 11.043	0.257					T
AAK	34.076	166.09	P1	P	22 55 12.572	1.413					T
UCH	34.479	166.10	P1	P	22 55 16.872	1.539	356.77	1.19	5.60	-3.07	TA
AML	34.530	167.18	P1	P	22 55 17.553	1.857	347.40	-8.52	7.62	-1.04	T
KZA	34.672	165.16	P1	P	22 55 17.858	0.915					T
INK	35.210	11.17	P1	P	22 55 20.239	-0.481	9.33	16.46	3.90	-4.72	T
ILAR	37.836	20.99	P1	P	22 55 43.333	0.117	345.53	-2.98	7.63	-0.83	TAS
GEYT	38.558	187.42	P		22 55 50.759	1.144	320.90	-41.33	7.68	-0.73	T S
ESDC	46.630	259.67	P1	P	22 56 56.876	1.641	15.34	-2.35	9.65	1.80	TA
KEST	47.395	244.32	P1	P	22 57 2.994	1.714					T
MJAR	51.107	95.24	P		22 57 27.214	-2.374	333.98	-8.88	9.75	2.23	T
CMAR	60.633	141.33	P1	P	22 58 36.289	-1.760	341.05	-9.93	7.42	0.59	T S
TORD	70.880	245.86	P1	P	22 59 44.285	0.088	355.81	-17.09	6.88	0.80	T S
TXAR	74.332	348.80	P		23 00 4.992	0.210	7.53	4.49	3.98	-1.85	TA

6.2.3 Spectral characteristics of SPITS and ARCES observations

The SPITS and the ARCES arrays are located at distances of 1178 and 1451 km, respectively, from the event epicenter (REB location). Waveforms, phase spectra and spectrograms for the SPITS and ARCES observations are shown in Figures 6.2.3 - 6.2.7. For the SPITS recordings, the presence of significant energy up to the Nyquist frequency of 40 Hz confirms the documented efficient high-frequency wave propagation from the Novaya Zemlya region to Svalbard, across the Barents Sea (Ringdal et. al, 2008).

For the ARCES high-frequency element, installed in March 2008, there has so far only been recorded two events from the eastern Barents Sea/Novaya Zemlya region. The magnitude 3.2 event on 11 November 2009 located in the eastern Barents Sea (labelled 5 in Figure 6.2.1), showed significant energy event up to 40 Hz both for the Pn and Sn phases (Kværna and Ringdal, 2010). The epicentral distance from ARCES to the 11 November 2009 event was about 800 km.

The 10 October 2010 event was located at a distance of about 1450 km from the ARCES array, and the spectra show signal energy up to about 25 Hz for the Pn and Sn phases. As compared to the SPITS spectra and the ARCES spectra of the 11 November 2009 event, the ARCES spectra for this event has comparatively less high frequency energy. We attribute this to a longer propagation path, and to signal attenuation when the seismic waves crossed the heterogeneous crustal structures of the Novaya Zemlya island. However, we nevertheless consider this as very efficient propagation of high-frequency energy.

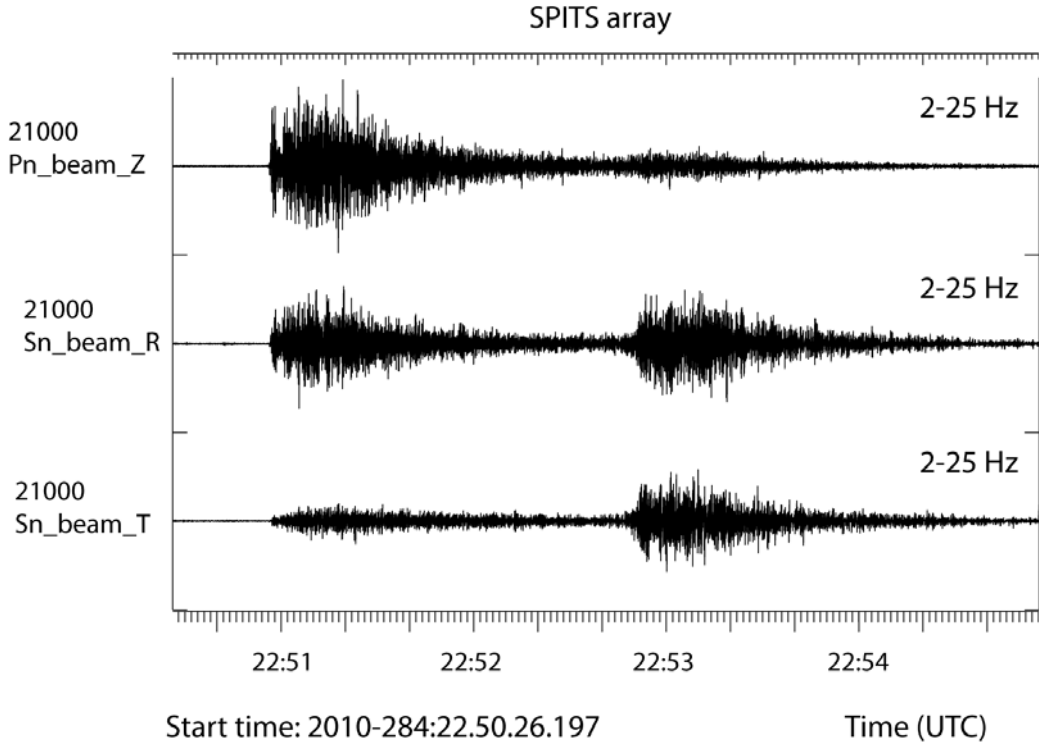

Fig. 6.2.3. Waveforms from the 11 October 2011 event recorded at the SPITS array. The upper trace shows the Pn beam of the 9 vertical-component sensors. The middle trace shows the Sn-beams of the 6 horizontal component sensors after rotation into the radial direction of the incoming wave. The lower trace shows the corresponding Sn beam of the transversely rotated horizontal sensors.All traces are bandpass filtered between 2 and 25 Hz.

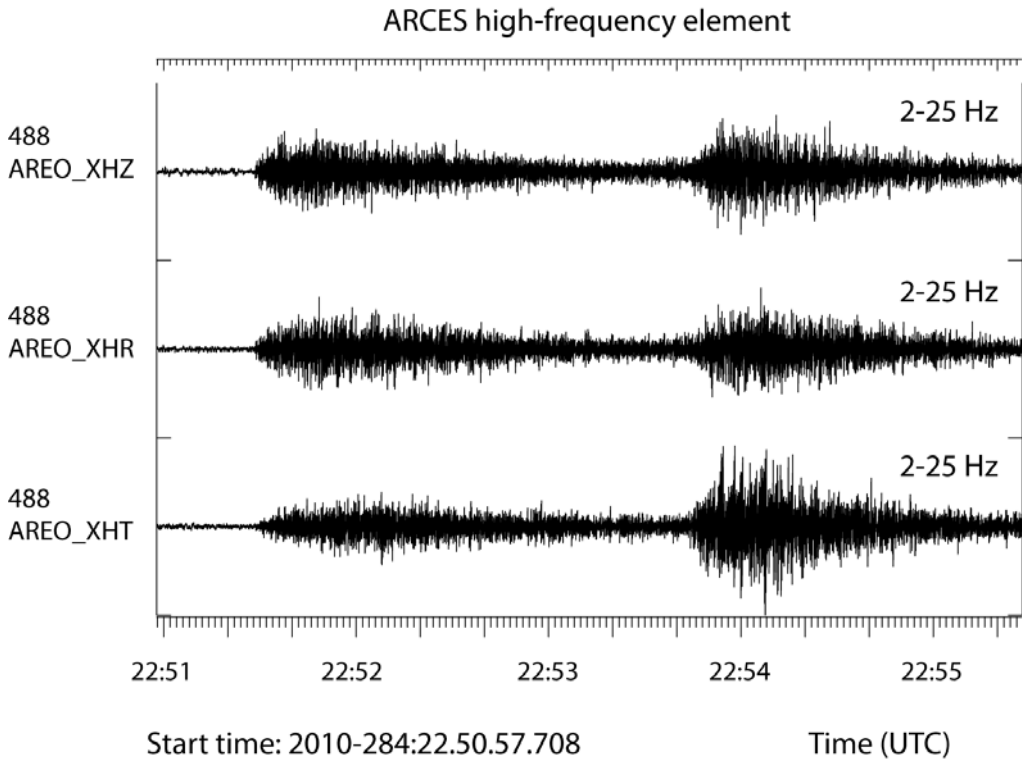

Fig. 6.2.4. Waveforms from the 11 October 2011 event recorded at the ARCES high-frequency element ARE0. The upper trace shows the vertical component sensor. The two lower traces show the horizontal components after rotation into the radial and transverse directions. All traces are bandpass filtered between 2 and 25 Hz.

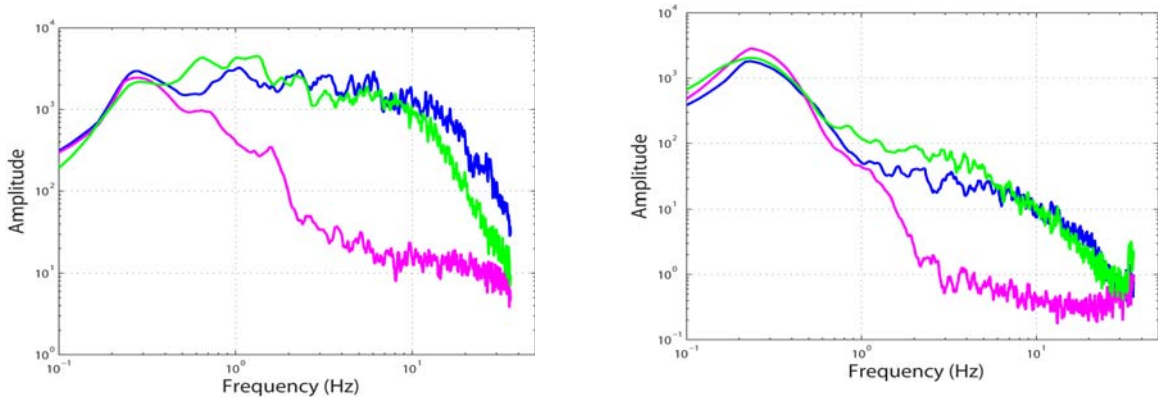

Fig. 6.2.5. Left: Spectra from the SPA0 three-component sensor of the SPITS array of the Pn (blue) and Sn (green) phases of the 11 October 2010 event. The noise spectrum (magenta) preceding the event is also shown. The Pn and noise spectra are calculated from the vertical component sensor, whereas the Sn spectrum is calculated from the transverse horizontal component.
Right: Corresponding spectra for the ARE0 high-frequency three-component sensor of the ARCES array. Time windows of 60 seconds were used for calculating all spectra.

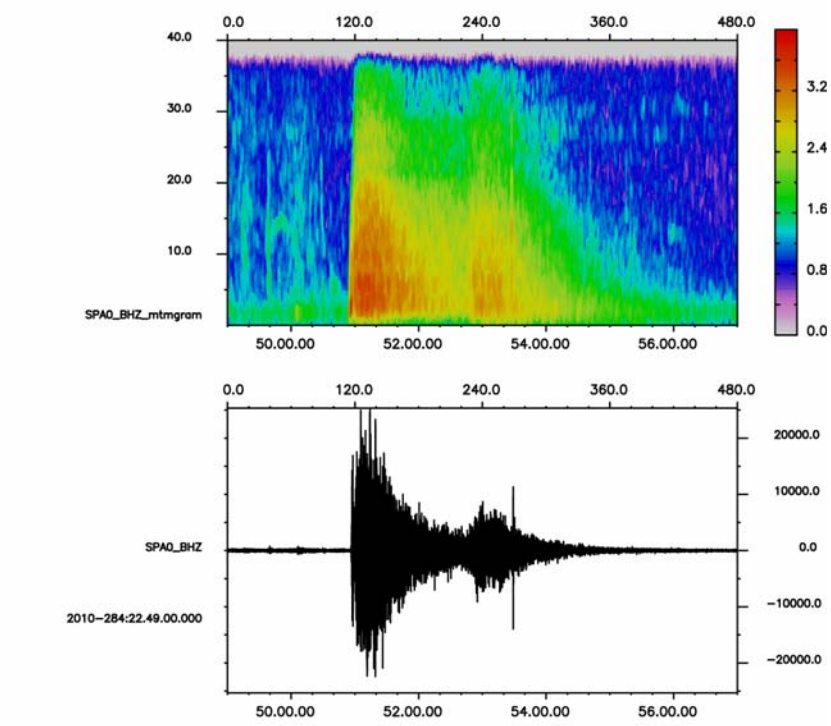

Fig. 6.2.6. Spectrogram for the vertical-component sensor SPA0_BHZ of the SPITS array for an eight minutes time interval around the P and S phases of the 11 October 2010 event.

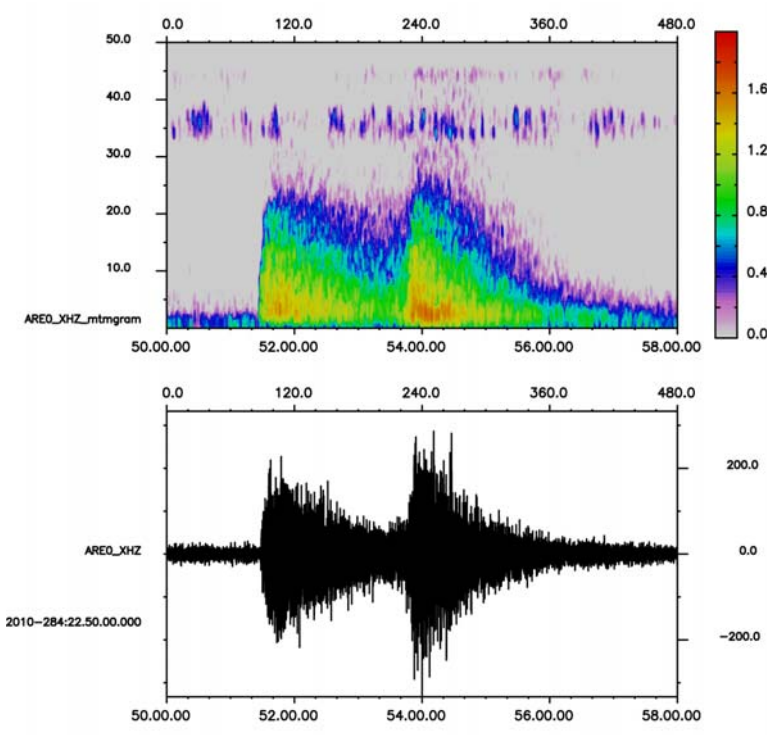

Fig. 6.2.7. Spectrogram for the vertical-component sensor ARE0_XHZ of the ARCES array for an eight minutes time interval around the P and S phases of the 11 October 2010 event.

References

Gibbons, S.J., J. Schweitzer, F. Ringdal, T. Kværna, S. Mykkeltveit and B. Paulsen (2011). Improvements to Seismic Monitoring of the European Arctic Using Three-Component Array Processing at SPITS. To be published in BSSA, December 2011.

Kværna, T. and F. Ringdal (2010). Seismic event in the Barents Sea, 11 November 2009. *In NORSAR Scientific Report No. 1-2010: Semiannual Technical Summary, NORSAR, Kjeller, Norway.*

Ringdal, F., Kværna, T., and Gibbons, S. J. (2008). Initial studies of high-frequency signals recorded at ARCES infrasound sensors. *In NORSAR Scientific Report No. 2-2008: Semiannual Technical Summary, NORSAR, Kjeller, Norway.*

Schweitzer, J. (2001): HYPOSAT – An Enhanced Routine to Locate Seismic Events. *Pure and Applied Geophysics,* **158**, No. 1, 277-289.

Schweitzer, J. and B.L.N. Kennett (2007). Comparison of Location Procedures: The Kara Sea Event of 16 August 1997. *Bull. Seism. Soc. Am.*, **97**, No. 2, 389-400.

Tormod Kværna
Steven Gibbons

6.3 The 21 July 2011 earthquake in Hedmark, Southern Norway

6.3.1 Introduction

On 21 July 2011, at 02:59 local time an earthquake with a local magnitude of about 3.8 awaked many people in Hedmark, Southern Norway. A very preliminary automatic location of the event clearly located the earthquake within the NORSAR array (NOA), between the communities of Elverum and Rena, about 40 - 50 km north of the 07 April 2004 Flisa earthquake (see Fig. 6.3.1 and Schweitzer (2005)). With the 42 seismic sites of the NORSAR array at epicentral distances between about 10 and 60 km from the event and several additional seismic stations in the region, it was possible to perform a high quality determination of the hypocenter.

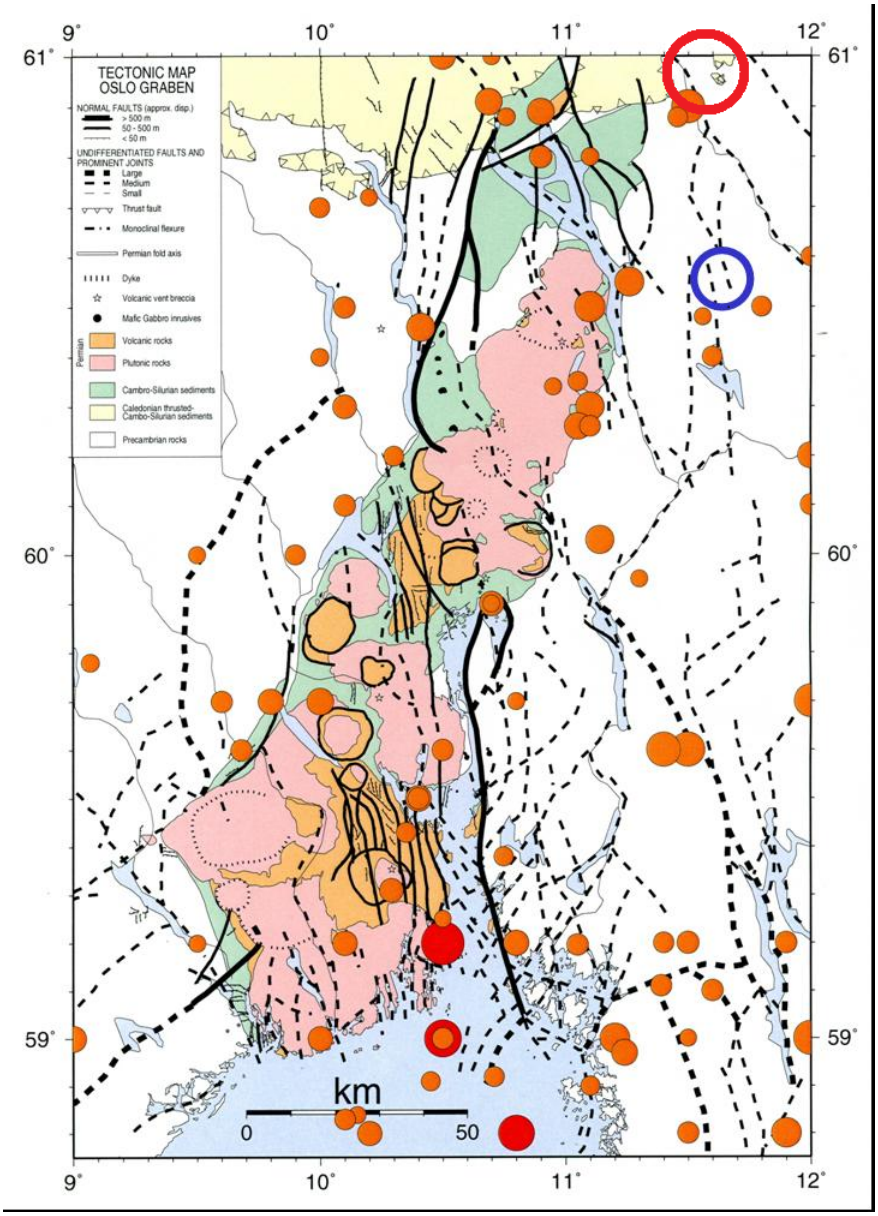

Fig. 6.3.1. Map (modified from Hicks, (1996)) of historical seismicity in south-east Norway around the Oslo Graben and the source regions of the 21 July 2011 Elverum-Rena (red circle) and of the 07 April 2004 Flisa earthquakes (blue circle, Schweitzer 2005).

6.3.2 Data analysis

Although the earthquake had been recorded with very impulsive first onsets by the different sensors at local distances, reading the exact onset times of the different seismic phases at the NOA stations became difficult; due to the large amplitudes, an acausal ringing effect of the antialias FIR filter in the digitizers is visible at all seismic traces and disturbs the onset time reading. The top trace in Fig. 6.3.2 shows the start of the raw earthquake recording, sampled with a rate of 40 Hz, at the closest NOA site NC403; the FIR filter effect is obvious. Bandpass filtering of the record between 0.01 and 15 Hz does not and cannot fully remove the filter effect (second trace from top). Since we know the FIR filter response of the SHI digitizers installed at NOA, we can use this to correct the observations. The third trace shows the original seismogram now deconvolved with the known instrument response (Pirli & Schweitzer, 2007). There is still some high frequency ringing visible, which totally disappears after filtering the seismogram with the mentioned Butterworth bandpass filter (Fig. 6.3.2, bottom trace). On such processed seismogram records, the onset time of the first P phase could be picked with an uncertainty of +/- 1 or 2 samples (0.025 - 0.05 s).

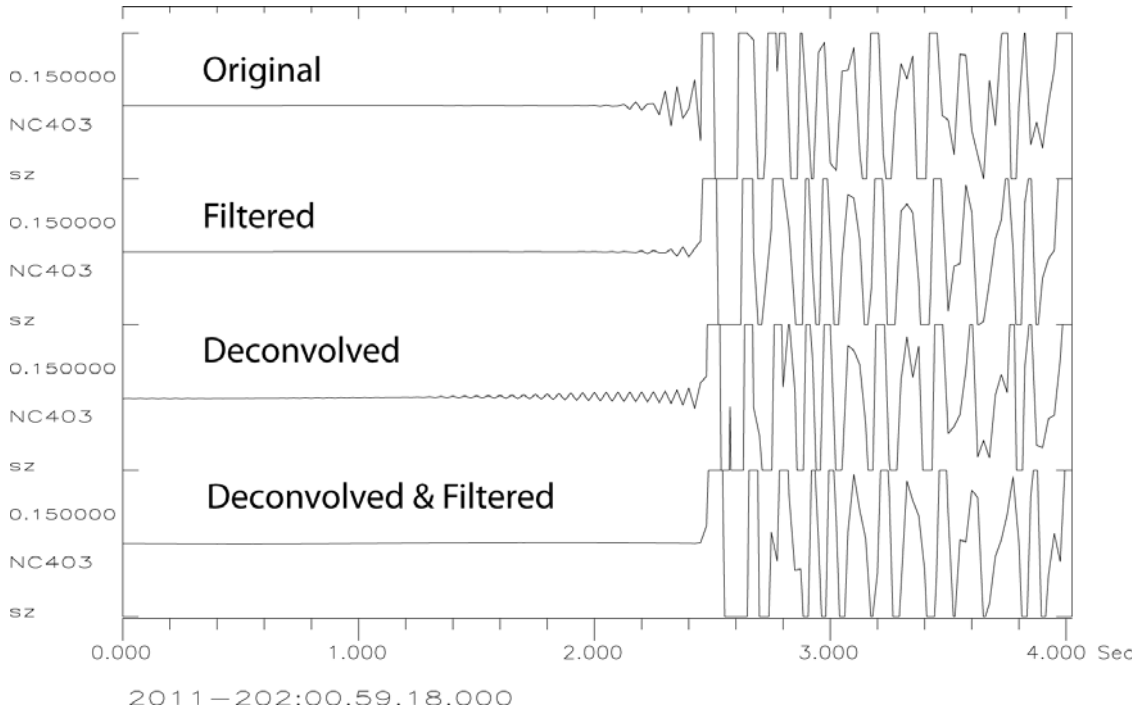

Fig. 6.3.2. First P-onset records of the 21 July 2011 earthquake at NOA site NC604. On top the original observations, as second trace a Butterworth bandpass 0.01 - 15 Hz filtered trace, as third trace the original trace deconvolved with the instrument and digitizer response, and on bottom the deconvolved trace additionally filtered with the Butterworth bandpass. All traces were normalized with the maximum P-wave amplitude.

The S-onsets could be read with an uncertainty of +/- 0.1 s on the rotated radial and transverse components at the 7 3-component NOA sites. S-onsets at the other NOA sites with vertical instruments only could be read with an uncertainty of +/- 0.3 s. For each of the 7 NOA subarrays, beams were calculated to estimate apparent velocities and backazimuths of the P and S onsets. With these 145 NOA observations plus some additional readings from the Hagfors array in Sweden, a seismic station at the University of Oslo and a test installation at NOA site NC6, altogether 165 observed parameters could be used to estimate the hypocenter (see also

Fig. 6.3.3). Fig. 6.3.4 shows a map of all stations, which have been used and the best achieved event location.

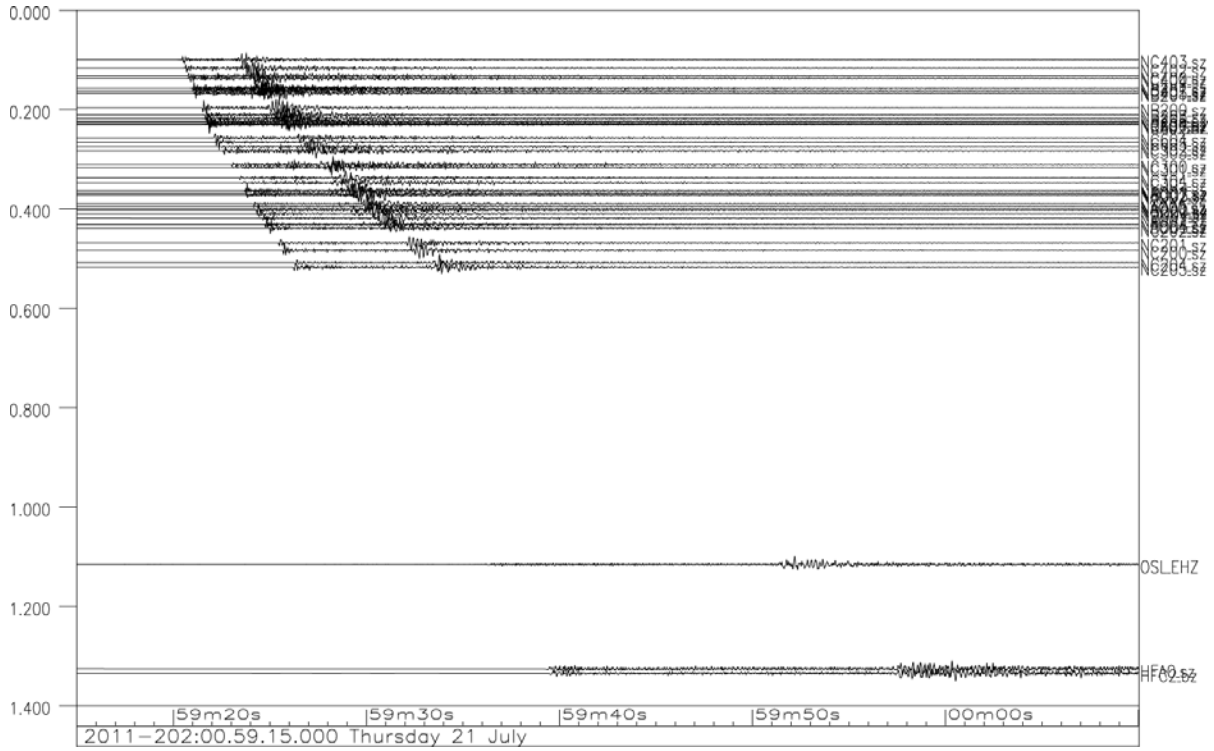

Fig. 6.3.3. All analyzed vertical traces used to locate the 21 July 2011 earthquake are shown as a function of epicentral distance. Normalized, unfiltered data are plotted.

6.3.3 The Elverum-Rena earthquake as ground-truth event

The 21 July 2011 earthquake was located using HYPOSAT (Schweitzer, 2001; 2002). The same velocity model as derived and systematically studied for the 7 April 2004 Flisa event could be used since the observing seismic stations are almost identical and the epicenters do not differ much; the seismic velocity model was published in Schweitzer (2005, Table 6.3.2 therein).

In Table 6.3.1 different locations for the 21 July 2011 earthquake are listed. All these locations with their error ellipses are plotted on the map of Fig. 6.3.4. All locations are very close to each other and their error bars overlap. The velocity model used had been defined by Schweitzer (2005) with discussing several parameters, which may influence the location (v_p/v_s velocity ratio and the depth of the main discontinuities Moho and Conrad). Applying this model for the 21 July 2011 event in the same larger source region together with only local and near regional observations gives very small (formal) location uncertainties and high confidence in the inversion results.

Although this event was not very large (reported magnitudes are between 3.3 and 3.8), it had been observed at local, regional, and teleseismic distances. With such a large number of close by seismic stations and observations, the GT level of this event is of interest. The given uncertainties for the location presented herein were calculated for 99.99% confidence limit. Based on these results, the epicenter can be addressed as a GT-1 event. With several NOA sites at epi-

central distances of 10 to 20 km and in different azimuthal directions even the depth of the event is well defined with an uncertainty of less than +/-1 km.

Table 6.3.1. List of locations for the 21 July 2011 earthquake in Hedmark, Southern Norway.

Source	Origin Time	dTo [s]	Latitude [deg]	Longitude [deg]	Depth [km]	dho [km]	Error Ellipse			RMS [s]
							Major [km]	Minor [km]	Azimuth [deg]	
NORSAR (web info)	00:59:16	-	60.98	11.58	~10	-	-	-	-	
NORSAR (analyst reviewed)	00:59:15.73		60.9774	11.5882	13.68		3.7	3.4	146.5	2.11
IDC (REB)	00:59:15.79	0.52	60.9571	11.5708	16.2	5.8	7.0	4.3	99	0.77
University of Bergen (web info)	00:59:16.9	-	60.955	11.579	17.7	-	-	-	-	-
NORSAR (this study)	00:59:16.38	0.08	60.9642	11.5849	22.8	0.8	0.5	0.5	55	0.13

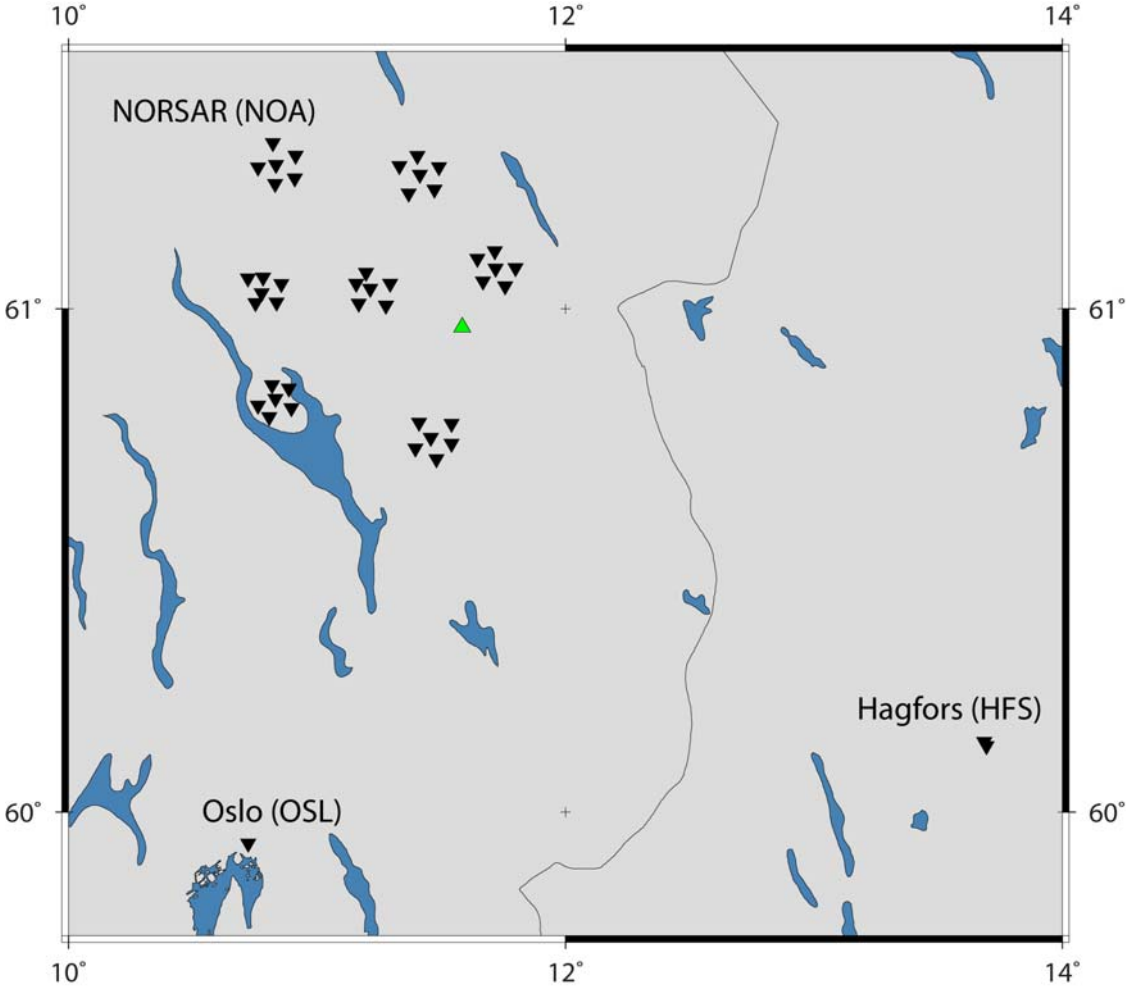

Fig. 6.3.4. Map of the new location of the 21 July 2011 (green triangle) and the seismic stations (black inverted triangles) used for its determination.

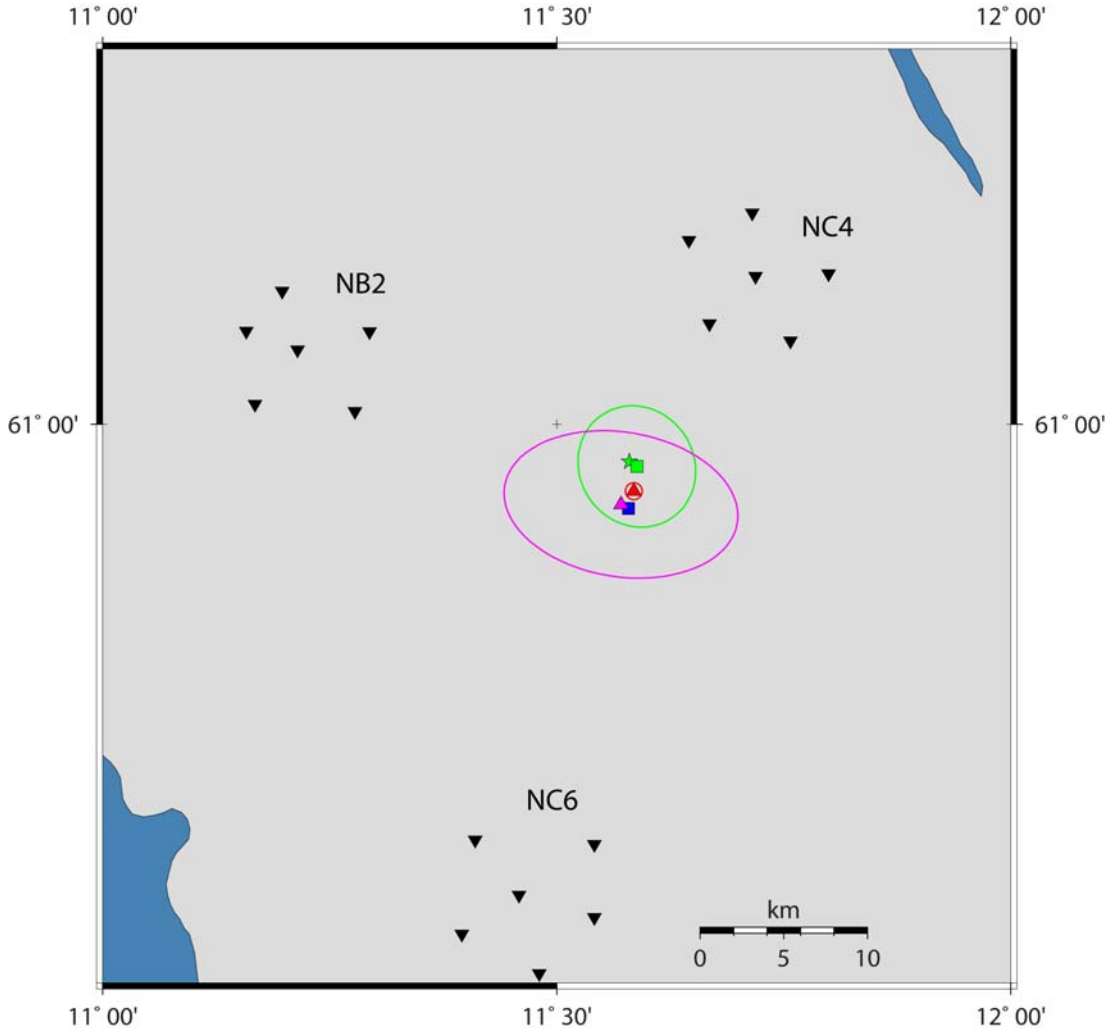

Fig. 6.3.5. Close up map with the different locations of the 21 July 2011 earthquake as listed in Table 6.3.1: NORSAR (Web info) green star, NORSAR (analyst reviewed) green square, IDC (REB) magenta triangle, University of Bergen (web info) blue square, NORSAR (this study) red triangle. Additionally, corresponding location uncertainty ellipses are shown, when available, as well as the nearest seismic stations of the NORSAR array.

6.3.4 Fault plane solution for the 21 July 2011 earthquake

At all stations used to locate the event and at a smaller number of stations at regional distances P-onset polarities and some SH and SV polarities could be read. In addition, some amplitude ratios between the P and the S (SV and SH) onsets were measured. All these data were inverted for the best fitting double couple solution. The FOCMEC inversion routine (Snoke, 2003) was applied to calculate all possible fault planes, which are in agreement with the observed data. The assumption for this type of inversion is that a single double couple can describe the source mechanism. Fig. 6.3.6 shows all observed P polarities and the results from FOCMEC. The triangles represent negative and the circles positive polarities. The B-axis, where the two possible fault planes intersect, is not very well defined due to station distribution and due to the fact that many stations in the South are located beyond the Teisseyre-Tornquist zone, which is known to block seismic wave propagation (Schweitzer, 1997). However, systematic search for more polarity data may constrain the solution better.

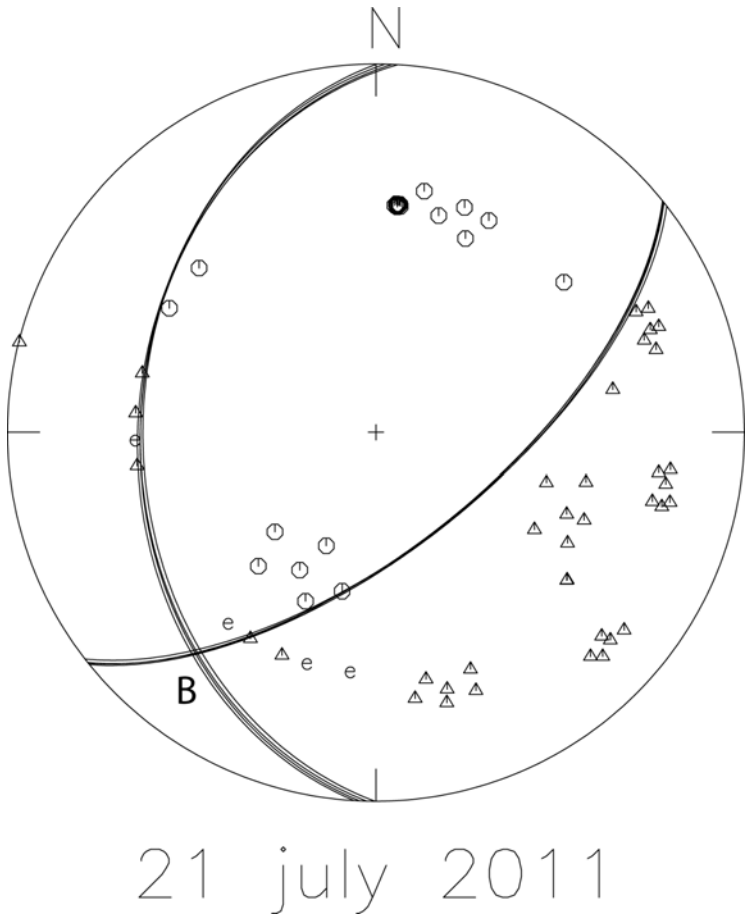

Fig. 6.3.6. The estimated fault plane solution for the 21 July 2011 earthquake and all P polarities (positive circles, negative triangles).

The presented double couple solution shows a reverse fault with a general NNE - SSW strike. This feature will also not change with a better defined solution. From the observed data, it is not possible to decide, which of the two possible planes is the actual fault plane.

However, many earthquakes in and around the Oslo Graben area show north-south striking fault planes with a large variation in the orientation of the auxiliary plane; almost every type of source mechanism can be observed: normal faulting, strike-slip movements, and reverse faulting (see e.g., Hicks et al., 2000; Lindholm et al., 2000).

Johannes Schweitzer

Acknowledgements

Thanks to the kind contribution of the station owners, seismic data from the Swedish Auxiliary IMS array Hagfors, the Norwegian National Seismic Network, the British Geological Survey, the University of Helsinki, the German Regional Seismic Network, the Geological Survey of

Denmark and Greenland, and the University of Oulu could be analyzed and were used to locate the event and to determine the focal mechanism.

References

Hicks, E. C. (1996). Crustal stresses in Norway and surrounding areas as derived from earthquake focal mechanism solutions and in-situ stress measurements. Cand. Scient. Thesis, University of Oslo, Norway, 164 pp.

Hicks, E.C., H. Bungum & C.D. Lindholm (2000). Stress inversion of earthquake focal mechanism solutions form onshore and offshore Norway. Norsk Geologisk Tidsskrift, **80**, 235-250.

Lindholm, C.D., H. Bungum, E. Hicks & M. Villagran (2000). Crustal stress and tectonics in Norwegian regions determined from earthquake focal mechanisms. In: Nottvedt et al. (eds). Dynamics of the Norwegian Margin. Geological Society London, **167**, 429-439.

Pirli, M. & J. Schweitzer (2007). Overview of NORSAR sytem response. NORSAR Sci. Rep., **1-2008**, 64-77.

Schweitzer, J. (1995). Blockage of regional seismic waves by the Teisseyre-Tornquist zone. Geophys. J. Int., 123, 260-276.

Schweitzer, J. (2001). HYPOSAT – An enhanced routine to locate seismic events. Pure Appl. Geophys., **158**, 277-279.

Schweitzer, J. (2002). PD11.1: User Manual for HYPOSAT (including HYPOMOD). In: Bormann, P. (ed.) (2002). IASPEI New Manual of Seismological Observatory Practice, GeoForschungsZentrum Potsdam, Vol. 2, 15 pp.

Schweitzer, J. (2005). The 7 April 2004 Flisa, Southern Norway earthquake sequence - eight hypocenter determinations and one focal mechanism. NORSAR Sci., **Rep. 1-2005**, 62-75.

Snoke, J. A. (2003). FOCMEC: FOcal MEChanism determinations. In: Lee, W. H. K., H. Kanamori, P. C. Jennings & C. Kisslinger (eds). International Handbook of Earthquake and Engineering Seismology. Academic Press, San Diego, Chapter 85.12.

6.4 The International Polar Year (IPY) broadband ocean-bottom seismograph deployment: observations, limitations and integration with the IPY land network

6.4.1 Introduction

Within the framework of the International Polar Year 2007-2008 (IPY) project "The Dynamic Continental Margin Between the Mid-Atlantic-Ridge System (Mohns Ridge, Knipovich Ridge) and Bear Island" (Schweitzer et al., 2008), several temporary seismic stations were installed in the wider area of the Western Barents Sea margin (Fig. 6.4.1). Among them was a three-component, broadband ocean-bottom seismometer and hydrophone (OBS/H) deployment, consisting of 12 stations distributed over the area between the Knipovich Ridge and Bear Island. Regarding land stations, the Norwegian National Seismic Network (NNSN) station HOPEN was upgraded with a broadband seismometer, a new broadband station (HSPB) was installed at Hornsund, and a small-aperture seismic array was installed on Bear Island for the summer season of 2008.

This network, together with the permanent stations in the wider region, was used to monitor and locate the seismicity around the continental margin and along the mid-ocean ridge, focusing on the sedimentary wedge between them. This contribution will mainly deal with a description of the seafloor network, its observations, and its integration with the land-based network in order to locate the seismicity in the target area.

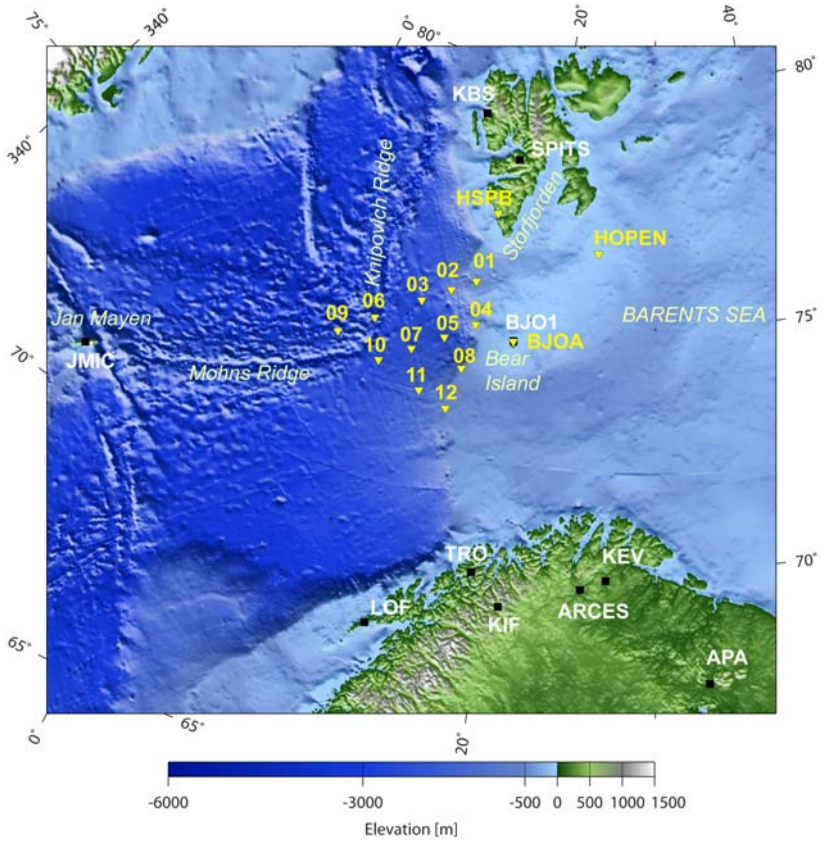

Fig. 6.4.1. Locations of seismic stations used within the IPY project. The IPY network is depicted in yellow, together with permanent seismic stations in the region, shown in black.

6.4.2 The IPY OBS/H deployment: instrumentation and data quality

The OBS/H stations were provided by the German Pool for Amphibian Seismology (DEPAS, www.awi.de/en/research/research_divisions/geosciences/geophysics/depas_german_instrument_pool_for_amphibian_seismology/), and were deployed by colleagues from the Alfred Wegener Institute, the University of Potsdam, KUM and the staff of the Polish research vessel HORYZONT II in late September 2007. The particular station model, known as LOBSTER (Longterm OBS for Tsunami and Earthquake Research), consists of a titanium frame that carries the broadband seismometer, recorder, releaser and batteries, each in a titanium pressure tube, as well as float units of syntactic foam, hydrophone, flasher, radio beacon and signal flag (Fig. 6.4.2). The seismometer is a CMG-40T by Güralp Systems Ltd. and the hydrophone is an HTI-04-PCA/ULF by High Tech Inc., USA, while data acquisition is performed by a GEOLON-MCS recorder in a Titanium tube, manufactured by SEND Off-Shore Electronics GmbH.

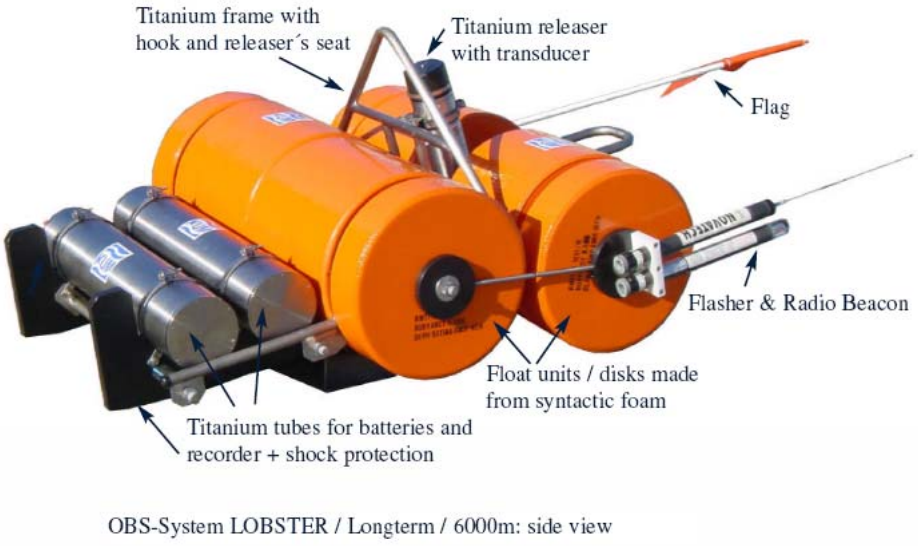

Fig. 6.4.2. The LOBSTER OBS/H system (picture taken from K.U.M. GmbH LOBSTER brochure).

The instrument response for the seismic channels was calculated, using information by the manufacturers of the sensors and data recorders (Güralp Systems, Ltd. and SEND Off-Shore Electronics GmbH, respectively). The pole-zero set for the CMG-40T is the following:

Table 6.4.1. Poles and zeroes of the Güralp CMG-40T seismometers of the DEPAS OBSs.

POLES (HZ)	ZEROES HZ
$-11.78 \times 10^{-3} \pm j11.78 \times 10^{-3}$	0
$-80.0 \pm j\ 95.0$	0

The normalizing factor at 1 Hz is A = 15.41 K. Sensitivity values are channel specific, a nominal value being about 2000 V/m/s.

The GEOLON-MCS recorder features software selectable pre-amplification, achievable in seven 6 dB steps, and which in the case of the OBS channels is set to GAIN = 1. This defines the sensitivity of the 24-bit A/D converter, based on the formula (SEND GmbH, 2009):

$$UIN_{0dB} = 5\ V\ /\ GAIN\ [Vpp\ differential]$$

Thus, the sensitivity is equal to 2x(5/1) Vfull-scale / 2^{24} = 0.59605 μV/bit.

Apart from the pre-amplifier, the GEOLON-MCS A/D converter consists of a sigma-delta modulator and a digital filter, which decimates down to the desired data sampling rate (SEND GmbH, 2007). The Cirrus Logic CS5378 low-power, single-channel, digital filter is used for this purpose (Cirrus Logic, 2010). A cascade of a multi-staged SINC filter with variable decimation stages and two FIR filters are employed to decimate from the 512 kHz of the modulator to a diversity of sampling rates. In the case of the IPY OBS/H deployment, 50 sps data was outputted. The employed digital filter cascade is the following:

FIR filter SINC-1, decimates by 8, symmetric, 36 coefficients: 512 kHz –> 64 kHz

FIR filter SINC-2-stage-2, decimates by 2, symmetric, 5 coefficients: 64 kHz –> 32 kHz

FIR filter SINC-2-stage-3, decimates by 2, symmetric, 6 coefficients: 32 kHz –> 16 kHz

FIR filter SINC-2-stage-4, decimates by 2, symmetric, 7 coefficients: 16 kHz –> 8 kHz

FIR filter SINC-3-stage-3, decimates by 5, symmetric, 17 coefficients: 8 kHz –> 1600 Hz

FIR filter SINC-3-stage-5, decimates by 2, symmetric, 6 coefficients: 1600 Hz –> 800 Hz

FIR filter SINC-3-stage-7, decimates by 2, symmetric, 7 coefficients: 800 Hz –> 400 Hz

FIR filter FIR1 (set 0), decimates by 4, symmetric, 48 coefficients: 400 Hz –> 100 Hz

FIR filter FIR2 (set 0), decimates by 2, symmetric, 126 coefficients: 100 Hz –> 50 Hz

As an example, the displacement amplitude and phase response for the vertical component of OBS01 is shown in Fig. 6.4.3. The shaded area notes the frequency range beyond the Nyquist (25 Hz).

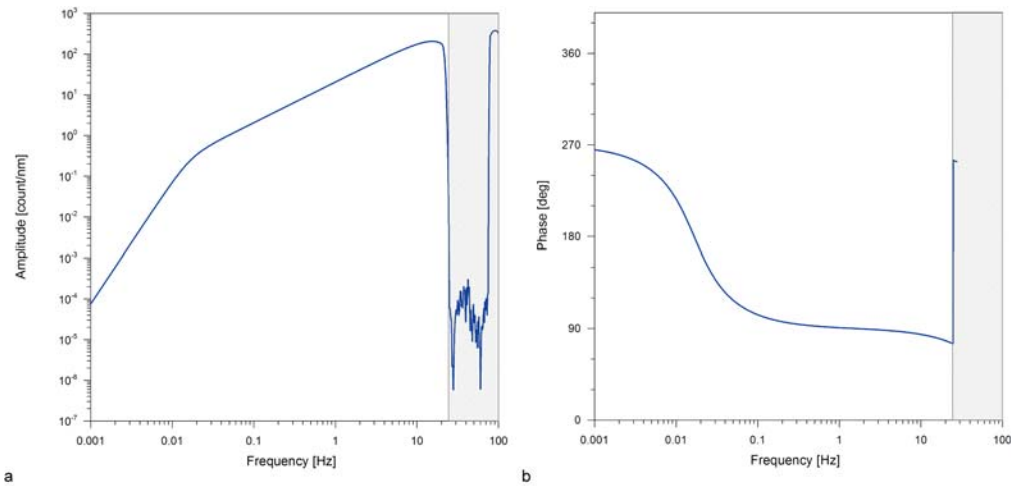

Fig. 6.4.3. a. Displacement amplitude response for the vertical, seismic channel of OBS01. b. Phase response for the same channel. The shaded area lies beyond the Nyquist frequency (25 Hz).

Regarding the response of the pressure sensor, only its gain is known, provided by the manufacturer in the brief documentation accompanying the shipped instruments (High Tech, Inc., 2005), a nominal value being equal to -195 dB relative to 1 V/μPa. A response curve is given in the same document, but without any information on how to reconstruct it.

The stations covered a wide variety of oceanic environments, from the shallow waters of the Barents Sea shelf (minimum depth 325 m for OBS01) to depths of about 2900 m close to the mid-ocean ridge (OBS09) and had a minimum inter-station distance of about 60 km. They were collected again in August 2008, after recording for a time interval of approximately 11 months. One of the shallowest stations (OBS04) was already fished out in April 2008 by a Russian trawler, while OBS03 was lost during recovery. OBS10 could not be recovered and was eventually found in April 2009 on the northern coast of Iceland, without having recorded data. Thus, there is partial data loss for OBS04 and total loss for OBS03 and OBS10.

Regarding the quality of the retrieved data, it mostly depends on additional possible problems, such as coupling conditions to the seafloor, low amplification etc., the possibility to apply the skew correction for timing, and the general noise conditions. Some problems were observed with particular seismometer components (vertical of OBS02, Y-component of OBS07, X-component of OBS12), while OBS02 had stopped recording a week before recovery, presumably due to problems with its power supply. This resulted in no skew correction for this station, as well as for the fished out station, OBS04. The rather frequent clipping of the horizontal components of OBS04 is suggestive of poor coupling to the seafloor, which may have been the reason that the station was fished out. No problems were detected on the hydrophone data.

Noise conditions are a very decisive factor affecting OBS/H data. The noise spectrum in the ocean is quite complex, with numerous sources contributing to it, including among others weather related phenomena, ocean currents, marine biologics and boat traffic (e.g., Wenz, 1962). In the case of the IPY OBS/H deployment, noise conditions were rather bad, extreme even in cases, with the shallower stations being worse. By far the best noise conditions were encountered at OBS09, the deepest station, close to the Mohns – Knipovich Ridge Bend, with second best being OBS06, also at a depth larger than 2300 m. The power spectral density plots of Figs. 6.4.4 and 6.4.5 show the average noise level (red line) at different stations for a period of one month (April 2008) and positive deviations from it (color scaled), for the OBS vertical component and the hydrophone, respectively. High noise conditions at all stations except for OBS09 can be observed in the typical seismic body-wave frequency range (1 – 10 Hz) in Fig. 6.4.4.

Comparing the same frequency range with Fig. 6.4.5, it becomes obvious that the hydrophones have lower noise levels, which has enabled in some cases the picking of first arrivals, when this was impossible on the seismic channels. A waveform example in Fig. 6.4.6 from the same time interval shows clearly the effect of poor signal-to-noise ratio (SNR) on the analysis of seismic events. The event occurred at the Mohns – Knipovich Bend (73.952°N, 8.819°E), on 27 April 2008, 23:49:52.6 UTC and waveforms are displayed sorted with epicentral distance and filtered between 3.5 and 12 Hz. Clear P-phase picks can be obtained on OBS06, OBS07 and OBS09, as well as the farther away OBS01, but not at in between distances. This is representative of how noise conditions affected the location capability of the network, taking also into account the quite small magnitude of most events.

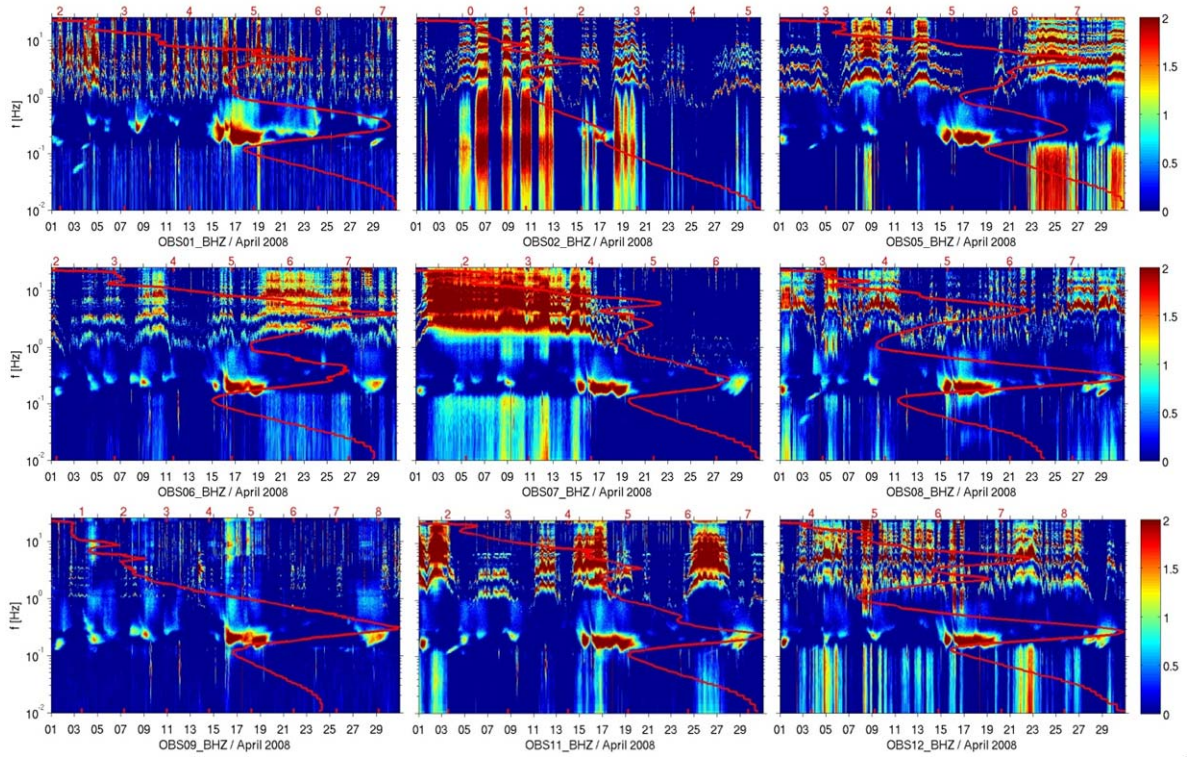

Fig. 6.4.4. Power spectral density plots for the vertical seismic components of the IPY OBS/H stations, for April 2008. The average noise level is shown by the red curve, while the applied color scale expresses positive deviations from the average.

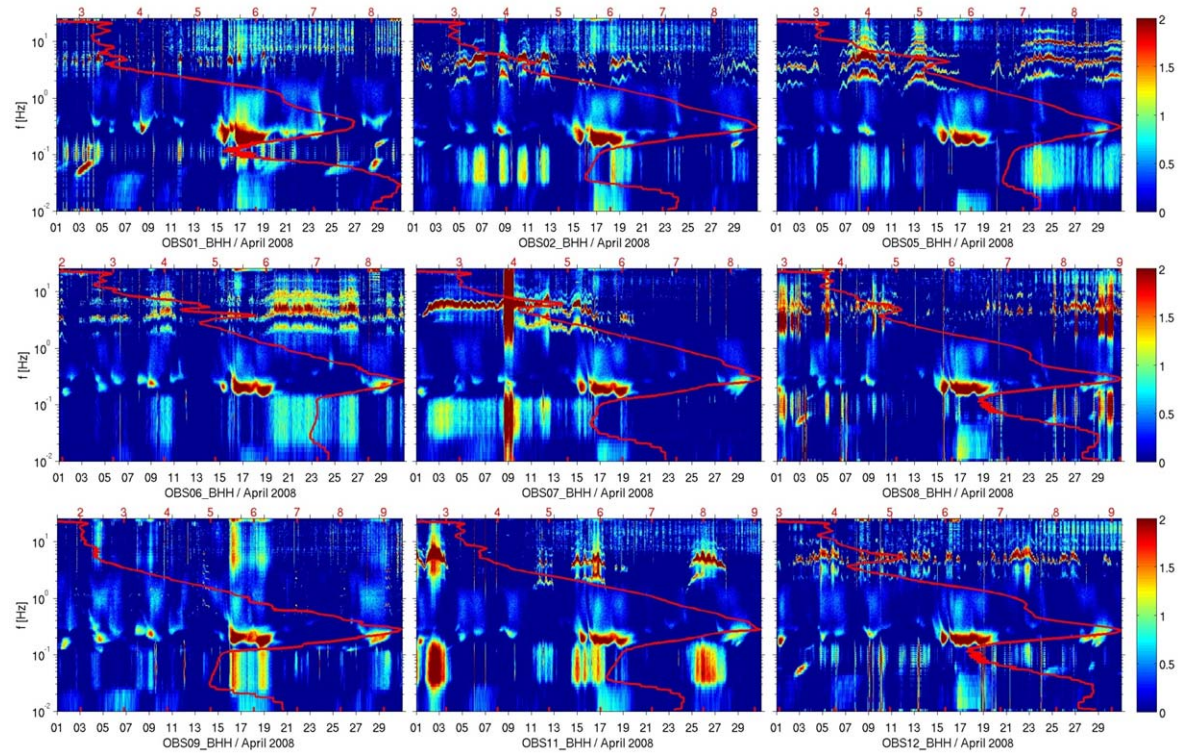

Fig. 6.4.5. As for Fig. 6.4.4, but for the hydrophone channels of the IPY OBS/H stations.

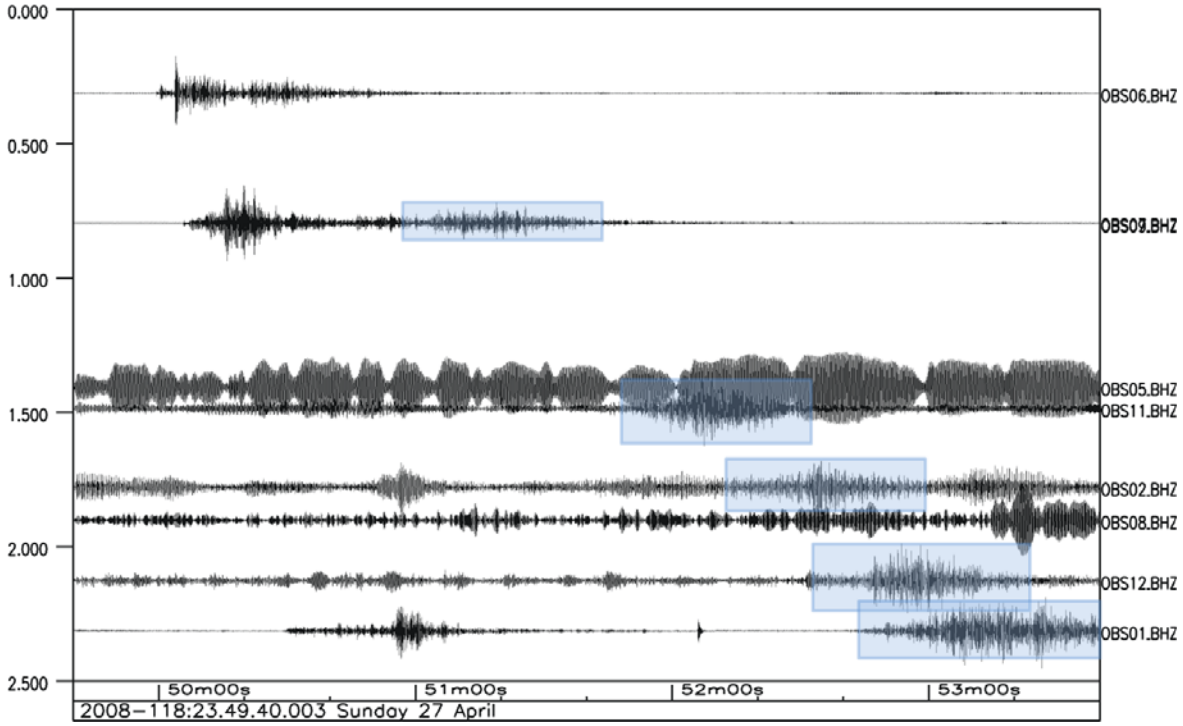

Fig. 6.4.6. Vertical component records on the OBS/H stations of a magnitude 3 event at the Mohns – Knipovich Bend, sorted by epicentral distance. Records are band-pass filtered between 3.5 and 12 Hz. Note that OBS07 and OBS09 are almost at the same distance from the epicenter. High noise conditions at several stations (e.g., OBS05) render picking of body-waves impossible. Colored rectangles enclose T-phases.

6.4.3 Examples of observations

A wide variety of signals was recorded on the seismic and acoustic components of the OBS/H network. There are teleseismic events, stronger regional earthquakes and a huge amount of small, local, seismic events, mostly distributed along the mid-ocean ridge. These can be seen both on the seismic sensors and the hydrophones. An example is shown in Fig. 6.4.7. It is a magnitude 2.6 local event on the Mohns Ridge, recorded on OBS09. It is noteworthy that P-phases appear with quite small amplitudes on all seismic channels, while they are more visible on the hydrophone (BHH). The opposite is true for S-phases, which are in general not well recorded on the pressure sensor, as theoretically expected. Another characteristic feature is the water reflection (Pw), seen on the hydrophone as an impulsive onset. The arrival time difference between the first P-phase onset and the water reflection is 3.9 s, while a water velocity of 1.48 km/s is considered typical for this area (e.g., Ehlers, 2009). This results in a water depth of about 2.9 km, which is in good agreement with our knowledge of the bathymetry in the region.

In addition, several T-phases have been recorded on the hydrophones, but also on the seismometers, mainly from events on the Mohns Ridge. T-phases are observed for events in a minimum distance of about 50 km from the recording station. Their excitation depends strongly on the bathymetry, since bathymetric features act as scatterers, and the effective impedance contrast between the ocean column and the seafloor, (e.g., de Groot-Hedlin and Orcutt, 2001; de Groot-Hedlin, 2004). An example recorded on the seismic sensor is shown in Fig. 6.4.6, where the T-phase, marked with a colored rectangle, can be seen following the body-waves.

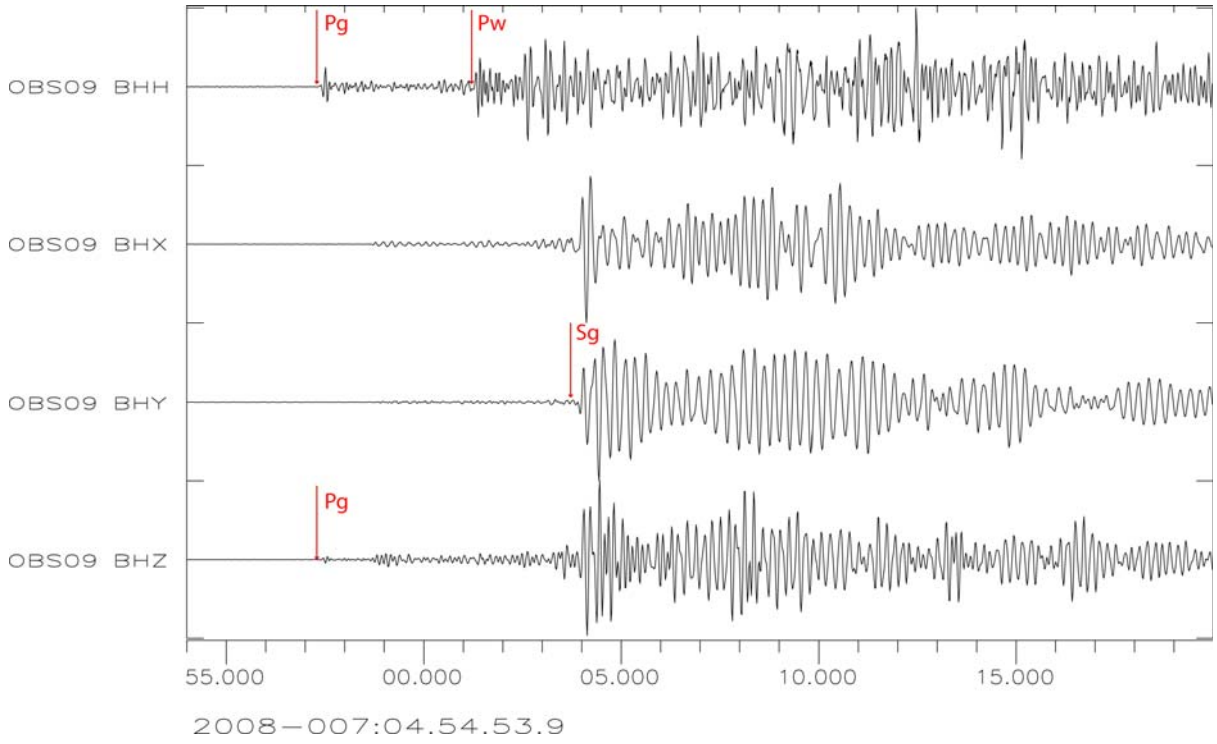

Fig. 6.4.7. Example of a local earthquake on the Mohns Ridge, as recorded on OBS09, band-pass filtered between 3.5 and 12 Hz. The arrivals of the first P-, S- and water-phase are shown. A water velocity of 1.48 km/s for this reflection phase gives a depth of about 2.9 km, which agrees with the bathymetry in this area. Note the rather small amplitudes of the P-phase and the fact that the S-phases cannot be recorded well on the pressure sensor (BHH).

An abundance of hydroacoustic signals was observed on the hydrophones of the IPY network. Among the anthropogenic sources that have been identified in several occasions are airguns (research and industrial), mostly at the southernmost stations closer to the continental shelf. It can be assumed that several signals are associated with boat traffic and marine life, such as whale vocalizations. However, the relatively low sampling rate of the data (50 sps) does not allow a secure identification. Finally, a large part of the recorded hydroacoustic signals remains unclassified.

A different example, shown in Fig. 6.4.8, is a tremor-like signal, consisting of several sub-harmonics, which is mostly visible on the horizontal and vertical components of the seismometer, but is very weak or almost absent on the pressure sensor. The signal is observed at several of the OBS/H, can last for several days and exhibits changes in the resonance frequencies over time. We provisionally interpret this signal as the effect of shear resonances in the upper sediment layers after Godin and Chapman (1999), although its presence at stations where the sedimentary layer is expected to be very thin (e.g., at OBS09) raises some questions on the likelihood of such an interpretation.

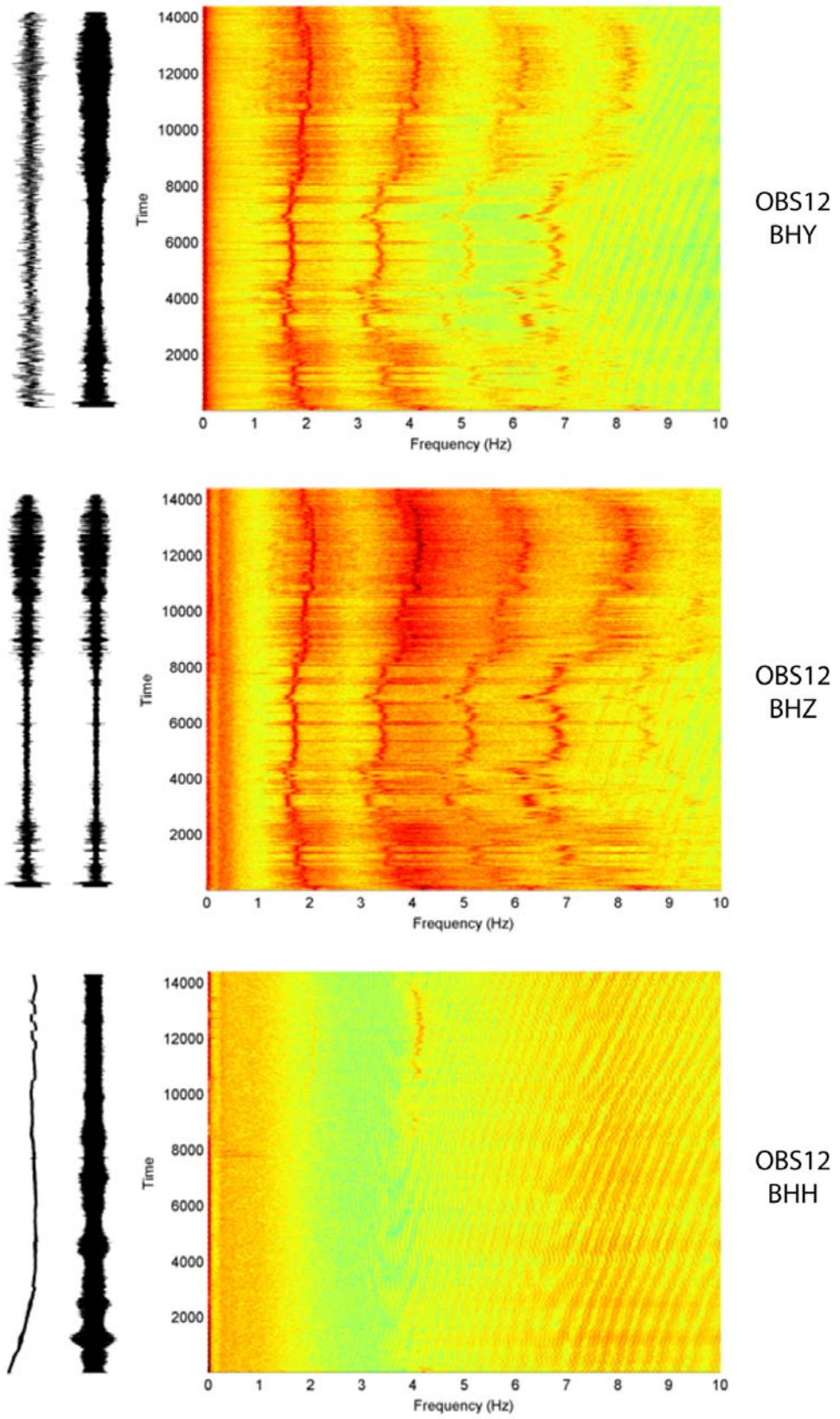

Fig. 6.4.8. Waveforms (left – raw; right – band-pass filtered between 1 and 10 Hz) and corresponding spectrograms up to 10 Hz, for 4 hours of data, on one of the horizontals (BHY), the vertical seismic (BHZ) and the hydrophone channel (BHH) of OBS12.

6.4.4 Location of seismicity

As mentioned in the introduction, the IPY OBS/H network was in operation for almost 11 months, from the end of September 2007 to the end of August 2008. During this time period, a total of 463 earthquakes were located in the wider project area. Our initial knowledge of the seismicity in the region during this time interval came mainly from NORSAR's analyst reviewed bulletin, which contains events with magnitude larger than 2. Its location results for 334 events are shown in Fig. 6.4.9a and reflect the quite large uncertainties introduced by the sparse regional network. Seismicity is mainly observed along the mid-ocean ridge, close to Spitsbergen, and at the sedimentary wedge between the ridge and the continental margin.

All events in NORSAR's bulletin were relocated using in addition all IPY data, as well as any data available from NNSN stations in northern Fennoscandia. The 256 seismic events in the area of Storfjorden, off the east coast of Spitsbergen, belong to the first six months of the aftershock sequence of the 21 February 2008 Mw 6.1 earthquake that was studied by Pirli et al. (2010) and will not be mentioned further herein. In addition to the events in NORSAR's bulletin, the Generalized Beamforming (GBF) algorithm (Ringdal and Kværna, 1989) was reapplied using also the temporary array on Bear Island and results within the project area were relocated manually, using all available data. The same applied for the results of an STA/LTA detector at OBS09 and OBS06, which mostly yielded events at the mid-ocean ridge. Due to the bad noise conditions on most OBS/H stations, power detectors could not be employed on any other ones. The spatial distribution of all (re)located events is shown in Fig. 6.4.9b.

In the relocated dataset, most of the seismicity follows the mid-ocean ridge system, with the largest concentration being observed at the Mohns – Knipovich Bend. Some earthquakes are observed on the sedimentary wedge, but they are fewer compared to the standard NORSAR bulletin results. No special focus will be given herein to the activity located at the southern terminus of the Mohns Ridge and around Jan Mayen, as it is situated outside the project area and lies outside the IPY network. It is however presented for completeness and is included in the statistics that follow.

For the 213 events located along the ridge and on the sedimentary wedge, several trials were performed with different velocity models, in order to define the combination that modeled best the very diverse paths followed by the seismic waves. For instance, stations with a predominantly oceanic path (e.g., JMIC) were modeled using the PREM model (Dziewonski and Anderson, 1981). Specifically for the areas of the sedimentary wedge and the Mohns – Knipovich Bend, the velocity models that provided the best fit to the data were local 1-D averages derived from the three-dimensional Barents3D model (Levshin et al., 2007; Ritzmann et al., 2007). However, even so, events on the sedimentary wedge were not modeled (in terms of velocity model fit) as adequately as events along the ridge, presumably due to the inability of the model to adjust to varying sediment structure. A three-dimensional model is expected to perform much better in this case.

A detailed study of the seismic activity on the sedimentary wedge cannot be achieved without an accurate determination of the hypocenter's location, so that the sediment unit containing the seismic source is identified. The same applies to the seismicity along the ridge, where hypocentral depth constitutes a diagnostic of different processes within the spreading regime. Unfortunately, the resolution achieved by the network was limited and the determination of focal depths was not possible.

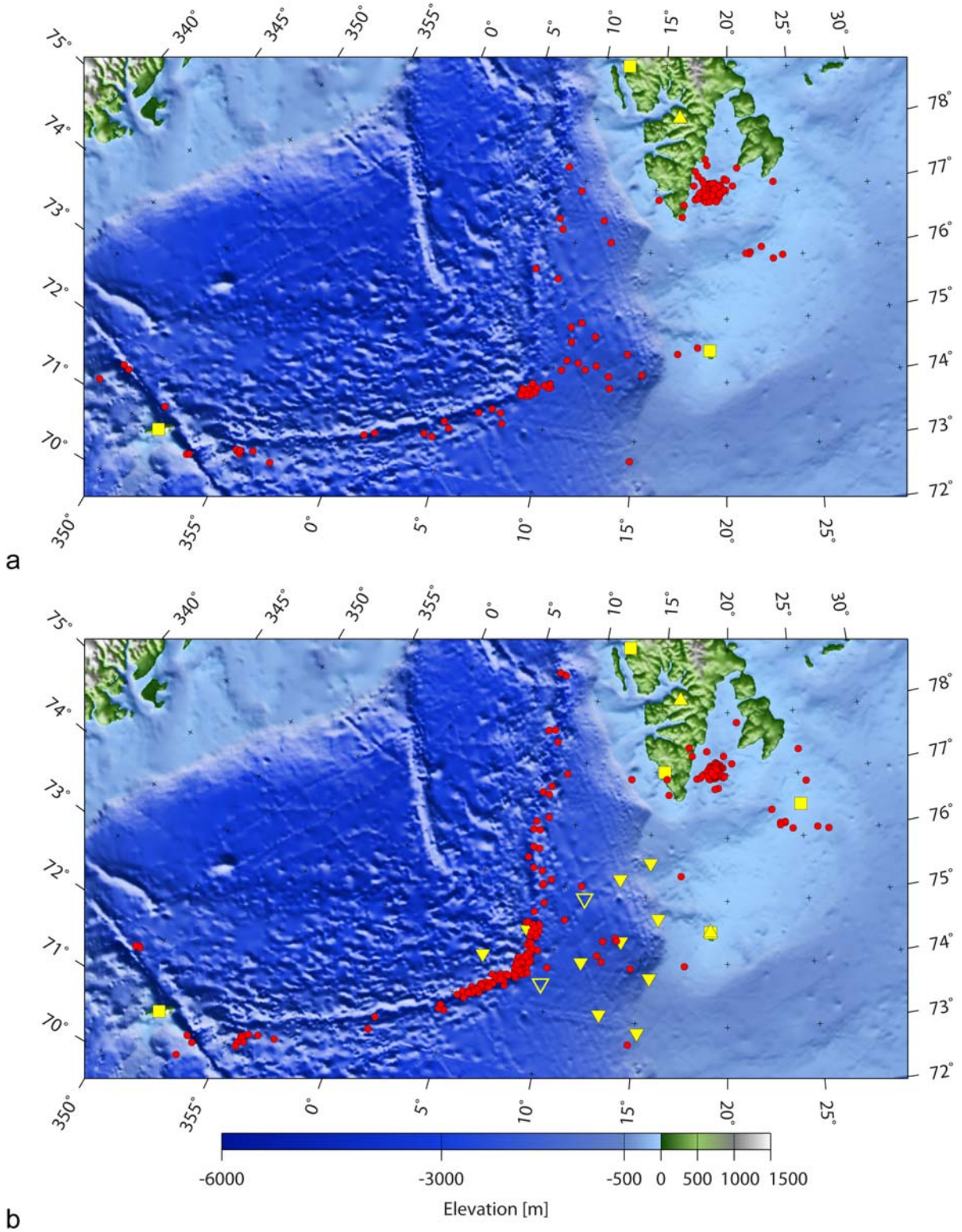

Fig. 6.4.9. a. NORSAR reviewed bulletin solutions for the time interval September 2007 – August 2008. b. Relocated events within the IPY context for the same time interval. The mapped epicenters belong to three different groups: relocations of NORSAR's bulletin solutions, relocations of GBF automatic locations, and locations of events detected on OBS09 and OBS06. Single 3C stations are noted as squares, seismic arrays as triangles and the OBS/H network as inverted triangles (open symbols: no data).

The graphs in Fig. 6.4.10 provide some insight into this problem. Fig. 6.4.10a shows the magnitude distribution for the 78 events (excluding the Storfjorden sequence) in NORSARS's bulletin. Magnitudes are based on amplitude measurements on STA traces for the stations of the permanent regional network. Most earthquakes in this dataset have moderate to small magnitudes, the larger (M > 4.5) ones corresponding to seismicity in the area of Jan Mayen. Fig. 6.4.10b displays the distribution of the number of stations that were actually used to locate the events with the number of events. It becomes clear that more than half of the events were located with a rather small network of 5 stations. This is mostly the effect of the poor SNR on the OBS/H stations, combined with the small magnitude of the events. Fig. 6.4.10c shows the distribution of the minimum epicentral distance in km for the resulting locations. Most of the epicenters are situated at a distance of 50 – 70 km from the nearest station, making the network rather sparse for focal depth determination. Finally, as shown in the rose diagram of Fig. 6.4.10d, there are very few solutions with a primary azimuthal gap less than 100°.

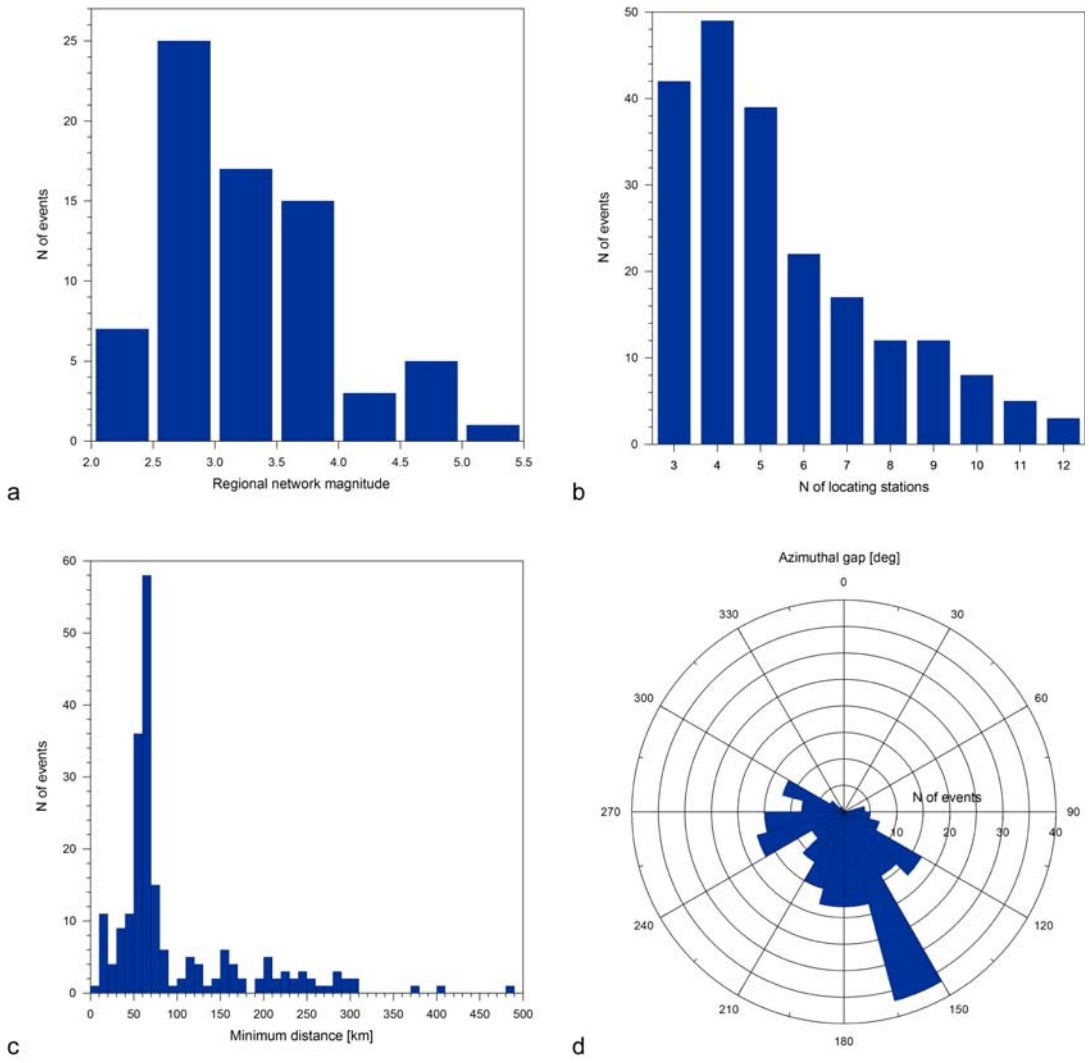

Fig. 6.4.10. a. Histogram of the regional network magnitude distribution for the 78 events in NORSAR's reviewed bulletin. b. Histogram of the number of stations used for location with the number of events for the entire dataset (213 events). c. Histogram of the minimum epicentral distance with the number of events for the entire dataset. d. Rose diagram of the distribution of the primary azimuthal gap in event location for the entire dataset. Intervals of 15° are used.

Despite these shortcomings, the IPY OBS/H network has contributed significantly in enhancing our knowledge of the seismicity in the region. Two examples of event relocation are shown. The first one deals with an event originally located on the Barents shelf, close to Bear Island (2008/01/21 19:31:51, M 3) and the second one with an event on the sedimentary wedge (2008/01/03 21:17:27, M 3), according to NORSAR's reviewed bulletin.

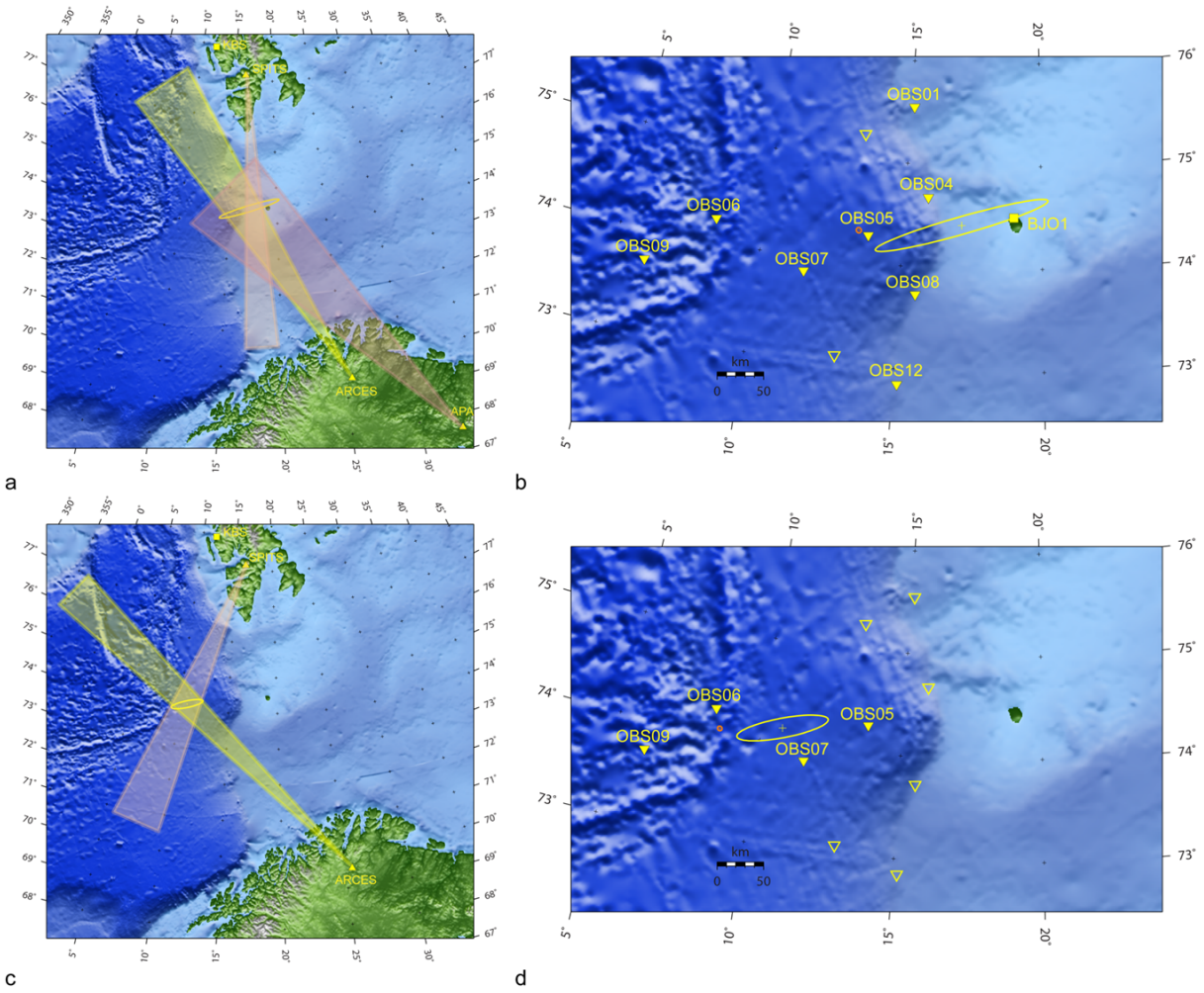

Fig. 6.4.11. a. NORSAR regional reviewed bulletin solution of the 2008/01/21 19:31 M 3 event. Colored triangles denote array backazimuth observations and corresponding uncertainties, while the 90% confidence-level error ellipse is shown in yellow. b. Zoomed-in view of the initial (yellow) and relocated (orange) solutions. The 95% confidence-level error ellipse is calculated for the relocated epicenters. Stations used for the location appear as filled symbols. Seismic arrays are noted as triangles, NNSN stations as squares and IPY stations are inverted triangles. c. Same as a. for the 2008/01/03 21:17 M 3 event. d. Same as b. for the 2008/01/03 21:17 M 3 event. Note the very small dimensions of the relocated error ellipses (in orange) for both events.

The 21 January 2008 earthquake (Fig. 6.4.11a) was located for NORSAR's bulletin using three seismic arrays at regional distances (ARCES, APA and SPITS) and station KBS. The location result is dominated by the backazimuth observations from the three arrays and their corresponding uncertainties (colored triangles in Fig. 6.4.11a,c). Relocating the event using in addition the OBS/H network, BJO1, HSPB and HOPEN results in the epicenter moving approximately 130 km westwards, on the sedimentary wedge (Fig. 6.4.11b). In fact, the intro-

duction of P- and S-phase readings from BJO1 is enough to move the epicenter off the continental shelf, but the addition of the OBS/H stations (8 out of 10 could be used in this case, with a minimum epicentral distance of 12 km from OBS05) refines the solution. The 3 January 2008 event (Fig. 6.4.11c) was located for NORSAR's bulletin near the end of the sedimentary wedge and close to the southern end of the Knipovich Ridge, using two seismic arrays (SPITS and ARCES) and station KBS. It was relocated using in addition OBS06, OBS09, OBS07 and OBS05, the epicenter moving to the mid-ocean ridge (Fig. 6.4.11d).

These two examples illustrate clearly the significance of the IPY network to the connection of located events with the correct geodynamic environment. The relocated seismicity in Fig. 6.4.9b is not only more populous, compared to the listings of NORSAR's reviewed bulletin, but the geographic spread is significantly less and seismic events are better associated with their corresponding geodynamic sources. Thus, sedimentary wedge seismicity has noticeably decreased, compared to the impression given by the bulletin, since several events are now correctly attributed to the mid-ocean ridge system. It should be noted that it cannot be expected that routine analysis results can be used for a seismotectonic or geodynamic study, especially in such cases, where seismicity is remote, in an offshore area that is covered only by a very sparse, regional network. However, this highlights the importance of temporary deployments to provide, even for limited time intervals, a more accurate image of the spatiotemporal distribution of the seismic activity for a given region.

6.4.5 Conclusions

We presented the contribution of the IPY OBS/H network to the study of the seismicity at the wider region of the western Barents Sea continental margin. Some equipment and data loss took place within the experiment, but most of the stations of the deployment contributed seismic and pressure data for approximately 11 months.

A variety of seismic and acoustic signals were recorded during the project; they included seismicity from different epicentral distance ranges and geodynamic environments, hydroacoustic phases, signals from anthropogenic sources (e.g., airgun shots, boat traffic), weather related phenomena, ocean currents, as well as many unclassified signals. In general, the noise level among the OBS/H stations was rather high, imposing restrictions to the analysis of seismic data. The two deepest stations (OBS09 and OBS06) were the ones with the best SNR, and therefore a strong focus was put on the exploitation of their data.

Unfortunately, the network did not achieve the required resolution to allow the determination of focal depth for the events along the mid-ocean ridge and the sedimentary wedge, which was one of the aims of the project. However, and despite all difficulties, the network had a significant contribution to the monitoring and location of the seismic activity in the region. Comparisons of our knowledge of the seismicity only with the use of the permanent, regional network, and with the use of the IPY stations, show not only a quantitative increase in the number of located events, but a clearly enhanced resolution. This is particularly important for such remote, offshore areas, since it allows us, even if it is only for a relatively short time interval, to obtain accurate images of the spatiotemporal distribution of the seismic activity.

Acknowledgements

The power spectral density plots of Figs. 6.4.4 and 6.4.5 were prepared by Michael Roth. The project "The Dynamic Continental Margin Between the Mid-Atlantic-Ridge System (Mohns Ridge, Knipovich Ridge) and Bear Island" was part of the Norwegian contribution to the International Polar Year 2007-2008 activities organized by the Norwegian IPY Committee and mainly financed by the Norwegian Research Council (Contract Number 176069/S30).

Myrto Pirli
Johannes Schweitzer
The IPY Project Consortium

References

Cirrus Logic (2010): Crystal CS5378 Low-Power Single-Channel Decimation Filter. CS5378_F3.pdf, Cirrus Logic Inc., Austin, Texas, 88 pp.

de Groot-Hedlin, C. & J.A. Orcutt (2001): Excitation of T-phases by seafloor scattering. J. Acoust. Soc. Am., **109(5)**, 1944-1954.

de Groot-Hedlin, C. (2004): Criteria for discretization of seafloor bathymetry when using a stairstep approximation: Application to computation of T-phase seismograms. J. Acoust. Soc. Am., **115(3)**, 1103-1113.

Dziewonski, A.M. & D.L. Anderson (1981): Preliminary reference Earth model. Phys. Earth Planet. Interiors, **25**, 297-356.

Ehlers, B.-M. (2009): A geodynamic model of the northern North Atlantic. PhD Thesis, Alfred Wegener Institute for Polar and Marine Research, Bremerhaven, Jacobs University Bremen, Bremen, 228 pp.

Godin, O.A. & D.M.F. Chapman (1999): Shear-speed gradients and ocean seismo-acoustic noise resonances. J. Acoust. Soc. Am., **106(5)**, 2367-2382.

High Tech, Inc. (2005): HTI-01-PCA/ULF Hydrophones 31205605 – 31208505. High Tech, Inc., Gulfport, Mississippi, 4 pp.

Levshin, A., J. Schweitzer, Ch. Weidle, N. Shapiro & M. Ritzwoller (2007): Surface wave tomography of the Barents Sea and surrounding regions. Geophys. J. Int., **170**, 441-459.

Pirli, M., J. Schweitzer, L. Ottemöller, M. Raeesi, R. Mjelde, K. Atakan, A. Guterch, S.J. Gibbons, B. Paulsen, W. Dębski, P. Wiejacz & T. Kværna (2010): Preliminary analysis of the 21 February 2008, Svalbard (Norway), seismic sequence. Seism. Res. Lett., **81(1)**, doi:10.1785/gssrl.81.1.50.

Ringdal, F. & T. Kværna (1989): A multichannel processing approach to real time network detection, phase association and threshold monitoring. Bull. Seism. Soc. Am., **79**, 1927-1940.

Ritzmann, O., N. Maercklin, J. I. Faleide, H. Bungum, W. D. Mooney & S. T. Detweiler (2007): A 3D geophysical model for the crust in the greater Barents Sea region: Database compilation, model construction and basement characterisation. Geophys. J. Int., **170**, 417-435.

Schweitzer, J. & the IPY Project Consortium Members (2008): The International Polar Year 2007-2008 Project "The Dynamic Continental Margin between the Mid-Atlantic-Ridge System (Mohns Ridge, Knipovich Ridge) and the Bear Island Region". NORSAR Scientific Report, **1-2008**, 53-63.

SEND GmbH (2007): Application Note: Geolon-MCS Digital Filtering. Digital_filtering_mcs.doc, SEND GmbH, Hamburg, Germany, 8 pp.

SEND GmbH (2009): GEOLON-MCS Marine Compact Seismocorder, User Manual. MCS1.09.mnl.doc, SEND GmbH, Hamburg, Germany, 38 pp.

Wenz, G.M. (1962): Acoustic ambient noise in the ocean: spectra and sources. J. Acoust. Soc. Am., **34(12)**, 1936-1956.